De-noising of ECG signal using FIR filter and QRS detection

by

Jannatul Robaiat Mou

A thesis submitted in partial fulfillment of the requirements for the degree of

M.Sc. Engineering

in the Department of Electronics and Communication Engineering

Department of Electronics and Communication Engineering

Khulna University of Engineering & Technology

Khulna 9203, Bangladesh

May, 2017

Declaration

This is to certify that the thesis work entitled ***"De-noising of ECG signal using FIR filter and QRS detection"*** has been carried out by **Jannatul Robaiat Mou** in the Department of Electronics and Communication Engineering, Khulna University of Engineering & Technology (KUET), Khulna, Bangladesh. The above thesis work or any part of this work has not been submitted anywhere for the award of any degree or diploma.

---------- ----------

Signature of Supervisor Signature of Candidate

Approval

This is to certify that the thesis work submitted by **Jannatul Robaiat Mou** entitled ***"De-noising of ECG signal using FIR filter and QRS detection"*** has been approved by the board of examiners for the partial fulfillment of the requirements for the degree of **M.Sc. Engineering** in the Department of **Electronics & Communication Engineering**, Khulna University of Engineering & Technology (KUET), Khulna, Bangladesh in May,2017.

Board of Examiners

1. ---------- **Chairman**
   Dr. Sheikh Md. Rabiul Islam **(Supervisor)**
   Associate professor
   Department of Electronics and Communication Engineering
   Khulna University of Engineering & Technology (KUET)
   Khulna-9203, Bangladesh.

2. ---------- **Member**
   Prof. Dr. Md. Faruque Hossain
   Head of the Department
   Department of Electronics and Communication Engineering
   Khulna University of Engineering & Technology (KUET)
   Khulna-9203, Bangladesh.

3. ---------- **Member**
   Prof. Dr. Md. Foisal Hossain
   Department of Electronics and Communication Engineering
   Khulna University of Engineering & Technology (KUET)
   Khulna-9203, Bangladesh.

4. ---------- **Member**
   Prof. Dr. A. B. M. Aowlad Hossain
   Department of Electronics and Communication Engineering
   Khulna University of Engineering & Technology (KUET)
   Khulna-9203, Bangladesh.

5. ---------- **Member**
   Prof. Dr. Md. Maniruzzaman **(External)**
   Electronics and Communication Engineering Discipline
   Khulna University, Khulna – 9208, Bangladesh.

Acknowledgement

For a start, all praise goes to Allah, the Almighty, on whom ultimately, we depend for sustenance and guidance and also for giving me the opportunity and confidence to complete my thesis work with great success.

I would like to express my sincere gratitude and profound respect to my honorable supervisor, **Dr. Sheikh Md. Rabiul Islam**, Associate professor, Department of Electronics and Communication Engineering, KUET, for his valuable guidance, constructive suggestion, and support throughout my study. Besides providing excellent academic guidance, he has been incredibly encouraging, supportive, kind, patient. I really enjoy all our meetings and during all the meetings, he talked with such enthusiasm about my research, presentation, publications, etc. those made it always very interesting. He has been great sources of inspiration to me and I thank him from the bottom of my heart.

I wish to thank the course teachers of my M. Sc. Engineering degree –Prof. Dr. Md. Mostafizur Rahman, Prof. Dr. Pallab Kumar Choudhury, and Prof. Dr. Monir Hossen, with Course Co-coordinator Prof. Dr. Md. Foisal Hossain, Department of Electronics and Communication Engineering, Khulna University of Engineering & Technology (KUET). Then I would like to acknowledge my deep gratitude to my committee members who have granted me their valuable time and effort to review my thesis work. I would like to convey my heartiest gratitude to Head of the department as well as all teachers of the Department of Electronics and Communication Engineering, KUET, for their co-operations and constant encouragements in various ways through this work.

Last, but not least, I would like to express my thanks to my parents, my husband, family members for their prayer and blessing, which has helped me becoming what I am today. I am grateful to all my friends for their help, support, and endless inspirations to complete my work.

Abstract

Electrocardiogram (ECG) machines are usually used for medical diagnosis of heart activities of human body now days. Every portion of ECG is very essential for the diagnosis of different cardiac problems. But the amplitude and duration of ECG signal is usually corrupted by different types of noise and interference based on interfaces between ECG machines and human body. It can change the real amplitude and duration of the signal.

In electrocardiogram (ECG), noise removal and QRS complex play the vital role for detecting various heart diseases. So, noise free and accurate QRS detection becomes very important in ECG signal. In this thesis we proposed new algorithms which are able to make it noise free and detect QRS complex in ECG signal. Generally, a noise free algorithm removes the noisy signal and we have used Remez exchange algorithm for 1st algorithm, designed an arbitrary magnitude with FIR filter for 2nd algorithm, FIR filter with window method for 3rd proposed algorithm, We have also proposed moving average filter and moving average weighted window, and an algorithm based on forward difference quotient and threshold for corresponding algorithms respectively for noise elimination of ECG. QRS complex of noise free ECG signal have been detected by proposed detection algorithm. The performance parameters are SNR, MSE and Correlation and accuracy, sensitivity, specificity, precision are used to justify the proposed noise free algorithm and QRS detection. The real data examples and experimental results approve new algorithms and prove the robustness of the algorithms which are more effective in ECG applications.

Keywords—ECG, QRS complex, Threshold, SNR, MSE, Correlation.

Table of Contents

Chapter 6 Conclusion and Future Work

List of Figures

List of Tables

Chapter 1

Introduction

1.1 Introduction

Electrocardiogram (ECG) is the recording of electrical activity of the heart and used to investigate the heart diseases. Due to its non-invasive nature it is a most popular diagnostic tool. This is done by measuring the potential difference between several electrodes which are placed on the skin at predefined points of the human body [1]. As ECG is a graphical representation of heart based on electrical impulses, it is needed to be done when chest pain occurred such as heart attack, rapidity of breath, faster heartbeats, high blood pressure, high cholesterol and to check the heart's electrical activity [2]. An ECG is very sensitive, different types of noise and interference can corrupt the ECG signal as the real amplitude and duration of the signal can be changed.

1.2 Motivation

At present high rate of heart diseases is facing in the world. This has become the leading cause of death and World Health Organization (WHO) says that more than 17 million people die annually from cardiovascular disease. "The Global Hearts", a new initiative fair from WHO, as it aims to beat back the global measures threat of cardiovascular disease, including heart attacks and stocks to people living in countries with limited resources or in low-income groups [3]. Most of the low and middle-income peoples die from heart attacks and strokes in the world. This death rate can be minimized to a large extent by early detection of the symptoms of cardiovascular diseases. The different types of cardiovascular disease diagnosis is based on the ECG pattern. The cardiovascular diseases are Congestive Heart Failure, Coronary Artery Disease, Heart Attack, Cardiac Dysrhythmia, Ventricular Fibrillation, Tachycardia, Angina, Arthrosclerosis and so many cardiovascular diseases.

1.3 Problem Statement

There are many reasons for the corruption of ECG signal while recording in hospital or some other place due to the power line interference, electromyographic (EMG) interference, base line drift, abrupt shift in base line, electrosurgical noise, instrumentation noise, electrode contact noise etc. In a noise signal, the signal component holds harmonics with different

amplitude and frequency. A major source of interference when one is recording or monitoring the ECG is the electric-power system. Besides providing power to the electrocardiograph itself, power lines are connected to other pieces of equipment and appliances in the typical hospital room or physician's office. There are also power lines in the walls, floor, and ceiling running past the room to other points in the building. These power lines can affect the recording of the ECG and introduce interference at the line frequency in the recorded trace. EMG noise is caused by the contraction of other muscles besides the heart. When other muscles in the vicinity of the electrodes contract, they generate depolarization and repolarization waves that can also be picked up by the ECG. The extent of the crosstalk depends on the amount of muscular contraction (subject movement), and the quality of the probes. Variations in electrode-skin impedance and activities like patient's movements and breathe cause Baseline wander. Abrupt shift noise represents an abrupt shift in baseline due to movement of the patient while the ECG is being recorded. The most important part of ECG signal is QRS complex because heart beat detection depends on it. QRS complex of ECG signal can be definitely distinguished from P wave and T wave because of its high amplitude and peak with long time span. The peak detection difficulties occur when the input electrical signal is disrupted by unwanted noise and interference. Due to these noises the quality of ECG signal can't be ideal so it is needed to improve the quality of required output of ECG signal.

1.4 Review of Related Research Work on Thesis

This section presents an overview of the existing literature in areas related to the work in this thesis on denoising techniques of ECG signal using various methods and QRS detection.

Mostly ECG recording is very sensitive and its affects by different types of noise and it changes the amplitude and duration of the signal. In literature review, it has been seen that mostly ECG signals are affected by white noise, colored noise, electrode movement noise, muscle artifact noise, baseline wander, composite noise, electromyographic (EMG) noise, abrupt noise and power line interference [4],[5]. These noises create more complication for diagnosis of the ECG signal. Some of the authors have solved this problem by proposing different algorithms for removal of noise [6]-[8]. In [4], the authors have found the performance of adaptive NLMS filter better than adaptive LMS filter. But in practical way, the performance parameters such as SNR, MSE, PRD have shown lowest values than others. The proposed algorithm with Discrete Wavelet Transform (DWT) in [5] have shown good results based on WGN noise and Poisson noise using several measureable parameters, such as wavelet filters [Daubechies2 (DB2),

Symlets (Sym2), Coiflet (coif2), DMeyer (demey), BiorSplines (bior2.2), Reverse Bior (rbio2.2)]. But performance parameters have not been measured. A.D. Jeyarani *et al.* have applied the different filters like band-stop filter, low pass filter, high pass filter for removing Power line Interference, Electromyographic noise (EMG noise), Baseline wander from noisy ECG signal [6]. Y. Lian *et al* proposed algorithm based on linear FIR filter with Recursive Running Sum (RRS) filters [7]. They have considered 50 or 60 HZ power line noise for a high-resolution ECG signal sampling at 600Hz. This algorithm have shown low resolution smooth signal. A. Mirza *et al* have proposed enhanced adaptive impulsive noise cancellation technique using State Space Recursive Least Square (SSRLS) algorithm [8]. This algorithm has used only MSE for performance of proposed algorithm and shown lowest results than others. M. Butt *et al*. proposed SSRLS based filter for removing only powerline interference noise from ECG signal and also didn't measure any performance parameters [9].

ECG consists of three wave components and they are P wave, QRS complex and T wave. The most important part of ECG signal is QRS complex because heart beat detection depends on it. QRS complex of ECG signal can be definitely distinguished from P wave and T wave because of its high amplitude and peak with long time span. Many researchers have developed methodology or algorithm for the use of R peak / QRS complex detection. The peak detection difficulties occur when the input electrical signal is disrupted by unwanted noise and interference [2]. M. Elgendi *et al* have improved QRS detection algorithm using dynamic thresholds which has shown 97.5% sensitivity and 99.9% positive predictivity [10]. J. Pan *et al* also developed an algorithm for QRS detection which was based on slope, amplitude, and width [11]. But the algorithm failed to properly detect only 0.675 percent of the beats. R. G. Lee *et al* developed a new QRS detection algorithm [12]. This algorithm has enhanced the accuracy of R wave detection by reverse R wave. They have not shown other detection parameter values such as sensitivity, specification, precision. Q. Xue *et al* developed a neural-network-based adaptive matched filtering for QRS detection. The main focus is put on low computational complexity and low signal-to-noise ratio. It is tested on several signals of MIT/BIH database, which obtained sensitivity above 90% in QRS detection. V.S. Chouhan *et al*. developed a methodology to detect of QRS complexes in 12-lead ECG using adaptive quantized which has Differentiation at preprocessing stage and Dynamic threshold to detect R peaks [14]. It also needs complex computation. However, the detection parameter have not been improved for detection of ECG signal. Therefore the development of robust method of

ECG signal detection still requires the improvement in noise elimination as well as in QRS detection.

1.5 Objectives

The fundamental objective of this thesis is,

(i) To propose improved de-noising methods of ECG signals, more specifically: (a) designing linear phase FIR low pass filters using Remez exchange algorithm, (b) designing of FIR filter with arbitrary magnitude response, (c) designing an FIR low pass filter using window method, (d) designing moving average filter, (e) designing moving average weighted window filter, (f) designing forward difference quotient and amplitude thresholding based algorithm.

(ii) Various noises such as baseline wander, composite noise, electromyography (EMG) noise, abrupt noise and power line interference will be investigated in this case.

(iii) The performance of algorithms will be compared with the existing de-noising algorithms in terms of mean square error (MSE), signal-to-noise ratio (SNR) and correlation coefficients values for different noise removal methods.

(iv) For comparison between the ECG signal and filtered signal by proposed algorithm, three processes such autocorrelation, cross-correlation and power spectral density (PSD) will be considered.

(v) To propose QRS detection algorithm for noise filtered ECG signal.

(vi) Propose detection algorithm will be compared in terms of accuracy, sensitivity, specificity, precision.

1.6 Organization of Thesis

This section provides a summary of the all the chapters covered in this thesis.

Chapter-1:

This chapter gives the introduction to the thesis, the problem description, objective and also detail of report layout of the thesis report.

Chapter-2:

This chapter gives the basic knowledge of ECG and its history. Here types of ECG, acquisition process of ECG, different waves of ECG such as P, U, QRS complex, T waves;

different types of ECG electrodes and their descriptions are described. Different types of noises which affects the ECG signal and previous related works are also described.

Chapter-3:

This chapter presents the brief description of six algorithms which are to be employed in this thesis to perform the noise cancellation. It also gives the overview of the process and operations of the algorithm.

Chapter-4:

In this chapter, a description of two algorithms is given which will be used for QRS detection. It gives the overview of the process and operation of the algorithm.

Chapter-5:

In this chapter, the analysis and simulation results of the algorithm are described. It also gives the figures and wave shapes of removing of high frequency noise from ECG signal. Finally, the algorithm result, discussion, verification and comparison study will be presented.

Chapter-6:

This chapter will provide the conclusion and future research. It also gives the detail of the thesis goal, its achievement and what has been concluded after completion this thesis.

References:

The list of information gathered from books, papers, database, journals and internet sites.

Chapter 2

Background and Related Work

2.1 Introduction

For analyzing of ECG signal, it is important to understand the physiology of ECG. In this chapter, at first a brief introduction of ECG is given. Then a detail discussion on various noises in ECG signal will be given. Finally, a review on previous related work will be discussed.

2.2 Electrocardiography

Electrocardiography is the process of recording of electrical activity of the heart. An electrocardiogram — abbreviated as EKG or ECG — is a test that measures the electrical activity of the heartbeat. With each beat, an electrical impulse (or “wave”) travels through the heart. This wave causes the muscle to squeeze and pump blood from the heart. A normal heartbeat on ECG will show the timing of the top and lower chambers.

The right and left atria or upper chambers make the first wave called a “P wave" — following a flat line when the electrical impulse goes to the bottom chambers. The right and left bottom chambers or ventricles make the next wave called a “QRS complex." The final wave or “T wave” represents electrical recovery or return to a resting state for the ventricles [15]. The different peaks P, Q, R, S, T, and U are noticeable at these stages, as observed in Figure 2.1. If ECG is properly analyzed, can provide us information regarding various diseases related to heart. Moreover, visual analysis cannot be relied upon. This calls for computer-based techniques for ECG analysis.

An ECG gives two major kinds of information. First, by measuring time intervals on the ECG, a doctor can determine how long the electrical wave takes to pass through the heart. Finding out how long a wave takes to travel from one part of the heart to the next shows if the electrical activity is normal or slow, fast or irregular. Second, by measuring the amount of electrical activity passing through the heart muscle, a cardiologist may be able to find out if parts of the heart are too large or are overworked.

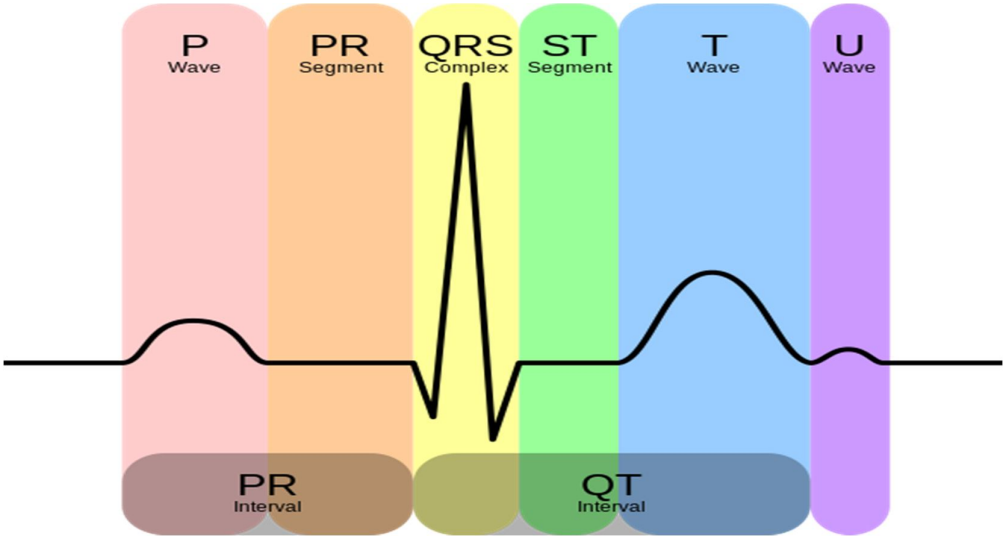

Figure 2.1: A General ECG waveform with P, Q, R, S, T and U peak.

2.2.1 Uses of ECG

An ECG is often used alongside other tests to help diagnose and monitor conditions affecting the heart. It can be used to investigate symptoms of a possible heart problem, such as chest pain, suddenly noticeable heartbeats (palpitations), dizziness and shortness of breath [3], [15].

An ECG can help detect:

- Arrhythmias – where the heart beats too slowly, too quickly, or irregularly.
- Coronary heart disease – where the heart's blood supply is blocked or interrupted by a build-up of fatty substances.
- Heart attacks – where the supply of blood to the heart is suddenly blocked.
- Cardiomyopathy – where the heart walls become thickened or enlarged.

A series of ECGs can also be taken over time to monitor a person already diagnosed with a heart condition or taking medication known to potentially affect the heart.

2.2.2 Types of ECG

There are three main types of ECG:

- a resting ECG – carried out while you're lying down in a comfortable position
- a stress or exercise ECG – carried out while you’re using an exercise bike or treadmill

- an ambulatory ECG – the electrodes are connected to a small portable machine worn at your waist so your heart can be monitored at home for one or more days

The type of ECG recommended for you will depend on your symptoms and the heart problem suspected. For example, an exercise ECG may be recommended if your symptoms are triggered by physical activity, whereas an ambulatory ECG may be more suitable if your symptoms are unpredictable and occur in random, short episodes.

2.2.3 Recording of ECG signal

- There are several different ways an ECG can be carried out. Generally, the test involves attaching a number of small, sticky sensors called electrodes to patient arms, legs and chest. These are connected by wires to an ECG recording machine.
- Patient don't need to do anything special to prepare for the test. They can eat and drink as normal beforehand.
- Before the electrodes are attached, they will usually need to remove their upper clothing, and sometimes their chest may need to be shaved or cleaned. Once the electrodes are in place, they may be offered a hospital gown to cover themselves.
- The test itself will normally only last a few minutes, and they can usually go home soon afterwards or return to the ward if they're already staying in hospital.

2.2.4 Different ECG Waves

- **P Wave**
  - The P wave [Fig. 2.2] is the first positive deflection on the ECG
  - It represents atrial depolarization

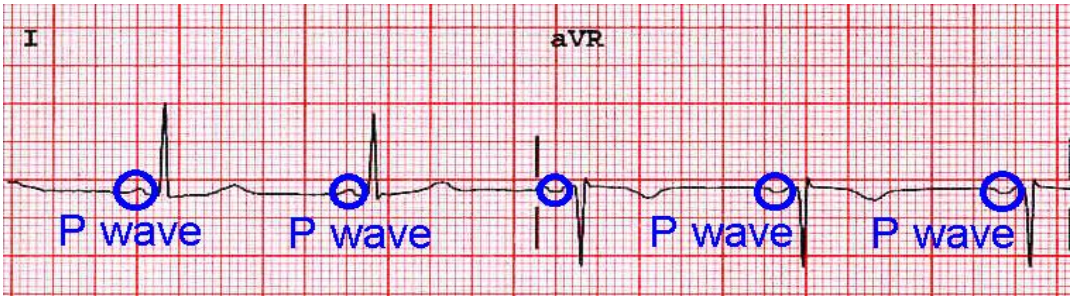

Figure 2.2: P-waves in ECG signal.

Morphology

- Smooth contour
- Monophasic in lead II
- Biphasic in V1

Axis

- Normal P wave axis is between 0° and +75°
- P waves should be upright in leads I and II, inverted in aVR

Duration

- < 120 ms
- Amplitude
- < 2.5 mm in the limb leads,
- < 1.5 mm in the precordial leads

➢ **QRS Complex**

The QRS complex represents in Figure 2.3 the rapid depolarization of the right and left ventricles. The ventricles have a large muscle mass compared to the atria, so the QRS complex usually has a much larger amplitude than the P-wave.

If the QRS complex is wide (longer than 120 ms) it suggests disruption of the heart's conduction system, such as in Left bundle branch block (LBBB), Right bundle branch block (RBBB), or ventricular rhythms such as ventricular tachycardia. Metabolic issues such as severe hyperkalemia, or TCA overdose can also widen the QRS complex. An unusually tall QRS complex may represent left ventricular hypertrophy while a very low-amplitude QRS complex may represent a pericardial effusion or infiltrative myocardial disease.

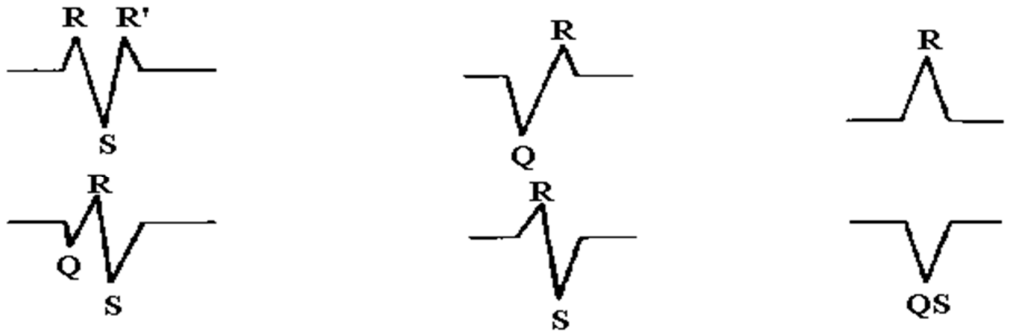

Figure 2.3: QRS complex in ECG signal.

- **T Wave**

  - The T wave [Fig. 2.4] is the positive deflection after each QRS complex
  - It represents ventricular repolarization
  - Upright in all leads except aVR and V1
  - Amplitude < 5mm in limb leads, < 15mm in precordial leads
  - Duration 160ms

Figure 2.4: T-waves in ECG signal.

- **U Wave**

The U wave as shown in Fig. 2.4 is a small (0.5 mm) deflection immediately following the T wave, usually in the same direction as the T wave. It is best seen in leads V2 and V3. The source of the U wave is unknown. Three common theories regarding its origin are:

- Delayed repolarization of Purkinje fibres
- Prolonged repolarization of mid-myocardial “M-cells”
- After-potentials resulting from mechanical forces in the ventricular wall

Features of Normal U waves

- The U wave normally goes in the same direction as the T wave
- U -wave size is inversely proportional to heart rate: the U wave grows bigger as the heart rate slows down
- U waves generally become visible when the heart rate falls below 65 bpm
- The voltage of the U wave is normally < 25% of the T-wave voltage: disproportionally large U waves are abnormal
- Maximum normal amplitude of the U wave is 1-2 mm

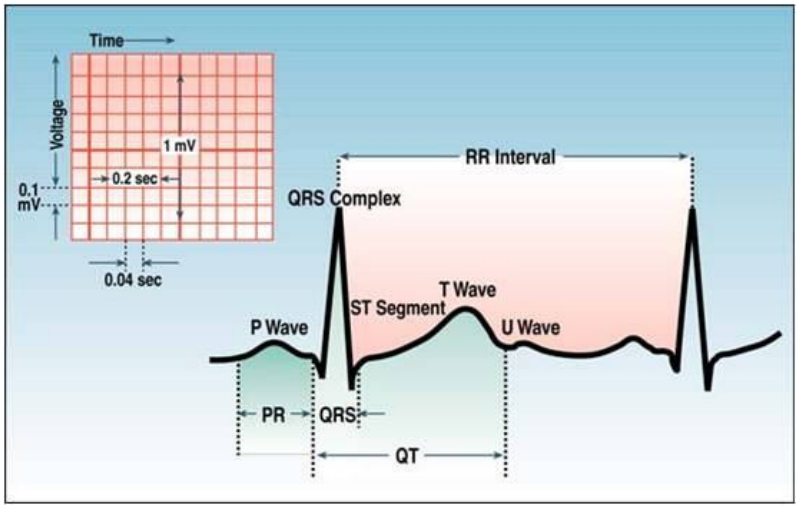

Figure 2.5: U-waves in ECG signal.

2.2.5 ECG Register

An electrocardiogram (ECG or EKG) is a register of the heart's electrical activity. Just like skeletal muscles, heart muscles are electrically stimulated to contract. This stimulation is also called *activation* or *excitation*. Cardiac muscles are electrically charged at rest. The inside of the cell is negatively charged relative to the outside (resting potential). If the cardiac muscle cells are electrically stimulated, they depolarize (the resting potential changes from negative to positive) and contract. The electrical activity of a single cell can be registered as the action potential [15]. As the electrical impulse spreads through the heart, the electrical field changes continually in size and direction. The ECG is a graph of these electrical cardiac signals.

2.2.6 The Electric Discharge of the Heart

Sinoatrial node (SA node) contains the fastest physiological pacemaker cells of the heart; therefore, they determine the heart rate [16]. First the atria depolarize and contract. After that the ventricles depolarize and contract. The electrical signal between the atria and the ventricles goes from the sinus node via the atria to the AV-node (atrioventricular transition) to the His bundle and subsequently to the right and left bundle branches, which end in a dense network of Purkinje fibers. The depolarization of the heart results in an electrical force which has a direction and magnitude; an electrical vector. This vector changes every millisecond of the depolarization. In the animation vectors for atrial depolarization, ventricular depolarization and ventricular repolarization are shown in Fig. 2.6.

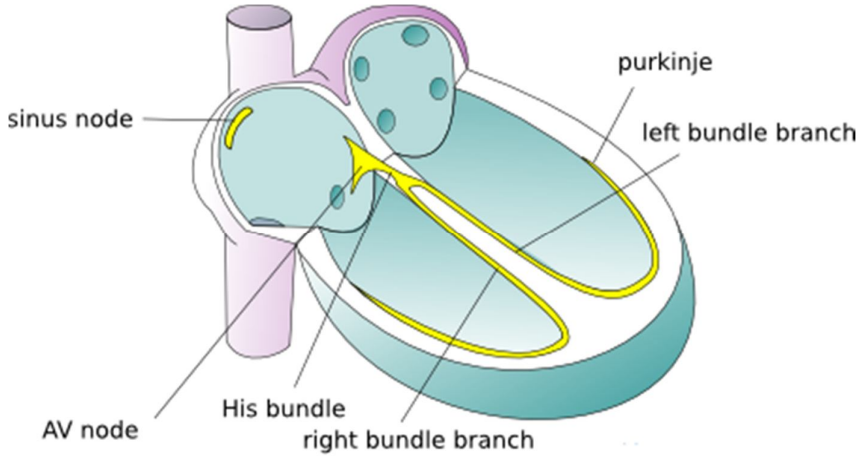

Figure 2.6: The conduction system of the heart.

2.2.7 The ECG Electrodes

Electrical activity going through the heart can be measured by external (skin) electrodes. The electrocardiogram (ECG) registers these activities from electrodes which have been attached onto different places on the body as shown in Fig. 2.7. In total, twelve leads are calculated using ten electrodes.

The ten electrodes are:

- **The four extremity electrodes:**
  - LA - left arm
  - RA - right arm

- N - neutral, on the right leg (= electrical earth, or point zero, to which the electrical current is measured)
- F - foot, on the left leg

It makes no difference whether the electrodes are attached proximal or distal on the extremities. However, it is best to be uniform in this. (e.g., do not attach an electrode on the left shoulder and one on the right wrist).

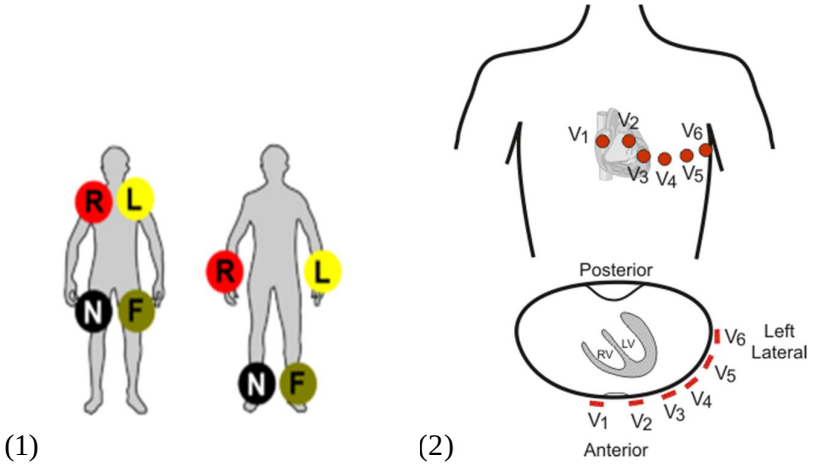

(1) (2)

Figure 2.7: (1) The limb leads and (2) The chest leads [4]

- **The six chest electrodes:**
  - V1 - placed in the 4th intercostal space, right of the sternum
  - V2 - placed in the 4th intercostal space, left of the sternum
  - V3 - placed between V2 and V4
  - V4 - placed 5th intercostal space in the nipple line. Official recommendations are to place V4 under the breast in women.
  - V5 - placed between V4 and V6
  - V6 - placed in the midaxillary line on the same height as V4 (horizontal line from V4, so not necessarily in the 5th intercostal space).

With the use of these 10 electrodes, 12 leads can be derived. There are 6 extremity leads and 6 precordial leads.

2.2.8 The Extremity Leads

The extremity leads position as shown in Figure 2.8, described are:

- **I** from the right to the left arm.
- **II** from the right arm to the left leg.
- **III** from the left arm to the left leg.

An easy rule to remember: lead **I** + lead **III** = lead **II** This is done with the use of the height or depth, independent of the wave (QRS, P of T). Example: if in lead I, the QRS complex is 3 mm in height and in lead III 9mm, the height of the QRS-complex in lead II is 12mm.

Other extremity leads are:

- **aVL** points to the left arm.
- **aVR** points to the right arm.
- **aVF** points to the feet.

The ‘a’ stands for "augmented" and ‘V’ for "voltage".

(aVR + aVL + aVF = 0)

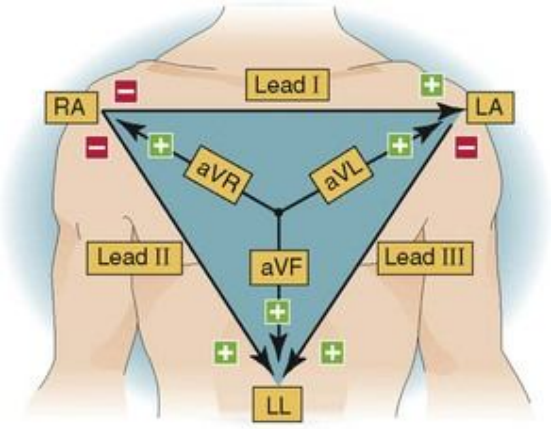

Figure 2.8: Connection of extremity leads.

2.2.9 The Chest Leads

The precordial, or chest leads, **(V1, V2, V3, V4, V5 and V6)** 'observe' the depolarization wave in the frontal plane. *Example*: V1 is close to the right ventricle and the right atrium. Signals in these areas of the heart have the largest signal in this lead. V6 is the closest to the lateral wall of the left ventricle.

2.2.10 ECG Variants

Besides the standard 12 lead ECG a couple of variants are in use:

- The **3 channel ECG** uses 3 or 4 ECG electrodes. Red is on the right, yellow on the left arm, green on the left leg ('sun shines on the grass') and black on the right leg. These basic leads yield enough information for rhythm-monitoring. For determination of ST elevation, these basic leads are inadequate as there is no lead that gives (ST) information about the anterior wall. ST changes registered during 3-4 channel ECG monitoring should prompt acquisition of a 12 lead ECG.
- The **5 channel ECG** uses 4 extremity leads and 1 precordial lead. This improves ST segment accuracy, but is still inferior to a 12 lead ECG [17], [18].
- In **vector electrocardiography** the movement of electrical activity of the P, QRS and T wave is described. Additional X, Y and Z leads are recorded. Vector electrocardiography is rarely used nowadays, but is sometimes useful in a research setting.
- In **body surface mapping** several arrays are used to accurately map the cardiac electrical wave front as it moves over the body surface. With this information the electrical activity of the heart can be calculated. This is sometimes used in a research setting.

2.2.11 Ladder Diagram

A ladder diagram is a diagram as shown in Fig. 2.9 to explain arrhythmias that shows the presumed origin of impulse formation and conduction in the heart. The figure shows a simple ladder diagram for normal sinus rhythm, followed by AV-nodal extra systole. The origin of impulse formation (sinus node for the first two beats and AV junction for the third beat) and the conduction in the heart are shown.

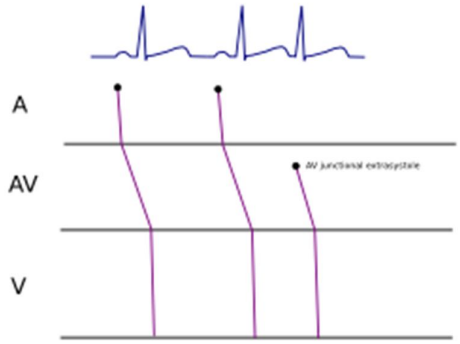

Figure 2.9: A ladder diagram where, A = atrial, AV = AV node, V = ventricles.

2.2.12 Color Coding of the ECG Leads

Two systems for ECG lead color coding are used: the AHA (*American Heart Association*) system and the IEC (*International Electrotechnical Commission*) system:

	AHA (*American Heart Association*)		**IEC (*International Electrotechnical Commission*)**	
Location	**Inscription**	**Color**	**Inscription**	**Color**
Right Arm	**RA**	White	**R**	Red
Left Arm	**LA**	Black	**L**	Yellow
Right Leg	**RL**	Green	**N**	Black
Left Leg	**LL**	Red	**F**	Green
Chest	**V1**	Brown/Red	**C1**	White/Red
Chest	**V2**	Brown/Yellow	**C2**	White/Yellow
Chest	**V3**	Brown/Green	**C3**	White/Green
Chest	**V4**	Brown/Blue	**C4**	White/Brown
Chest	**V5**	Brown/Orange	**C5**	White/Black
Chest	**V6**	Brown/Purple	**C6**	White/Violet

2.3 Overview of Basic Noises in ECG Signal

Electrocardiographic (ECG) signals may be corrupted by various kinds of noise. Typical examples are:

- power line interference
- electrode contact noise
- motion artifacts
- muscle contraction (Electromyogram, EMG)
- baseline drift and ECG amplitude modulation with respiration
- instrumentation noise generated by electronic devices used in signal processing, and
- electrosurgical noise,

and other, less significant noise sources [19].

2.3.1 Power-Line Interference Noise

Power line interference consists of 50/60 Hz pickup and harmonics which can be modeled as sinusoids and combination of sinusoids. A major source of interference when one is recording or monitoring the ECG is the electric-power system. Besides providing power to the electrocardiograph itself, power lines are connected to other pieces of equipment and appliances in the typical hospital room or physician's office. There are also power lines in the walls, floor, and ceiling running past the room to other points in the building. These power lines can affect the recording of the ECG and introduce interference at the line frequency in the recorded trace, as illustrated in figure. Such interference appears on the recordings as a result of two mechanisms, each operating singly or in some cases, both operating together.

Electric-field coupling between the power lines and the electrocardiograph and the patient is a result of electric fields surrounding main power lines and the power cords connecting different pieces of apparatus to electric outlets. These fields can be present even when the apparatus is not turned on, because current is not necessary to establish the electric field. These fields couple into the patient, the lead wires and the electrocardiograph [17].

Typical parameters:

- Frequency content-60 Hz(fundamental) with harmonics
- Amplitude-up to 50 percent of peak-to-peak ECG amplitude

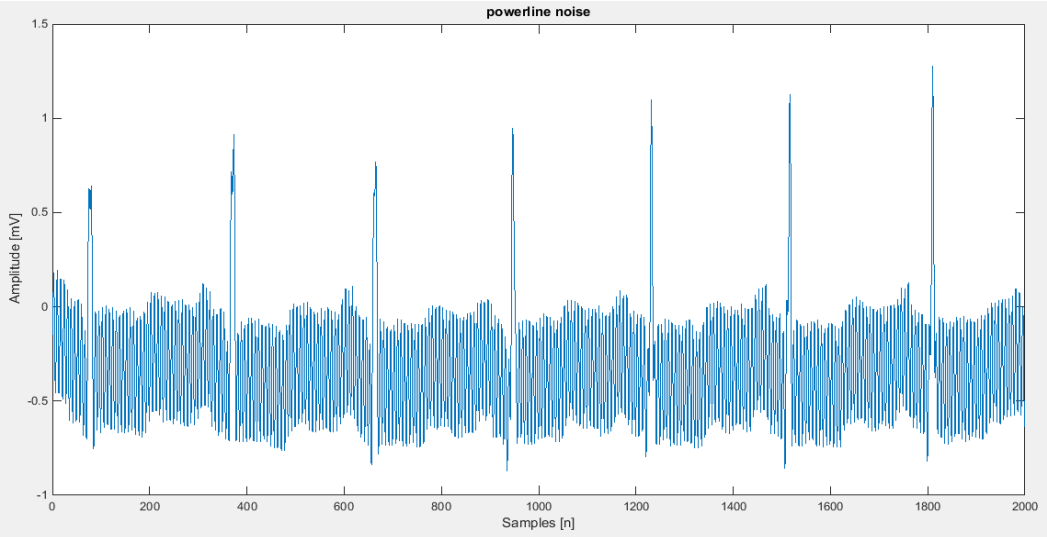

Figure 2.10: ECG signal corrupted by Power line noise

2.3.2 Electromyogram (EMG) noise

EMG noise is caused by the contraction of other muscles besides the heart. When other muscles in the vicinity of the electrodes contract, they generate depolarization and repolarization waves that can also be picked up by the ECG. The extent of the crosstalk depends on the amount of muscular contraction (subject movement), and the quality of the probes.

It is well established that the amplitude of the EMG signal is stochastic (random) in nature and can be reasonably modeled by a Gaussian distribution function [18]. The mean of the noise can be assumed to be zero; however, the variance is dependent on the environmental variables and will change depending on the conditions. Certain studies have shown that the standard deviation of the noise is typically 10% of the peak-to-peak ECG amplitude [19]. While the actual statistical model is unknown, it should be noted that the electrical activity of muscles during periods of contraction can generate surface potentials comparable to those from the heart, and could completely drown out the desired signal. The effects of typical EMG noise can be observed in the ECG signal shown in Figure 2.12, and is particularly problematic in the areas of the P and T complexes.

Typical parameters:

- Standard Deviation- 10 percent of peak-to-peak ECG amplitude
- Duration-50 ms
- Frequency Content-dc to 10 000 Hz

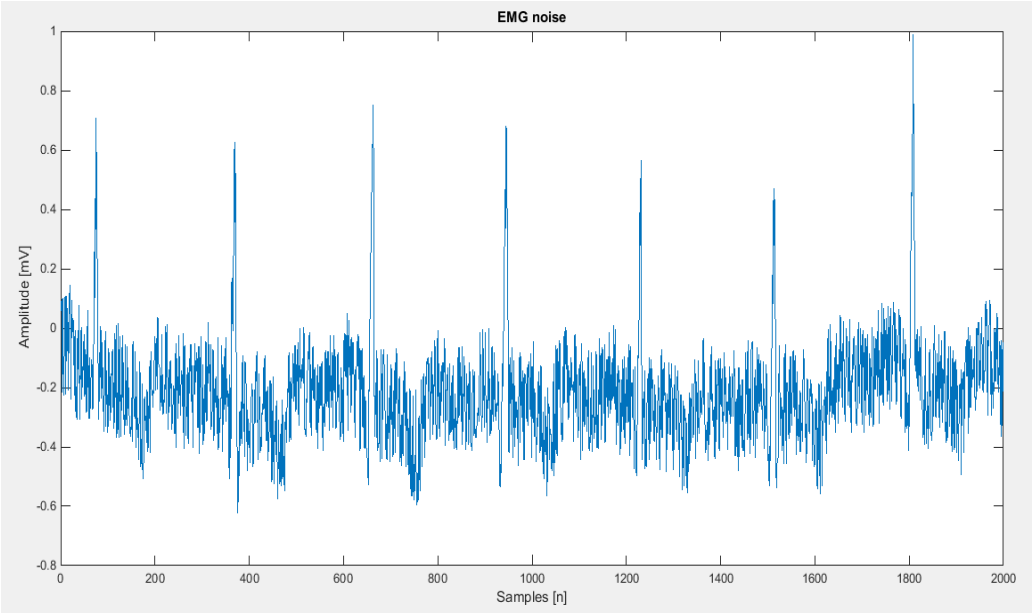

Figure 2.11: ECG signal corrupted by Electromyogram (EMG) noise.

2.3.3 Baseline Drift Noise

Variations in electrode-skin impedance and activities like patient's movements and breathe cause Baseline wander [20], [21]. Baseline wander disturbance is especially dominant in exercise electrocardiography, and in ambulatory and Holter monitoring. The range of frequency in which baseline wander is dominant is typically less than 1.0 Hz, however for exercise ECG this range can be wider [21]. It is caused by changes in electrode-to-skin polarization voltages, or by electrode movement, or by respiration movement or by body movement. In wandering baseline, the isoelectric line change positions. One possible cause is the movement of cables. Patient movement, dirty lead wires/electrodes, and a variety of other things can cause this as well. Fig. 2.13. Illustrates the ECG signal with significant baseline wander.

Typical parameters:

- Amplitude variation- 15 percent of peak-to-peak (p-p) ECG amplitude
- Baseline variation-15 percent of p-p ECG amplitude variation at 0.15 to 0.3 Hz

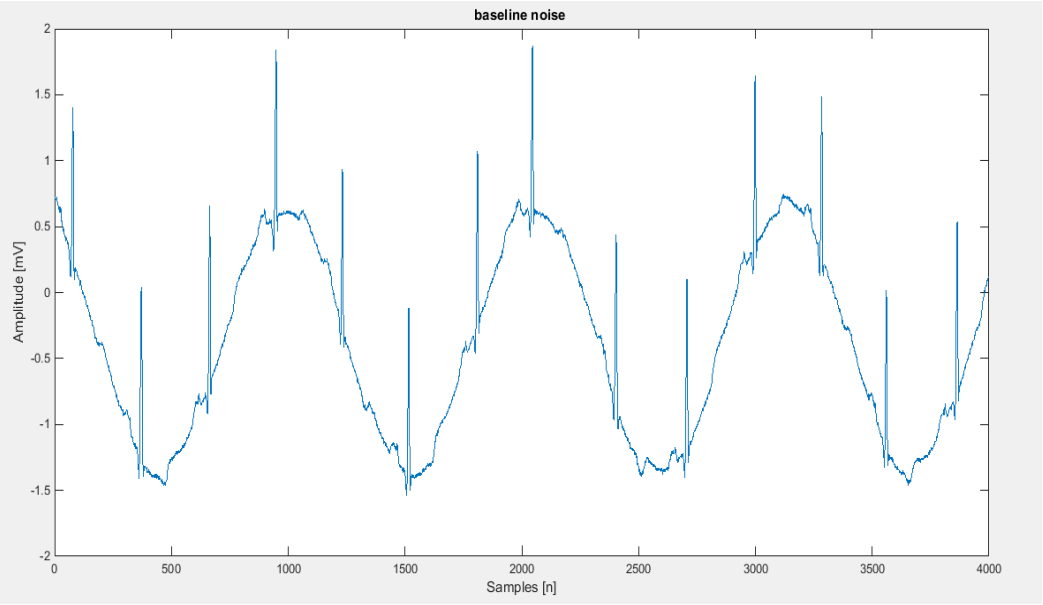

Figure 2.12: ECG signal corrupted by Baseline Drift noise.

2.3.4 Abrupt Baseline Shift Noise

This type of interference represents an abrupt shift in baseline due to movement of the patient while the ECG is being recorded as shown in Fig. 2.14.

Typical parameters:

- Duration-1 s
- Amplitude-maximum recorder output
- Frequency-60 Hz
- Time constant-about 1s

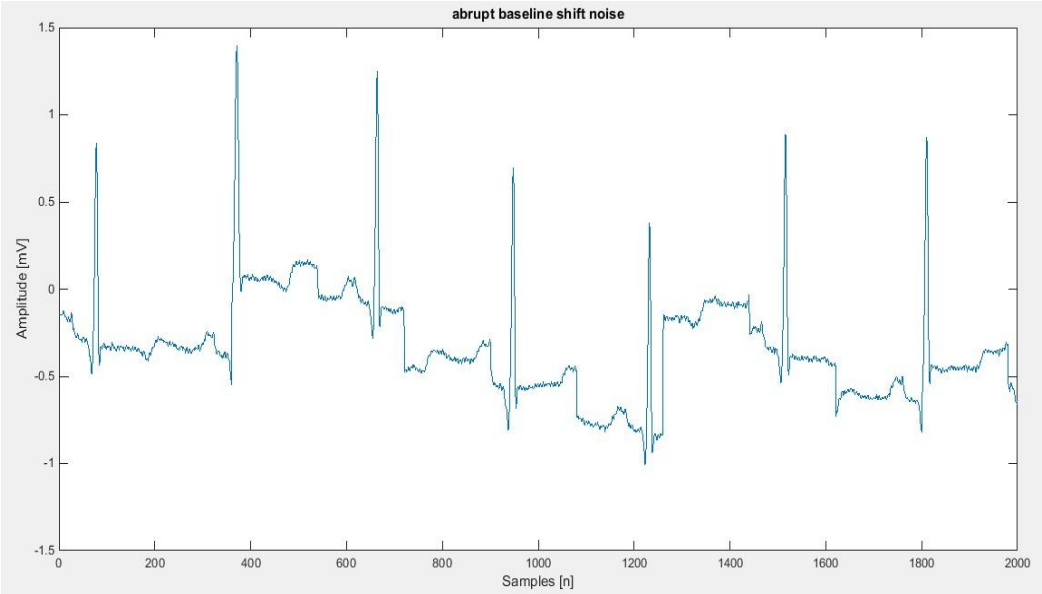

Figure 2.13: ECG signal corrupted by abrupt baseline shift noise.

2.3.5 Electrosurgical Noise

Electrosurgical noise completely destroys the ECG and can be represented by a large amplitude sinusoid with frequencies approximately between 100 kHz and 1 MHz. Since the sampling rate of an ECG signal is 250 to 1000Hz, an aliased version of this signal would be added to the ECG signal. The amplitude, duration, and possibly the aliased frequency should be variable [19].

Typical parameters:

- Amplitude-200 percent of peak-to-peak ECG amplitude
- Frequency Content-Aliased 100 kHz to 1 MHz Duration-1-10 **s**

2.3.6 Noise Generated by Electronic Devices Used in Signal Processing

Artifacts generated by electronic devices in the instrumentation system can't be corrected by a *QRS* detection algorithm. The input amplifier has saturated and no information about the ECG can reach the detector. In this case an alarm must sound to alert the ECG technician to take corrective action [19].

2.4 Summary

In this chapter, basic topics of ECG is discussed which is very important in analysis of ECG signal. It also discusses how ECG signal is generated and how to acquire it using electrodes. Various ECG waves are also discussed. Various noises in ECG signal such as power line interference, EMG noise, baseline shift, abrupt shift in base line, electrosurgical noise etc. are also mentioned in this chapter. This chapter outlines the literature related to the ECG signal denoising and QRS detection. From these literatures, there are some lack of novelty work. We have tried to find the problem statement of ECG diagnosis and QRS detection.

Chapter 3

Proposed Denoising Algorithms

3.1 Introduction

The real ECG signal from recorded of human body is always corrupted by several sources of noises such as being EMG (electromyogram) signal (a high frequency signal related to muscle activity), the BLW (the baseline wandering: a low frequency signal caused mainly by the breathing action), the electrode motion (usually represented by a sharp variation of the baseline). Different works had been established on denoising algorithms. In this chapter, some denoising algorithms will be discussed for removal of noise from corrupted ECG signal.

3.2 Noise Elimination methodology

We have proposed some algorithm for noise elimination of ECG signal which is described as below:

3.2.1 Algorithm-1/ FIR low pass filter using Remez exchange algorithm

The Remez exchange algorithm is based on optimal method where the concept of equiripple passband and stopband. Consider the lowpass filter freqiecy response depected in Figure 3.1. In the passband, the practical response oscillates between $1-\delta_p$ and $1-\delta_p$. In the stopband the filter response lies between 0 and δ_s. The difference between the ideal filter and the practical response can be viewed as an error function:

$$E(\omega) = W(\omega)|H_D(\omega) - H(\omega)| \tag{3.1}$$

Where $H_D(\omega)$ is the ideal or desired response and $W(\omega)$ is a weight function that allows the relative error of approximation between different bands to be defines. In the optimal method, the objective is to determines the filter coefficients, h(n), such, such that the value of the maximum weight error, $|E(\omega)|$, is minimized in the passband and stopband. Mathematically, this may be expressed as $min[max]|E(\omega)|$ over the passbands and stopbands.

For a given set of filter specifications, the locations of extremal frequencies, apart from those at band edges $\left(f = f_p \text{ and } f = {}^{F_S}/_{2}\right)$, are not priori. This the main problem in the

optimal method is to find the locations f the extremal frequencies. A powerful technique which employs the Remez exchange algorithm to find the extremal frequencies.

For a given set of specifications (that is passband edge frequencies, N, and the ratio between the passband and stopband ripples) the optimal method involves the following key steps

- Use the Remez exchange algorithm to find the optimum set of extremal frequencies;
- Determine the frequency response using extremal frequencies;
- Obtain the impulse response coefficients.

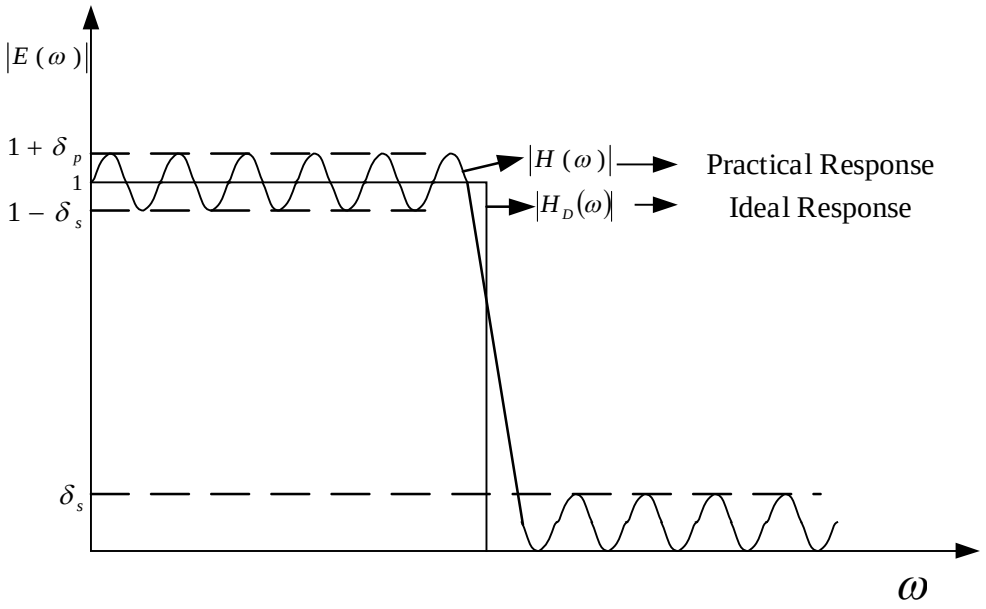

Figure 3.1: Frequency response of an optimal filter (Remez exchange algorithm).

For the above key steps, we consider to design linear phase FIR low pass filters using Remez exchange algorithm required to satisfy the following specifications:

Passband frequency	0-55Hz
Passband ripple	3dB
Stopband ripple	20dB
Stopband frequency	50-55Hz
Sampling frequency (F_s)	200Hz
Normalize frequency $F_N = {}^{F_s}/_{2}$	100 Hz

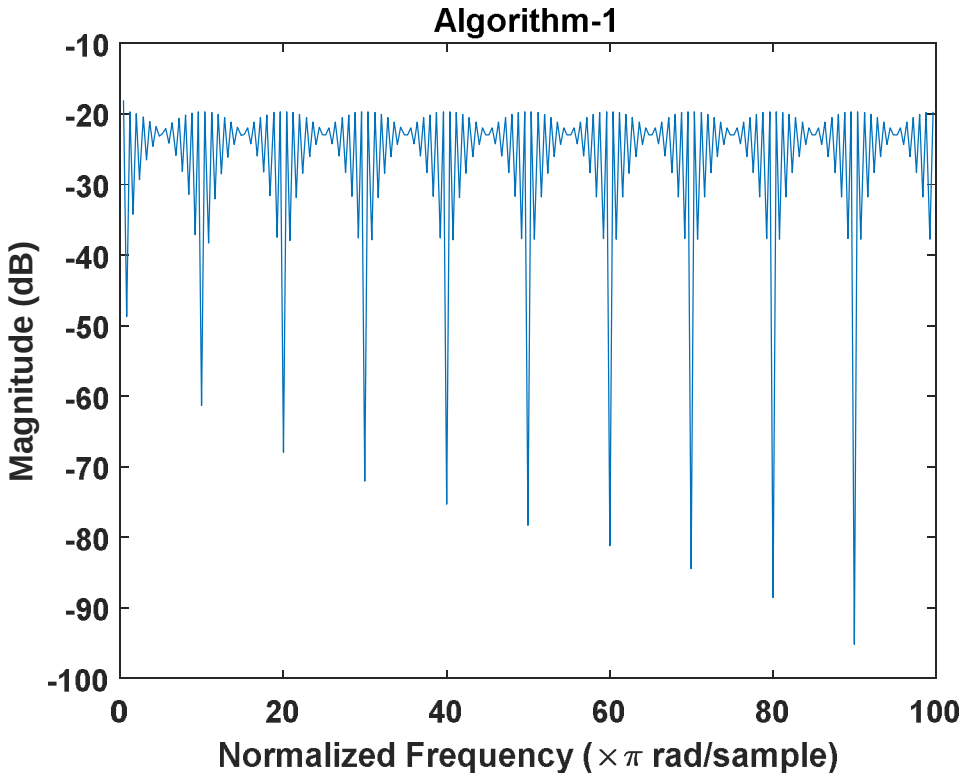

Figure 3.2: Frequency response of designed low pass FIR filter.

Estimate of filter length can be determined by using Remez exchange algorithm [2]. This require by need to calculate of passband and stopband deviation by [2]:

$$\delta_p = 2 \times \frac{10^{\frac{A_p}{20}} - 1}{10^{\frac{A_p}{20}} + 1}, \delta_s = 10^{-\frac{A_s}{20}} \quad (3.2)$$

Where $A_p$and A_s are the passband and stopband ripples respectively, in dB.

The input parameters are setting for optimal design program to obtain the coefficients of filter length and the frequency response of filter coefficient h[n] as shown in Figure 3.2.

3.2.2 Algorithm-2/ Frequency Sampling filter

Design of FIR filter with arbitrary magnitude response is described below.

A prerequisite FIR filter that the desired frequency response $(H(k))$ characteristics depicted as specified requirements:

Passband frequency	0-100Hz
Transition band	5 Hz

Passband ripple	0 dB
Stopband ripple	0 dB
Sampling frequency (F_s)	200 Hz
Normalize frequency $F_N = {F_s}/{2}$	100 Hz
Filter length, (N).	22

From the specification table can be designed as where the band edges frequency must have normalized to the half of the sampling frequency (The vector of normalized band edge frequencies point $f_k = \left({f_d}/{F_N}\right)$ and magnitude of frequency sample points$(|H(k)|)$ as shown in Table 3.1. A sample of the optimum values of transition band frequency samples is given in Table 3.1 for N=22. In the table, the band width refers to the number of frequency samples in the passband of the filter.

Table 3.1: Optimum transition band frequency samples for lowpass frequency sampling filters for N=22.

k	**f(k)**	**H(k)**	**k**	**f(k)**	**H(k)**
0	0	0.15	21	1	0
1	0.05	0.15	20	0.95	0
2	0.1	0.1	19	0.90	0
3	0.15	0.1	18	0.85	0
4	0.20	0.1	17	0.80	0
5	0.25	0.1	16	0.75	0
6	0.30	0.1	15	0.70	0
7	0.35	0.1	14	0.65	0
8	0.40	0.1	13	0.60	0.1
9	0.45	0.1	12	0.55	0.1
10	0.5	0.1	11	0.5	0.1

In the most cases, the values of the transition band frequency samples normally lie in the following ranges for one transition frequency sample which is depicted as Figure 3.3 (a):

$$0.1 \leq T_1 \leq 0.15$$

$$0 \leq T_2 \leq 0.1$$

From the specifications, the number of frequency samples, N=22. The sample numbers corresponding to the passband and stopband edges frequencies are 2 and 14, respectively. The transition band samples, M=2 and M=12. Form Table 3.1, is 0.1. Thus, the frequency samples for the ideal magnitude-frequency response are given the filter are given by:

$$|H(k)| = \begin{cases} 0.15 & for\ k = 0,1 \\ 0.1, for\ k = 2, \ldots .12 \\ 0, & for\ k = 13 \ldots 21 \end{cases}$$

The impulse response or filter coefficients $h(n)$ can be obtained as the inverse DFT of the frequency sample

$$h(n) = \frac{1}{N}\sum_{k=0}^{N-1} H(k)e^{j(2\pi/N)nk} \tag{3.3}$$

where $H(k), k = 0,1, \ldots, N-1$ samples of the ideal or target frequency response are.

We have chosen N=22 and the impulse response is

$$h(n) = \frac{1}{21}\sum_{k=0}^{21} H(k)e^{j(2\pi/N)nk}$$

$$h(n) = \frac{1}{21}\left[H(0)e^{j(2\pi/21)n*0} + H(1)e^{j(2\pi/21)n*1} + \cdots \ldots + H(21)e^{j(2\pi/21)n*21}\right]$$

Using the above parameters as an input, the coefficients h(n) were obtained and h(n) are listed in Table 3.2 and the filter spectrum is shown is Figure 3.3(b)and 3.3(c) represents the frequency response of frequency sampling filter.

Table 3.2: The impulse response h(n) or filter coefficients of frequency sampling filter (N=21, fs=200)

h(n)			h(n)
h[0]=	0.000286368367763920	0.000286368367763920	=h[21]
h[1]=	5.68354048174746e-05	5.68354048174745e-05	=h[20]
h[2]=	-0.000196969733948250	-0.000196969733948249	=h[19]
h[3]=	0.00136009302334421	0.00136009302334421	=h[18]
h[4]=	0.00117772018904162	0.00117772018904162	=h[17]
h[5]=	-0.00142159669903109	-0.00142159669903109	=h[16]

h[6]=	0.00444118010460193	0.00444118010460193	=h[15]
h[7]=	0.00627677638105475	0.00627677638105475	=h[14]
h[8]=	-0.00788416573826666	-0.00788416573826666	=h[13]
h[9]=	0.00745261427796247	0.00745261427796248	=h[12]
h[10]=	0.0562285227793611	0.0562285227793611	=h[11]

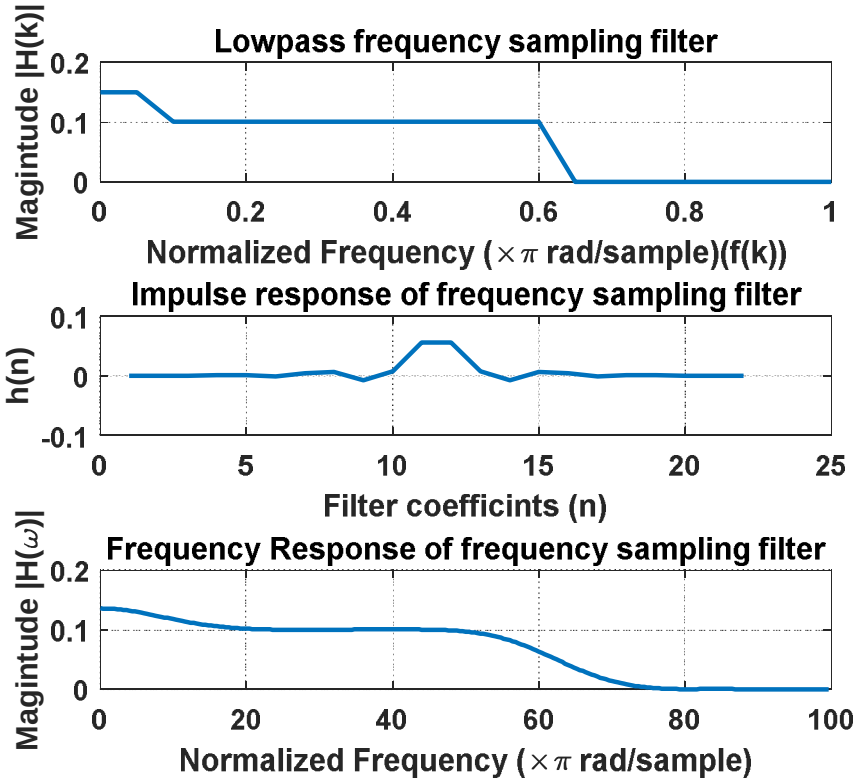

Figure 3.3: (a) Desired design Low pass frequency sampling filter; (b) impulse response $h(n)$ of it and also frequency response of this filter in (c).

The impulse response $h(n)$ coefficients is applied to noisy ECG signal to find the filtered ECG signal $y(n)$ by the following equation:

$$y(n) = h(0)x(n) + h(1)x(n-1) + h(2)x(n-2) + .. + h(20)x(n-20) \quad (3.4)$$

3.2.3 Algorithm-3/ FIR low pass filter using window method

Design an FIR low pass filter using window method to remove noise from signal and its algorithm is described as:

1. Specifying an FIR filter design of a low pass filter

$$H_D(\omega) = \begin{cases} 1, & |\omega| < \frac{\pi}{32} \\ 0, & otherwise \end{cases} \quad (3.5)$$

The subscript D used the distinguish between the ideal and practical impulse response.

2. If we know $H_D(\omega)$ we can be obtained the desired response $h_D(n)$ by evaluating the inverse Fourier transform of Equation (3.5). As we consider to design a low pass filter. We could start with the ideal lowpass response shown in Figure 3.**4** (b) where $\omega_c$the cut off frequency and the frequency scale is normalized*:* T=1. By letting the response go from $-\omega_c$ to ω_c , we simplify the integration operation. This the impulse response is given by

$$h_d(n) = \frac{1}{2\pi}\int_0^{\frac{\pi}{32}} H_d(\omega)e^{j\omega n}d\omega$$

$$h_d(n) = \begin{cases} \frac{1}{4} sinc\left(\frac{\omega_c}{\pi}\left(n - {}^{(M-1)}/_{2}\right)\right), & n = 1 \ldots . M-1 \\ 1, & n = 0 \end{cases} \quad (3.6)$$

Where $\omega_c = \frac{\pi}{32}$ is the cutoff frequency of the filter.

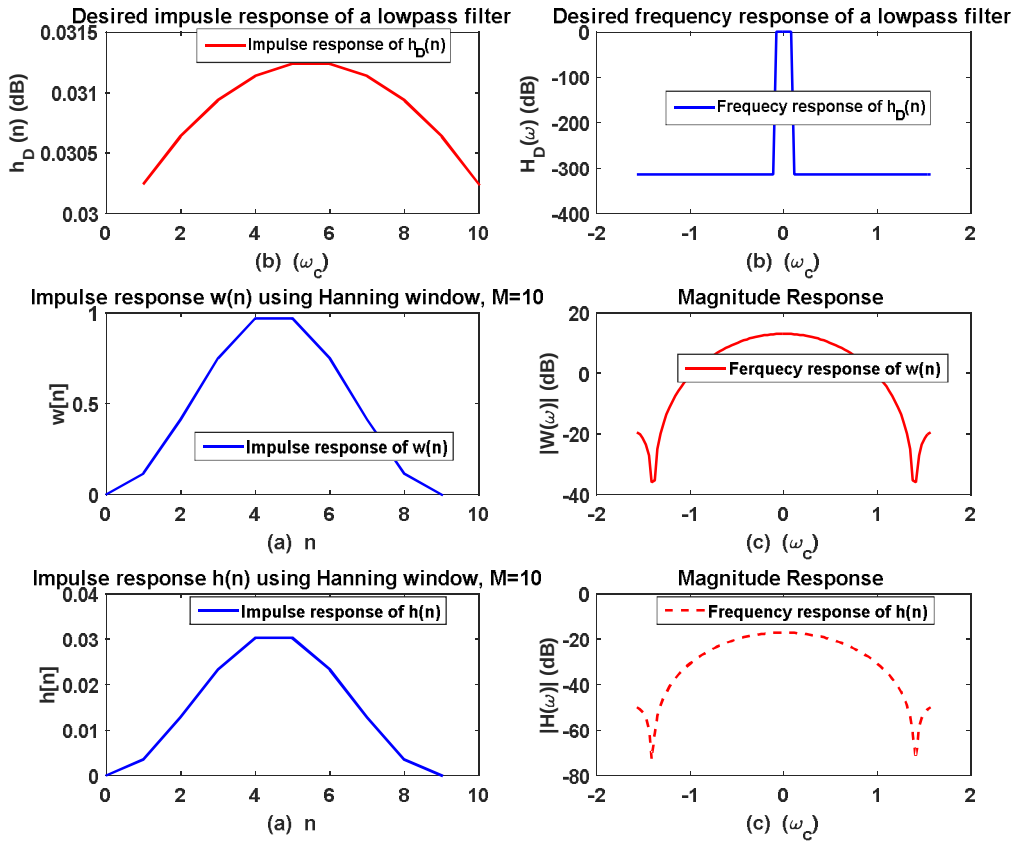

Figure 3.4: Impulse response of the ideal low pass filter $h_D(n)$ in (a), Hanning window function $w(n)$ in (c) final practical impulse response h(n) in (e); and its frequency response (b) ideal/desired, (d) window function, (f) practical frequency response of h(n).

3. Select a window function $w(n)$(such as Rectangular, Hamming, Hanning, Blackman, and Kaiser [9]) that satisfies the passband or stopband attenuation. The window function of Hanning window is given by

$$w_{Hann}(n) = \begin{cases} 0.5 - 0.5cos\frac{2\pi n}{M-1} & for\ 0 \le n \le M-1 \\ 0 & otherwise \end{cases} \quad (3.7)$$

4. Assume the filter length $M = 10$.
5. Obtained values of $w(n)$ for chosen window function and the values of the actual/practical FIR filter coefficients by

$$h(n) = h_D(n) * w_{Hann}(n)) \quad (3.8)$$

The equation (3.8) represents a practical approach is to multiply the ideal impulse response $h_D(n)$, by a suitable window function $w(n)$, whose duration is finite. This way

the resulting impulse response decays smoothly towards zero. The process is illustrated in Figure 3.**4**. Figure 3.**4** (b) shows the ideal frequency response and corresponding ideal impulse response Figure 3.4 (a). Figure 3.**4** (c) shows a finite duration window function and its spectrum in Figure 3.3 (d). Figure 3.**4** (e) shows h(n) which is obtained by multiplying $h_D(n)$ by $w(n)$. The corresponding frequency response shows that the ripples and overshoots, characteristic of direct truncation, are much reduced. However, the transition width is wider than for the rectangular case. The transition width of the filter is determined by the width of the main lobe of the window. The side lobes produce ripples in both passband and stopband.

Using Equations (3.4) and (3.5) the parameters as an input, the practical filer coefficients $h(n)$ were obtained by Equation (3.6) and $h(n)$ are listed in Table 3.3.

Table 3.3: List of filter coefficients $h(n)$.

h(n)			h(n)
h[0]	0	0	h[9]
h[1]	0.00358404441626496	0.00358404441626496	h[8]
h[2]	0.0127825047097972	0.0127825047097972	h[7]
h[3]	0.0233528803117899	0.0233528803117899	h[6]
h[5]	0.0302955272394288	0.0302955272394288	h[5]

6. Apply filter coefficients $h(n)$ to the ECG noisy signal and remove unwanted signal and get smoothed ECG signal by the following equation:

$$y(n) = h(0)x(n) + h(1)x(n-1) + h(2)x(n-2) + .. + h(9)x(n-9) \qquad (3.9)$$

3.2.4 Algorithm-4/ M point average with window length FIR filter

The M point average filter is a simple Low Pass FIR (Finite Impulse Response) filter [22**].** The M point average filter perform three important functions:

i. It consists of M input points and the average of those M-points and produces a single output point;

ii. The filter coefficient represents amount of delay;

iii. This filter performs as a low pass filter.

Consider M-point average defined by a window of length M. The equation of it is written as:

$$y[i] = \frac{1}{M}\sum_{j=0}^{M-1} x[i+j] \qquad (3.10)$$

where x [ ] is the input signal, y [ ] is the output signal, and M is the number of points in the average.

To noise eliminate, we can choose $M = 3, 5, 7 \ldots$ i.e., M should be choosing odd number. The following examples are described as below with the help of equation (3.5), we chose M=7 which is given by the following equation:

$$y(i) = [x(i) + x(i+1) + x(i+2) + x(i+3) + x(i+4) + x(i+5) + x(i+6)] \quad for\ 1 < i < n$$

$$y(i) = \frac{y(i)}{7} \qquad (3.\mathbf{11})$$

where $x(i)$, $x(i+1)$, $x(i+2)$, $x(i+3) \ldots\ldots\ldots\ldots x(n)$ is the input samples value of original ECG signal and $y(i)$ is the calculated output of filtered ECG signal and n is the number of samples for analysis, represents as one-dimensional array of sample points of the ECG signal.

Window length, specified as a numeric or duration scalar. When k is a positive integer scalar, the centered average includes the element in the current position plus surrounding neighbors. For example, a three-point average defined by a window of length three results in the following calculation for a vector A:

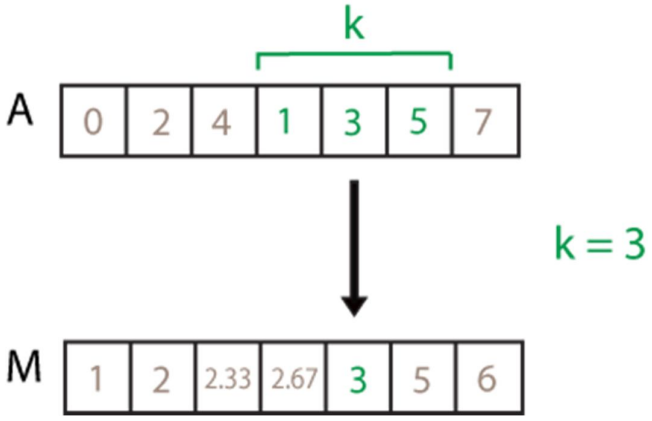

3.2.5 Algorithm-5/ Moving average weighted window filter

We developed an algorithm based on moving average weighted window. Let $\boldsymbol{x(n)} = \boldsymbol{x(1), x(2), x(3) \ldots\ldots x(k)}$ represents one-dimensional array of sample points of the synthesized digitized ECG. The algorithm is described as follows:

Step 1**:** The ECG signal x is calculated from x by following equation: $x = x - mean\ (x)$

Step 2**:** Use four points moving average filter to smooth $x(n)$which is given by the equation**:**

$$y(n-1) = [x(n+1) + 2x(n) + x(n-1)]/4;\ \ 2 < n < k-1 \qquad (3.12)$$

Where $x(n-1),\ x(n), x(n+1)$ is the input samples of input signal x and $y(n-1)$ is the output sample of y.

Step 3: Window size for moving weighted filtering is considered $-w$ to w, where w is the window size. The weighted window function equation is given by: $\frac{\left[1-\left(\frac{j}{w}\right)^2\right]}{w}$

Step 4: The final filtered equation is given by:

$$y(i) = y(i) + y(i+j)\frac{\left[1-\left(\frac{j}{w}\right)^2\right]}{w};\ \ if j > -i\ and\ j < (length(y) - i + 1) \qquad (3.13)$$

Step 5: Apply step 4 in ECG noisy signal and get ECG filtered signal.

Step 6: To prove of robustness of this algorithm, the performance parameters such as MSE, SNR and correlation are considered of this algorithm.

3.2.6 Algorithm-6/ Forward difference quotient and amplitude thresholding

The main concept of this algorithm is based on forward difference quotient and amplitude thresholding**.** We considered difference of the noisy signal by different order $(n)$to eliminate the ECG signal**.** The algorithm is described bellows**:**

Consider a small increment $\Delta x = T$, where T is sampling interval and the equation of M^{th}samples of noisy ECG signal $x_{noisyecg}$ represents as

$$y[i] = f(x) = \sum_{j=0}^{M-1} x_{noisyecg}[i+j] \qquad (3.14)$$

Consider the first forwards difference quotient is

$$\Delta f(x) = f(x+T) - f(x) \tag{3.15}$$

The second forwards difference is defined as

$$\Delta^2 f(x) = \Delta f(x+T) - \Delta f(x) = f(x+2T) - f(x+T) - \{f(x+T) - f(x)\}$$
$$= f(x+2T) - 2f(x+T) + f(x) \tag{3.16}$$

The third forwards difference is defined as

$$\Delta^3 f(x) = \Delta f(x+2T) - \Delta^2 f(x) = f(x+3T) - f(x+2T) - 2\{f(x+2T) - f(x)\} + \{f(x+T) - f(x)\} \tag{3.17}$$

The fourth forwards difference is defined as

$$\Delta^4 f(x) = \Delta f(x+3T) - \Delta^3 f(x) = f(x+4T) - f(x+3T) - 3\{f(x+3T) - f(x+2T)\} + 3\{f(x+2T) - f(x)\} - \{f(x+T) - f(x)\} = f(x+4T) - 4f(x+3T) + 6f(x+2T) - 4f(x+T) + f(x) \tag{3.18}$$

In general,

$$\Delta^i f(x) = \Delta f(x+(i-1)T) - \Delta^{i-1} f(x),\ for\ 1 < i < n \tag{3.19}$$

Where, n is the order of forward difference of noisy ECG signal

After applied of forward difference equation, if there is some noisy signal, then we can apply the threshold (Th)

$$Th = \frac{1}{N}\sum_{i=1}^{N} {x_{ecg}}_i^2$$

$$x_{noisyECG} = \begin{cases} abs\left(\Delta^i f(x)\right) < Th,\ 0 < Th < 1 \\ 0, otherwise \end{cases} \tag{3.20}$$

These values are the noisy data value. We have to find out their position/index and need to calculate their length between two consecutive noise peak values by the following iterations:

$$position\ of noisy\ data, i = 0$$

$$if \Delta^{i-1} f(x) - \Delta^i f(x) > 0\ and\ \Delta^{i+1} f(x) - \Delta^i f(x) > 0; 2 < i < k-1$$

$$i = i + 2$$

Now we have to create a new error vector which stores the amplitude of noisy value.

Initialization error vector,

$$newvector = 0$$

Initialization error noise amplitude,

$$previous\ amplitude = 0$$

Amplitude of the present noise sample is given by,

$$amplitude = \Delta f(x(i)) + previous\_amplitude$$

Duration of noise is defined by,

$$length = x(i+1) - x(i);\quad 1 < i < length(x)$$

Magnitude of noise is given by,

$$Z = ones(1, length) \times amplitude$$

Currently new error vector is defined by,

$$newvector = [newvectorZ]$$

New amplitude of noise is given by,

$$previous\ amplitude = amplitude$$

Finally, we can reconstruct ECG signal by

$$Reconstructed\ signal = x(length(new\_vector)) - new\_vector$$

3.3 Summary

Noise of ECG signal is a great problem in diagnosis of medical science. Therefore, researchers are developing different methodology for noise eliminations. However, the de-noised methods have not been improved for noisy ECG signal. Therefore, the development of robust method of ECG signal detection still requires the improvement in noise elimination. In this thesis we studied about various algorithms which are enabling to eliminate noises from noisy ECG signal**.**

Chapter 4

Proposed QRS Detection Algorithm

4.1 Introduction

The QRS complex is the most prominent wave component within the electrocardiogram. It reflects the electrical activity of heart during the ventricular contraction and the time of its occurrence. Its morphology provides information about the current state of the heart. The identification of QRS-complexes forms the basis for almost all automated ECG analysis algorithms. In this chapter detection algorithm is proposed which will detect a QRS complex.

4.2 QRS Detection Methodology

Before obtaining the QRS complex the ECG, it was applied to preprocessing by different noisy algorithm as described in chapter 3. Initial we have considered some parameter as shown in Figure 4.1 to detect of QRS complex. The algorithms described below approach the rectification stage in different ways algorithm is summarized as:

1. Introduce ECG signals from ECG database.
2. Perform the different noises (i.e., power line interference, Baseline wonder, EMG, abrupt noise) individual into the original ECG signal.
3. Filtered of ECG noisy signal by using Algorithm-1, Algorithm-2, and Algorithm-3 respectively.
4. Detection of QRS:
5. Apply proposed threshold (*T*) on ECG signal

$$T = \frac{1}{N}\sum_{i=1}^{N} {x_{ecg}}_i^2 \qquad (4.1)$$

where x_{ecg} is the raw ECG signal and N vectors of ${x_{ecg}}_i, i \in \{1,2,\dots\dots N\}$ of signal samples numbers.

With proposed threshold (*T*), QRS detection is calculated by

$$\hat{x}_{ecg} = \begin{cases} x_{ecg} for x_{ecg} \geq T \\ 0 \quad for x_{ecg} < T \end{cases} \qquad (4.2)$$

6. Repeat procedures:

   Input:

   i: present sample value,

$i-1$: past sample value,

$i+1$: future sample value

Assume detect position and values are zero, i.e.,

$R_p = 0, Q_p = 0, S_p = 0, R_v = 0, Q_v = 0, S_v = 0.$

// First find out the R-wave positions and values:

Old difference = $(\hat{x}_{ecg}(\mathrm{i}-1) - \hat{x}_{ecg}(i))$;

New difference = $(\hat{x}_{ecg}(\mathrm{i}) - \hat{x}_{ecg}(i+1))$;

For $i = 1: length\ (x_{ecg})$

if(Old difference <0 && New difference >0)

$R_p = [R_p\ \mathrm{i}]$;

$R_v = [R_v \hat{x}_{ecg}\ (\mathrm{i})]$;

else continue;

// First find out the Q-wave positions and values:

$Q = i - 1$;

$while\ (Olddifference < 0)$

Old difference = $((\widehat{x}_{ecg}(Q-1) - \hat{x}_{ecg}(Q))$;

$Q = Q - 1$;

end

$Q_p = [Q_p\ \mathrm{Q}]$;

$Q_v = [Q_v \hat{x}_{ecg}(\mathrm{Q})\ ]$;

// First find out the S-wave positions and values:

S=i+1;

while ($Newdifference > 0$)

New difference = $(\hat{x}_{ecg}(\mathrm{S}) - \hat{x}_{ecg}(\mathrm{S}+1))$;

$S = S + 1$;

end

$S_p = [S_p - S]$;

S_p=[$S_p \hat{x}_{ecg}(\mathrm{S})$];

end

end

7. Finally store and detect of QRS position and values.
8. Output: QRS detection from ECG signal
9. Until there is no further successive ECG signal.
10. Performance test based on accuracy, sensitivity, specification, precision.
11. Compare this algorithm with conventional algorithm.

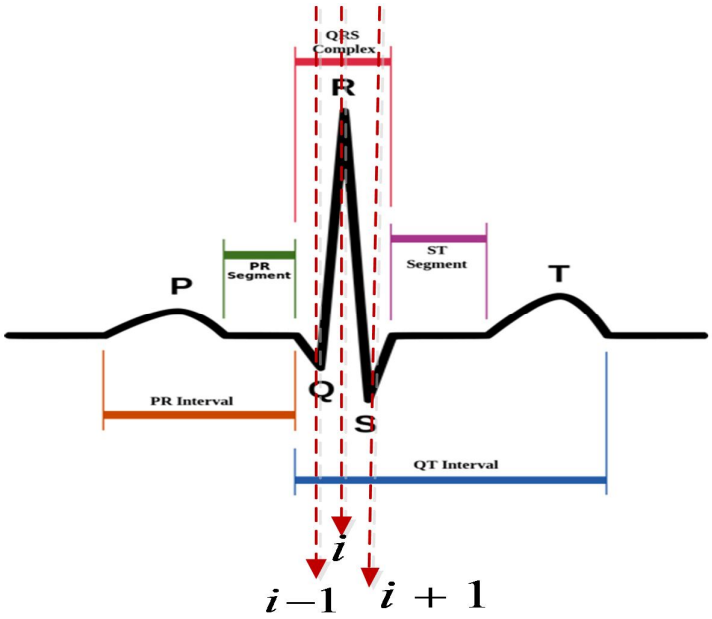

Figure 4.1: Maps of QRS detection of ECG signal (i= R wave detection, $i + 1$=S wave detection, $i - 1$=Q wave detection parameter).

4.3 Summary

The proposed detection achieved higher accuracy, sensitivity, specificity and precision value than other conventional methods. The heart beat rate will be measured accurately and 100% accuracy from the detected QRS complexes by proposed detection algorithm and also specified the heart diseases based on database.

Chapter 5

Results & Discussion

5.1 Introduction

In this chapter, we analyze the performance of our proposed algorithms**.** Many literature reviews have studied about the performance assessment of reconstructed signal and original signal and their comparative evaluation [24]. Some performance parameters are described below that were used in this research work**.** In this thesis, we considered different noises such as power line interference, baseline wonder and EMG and abrupt noise**.** Simulation results and performance analysis of proposed algorithms are described in following sections.

5.2 Performance Evaluations Parameters

To analysis the performance of the developed algorithm which is applied on different types of noisy ECG signal we have used some parameters [24]. They are following:

5.2.1 Signal to Noise ratio *(*SNR*)*

The signal-to-noise ratio can be defined as

$$SNR_{ecg} = \frac{\frac{1}{N}\sum_{i=1}^{N} {x_{ecg}}_i^2}{\frac{1}{N}\sum_{i=1}^{N} {x_{ecg}}_i^2 - \frac{1}{N}\sum_{i=1}^{N} {x_{Denoised\_ecg}}_i^2}$$

Where $SNR = 10log_{10}SNR_{ecg}dB$ and $x_{Denoised\_ecg}$ is the filtered ECG signal.

The larger value of SNR indicates that the algorithm performance is better. If SNR becomes low it indicates that the algorithm performance is degraded.

5.2.2 Mean Square Error *(*MSE*)*

It is measured between the original ECG signal and filtered ECG signal. It can be defined as

$$MSE = \frac{1}{N}\sum_{i=1}^{N}\left[{x_{ecg}}_i^2 - {x_{Denoised\_ecg}}_i^2\right]$$

Mean Square Error (MSE) should be as low as possible which indicates the better performance of the algorithm.

5.2.3 Correlation

The discrete autocorrelation between the two signal x and y is defined as

$$r_{xx} = \frac{1}{N}\sum_{k=1}^{N} x_{ecg}[n]x_{ecg}[n+k]$$

and the cross correlation is

$$r_{xy} = \frac{1}{N}\sum_{k=1}^{N} x_{Denoised\_ecg}[n]x_{ecg}[n+k]$$

The correlation coefficient (r) is measured with two numerical variables or signals for paired observations**.** If the correlation coefficient is normalized, its absolute value will range from 0 to 1, making it easier to judge the similarity between the signals. If the normalized correlation coefficient is equal to either 1 or -1, the two signals are perfectly correlated. If r value is close to $+1$, it indicates a perfect positive fit or positive relationship between the two signals x and y i.e., the values of x increases, the values of y also increases. If r value is close to -1, it indicates a perfect negative fit. If $r$value is close to 0, there is no relationship between x and y.

5.2.4 Power Spectral Density (PSD)

We have investigated three non-parametric methods for power spectral estimation (PSD) such as *Periodogram, Welch* and *Lomb-Scargle algorithm [*24*]*.

The Lomb-Scargle periodogram is a well-known algorithm for detecting and characterizing periodic signals in unevenly-sampled data. Lomb-Scargle algorithm can compute spectra of non-uniform sampled signals or signals with missing samples.

Taking Fourier transform of autocorrelation equation results are an estimate of power spectrum [24]:

$$P\left(e^{j\omega}\right) = \sum_{n=-N+1}^{N-1} r_{xx}e^{-j\omega n}$$

is called *Periodogram.*

Consider, an N point data ECG sequence is partition as $x[n], 0 \leq n \leq N-1$, into L segments of M samples each the segments $x_M^l[n]$ are formed we have $N \gg LM$. Thus,

$$x_M^l[n] = x[n + lM - M] \begin{cases} 0 \leq n \leq M-1 \\ 1 \leq l \leq L \end{cases}$$

For estimate of Welch PSD computation of L periodograms

$$P_M^l(e^{j\omega}) = \frac{1}{W}\left|\frac{1}{N}\sum_{n=0}^{N-1} x_M^l[n]e^{-j\omega k}\right|^2, 1 \leq l \leq M$$

Where, $W = \sum_{l=1}^{M} w^2(l)$ and $w(l)$ is window function. This is the Welch method of PSD.

5.3 Denoising Simulation Results

The ECG dataset used in this research work are collected from the MIT/BIH Database *[*25*]*. In Figure 5**.**1-5**.**23 we have plotted the raw ECG signal and noisy ECG signal and also filtered signal with different noise density such as $\sigma = 0, 0.25, 0.5, 0.75, 1$**.** We have considered different noises such as power line interference, baseline wonder and EMG and abrupt noise. For power line interference and baseline wonder, we have considered 50Hz noise frequency and 0.5mV amplitude for added into ECG signal. This electromyography (EMG) noise is simulated by adding random noise to the ECG. Array of random numbers was created consisting of values of ±0.50 of the ECG maximum amplitude to the uncorrupted ECG. The reduced noise levels are formed by scaling the random numbers by the appropriate amount. Electromyography (EMG) noise shows the greater noise and has broadband frequency characteristics, which overlaps the frequency spectrum of the QRS complex. For abrupt shift noise random numbers (within ±0.5 mV) were generated, but the same random number was taken for 500 ms duration cycle and then another random number was generated for next cycle and so on**.** We have considered the amplitude and frequency of powerline noise and baseline drift noise are same values for denoising in this thesis. All of these noises are filtered by Algorithm-1, Algorithm-2, Algorithm-3, Algorithm-4, Algorithm-5, and Algorithm-6 respectively**.**

To remove noisy signal based on proposed algorithms 1,2,3 4, 5 and 6, we have added the noise into the raw ECG signal at different intensity of noise such as 0, 0.25, 0.5, 0.75, and 1 as illustrated in Figure 5.1. The corrupted ECG signal for EMG noise is shown in Figure 5.1. Figure 5**.**1 shows the noisy ECG signal with different noise density such as $\sigma =$

$0, 0.25, 0.5, 0.75, 1$ on left column Figure and its ECG filtered signal by using Algorithm -1 on the right column Figure for the EMG noise. Similarly, Figurescan be shown for EMG noise, Baseline drift noise and abrupt noise. We have observed that Algorithm-1 is not showing good smooth signal if noise density is increases. Figure 5.2 shows noisy and ECG filtered signal by Algorithm-2 for powerline noise. This algorithm is also not showing smooth ECG signal with noise density increases. Figure 5.3 shows for Algorithm-3 for EMG noise, only abrupt noise is removed for $\sigma = 0 \& 0.25$ but $\sigma = 0.5$ to 1 does not show properly in algorithm 3.

Algorithm-4 applied on the corrupted ECG signal to eliminate the various noises. The Algorithm-4 is able to remove the noise from the corrupted ECG signal at different noise intensity level. The filtered baseline shift noise-free signal is shown in Figure 5.4.The ECG filtered signal with all different noise incorporate with powerline, EMG and baseline shift noise has properly remove the noise for Algorithm-4. On the other hand, the abrupt noise is properly remove by Algorithm-4. Figure 5.5 shows denoising Algorithm-5 with power line noise removal ECG filtered signal. This algorithm remove EMG noise with higher noised density as well as properly remove the noise of baseline drift. But it can not properly remove the abrupt noise from ECG.

To eliminate the abrupt baseline shift noise from ECG signal we have used the Algorithm-6 to remove the noise at each step of it as shown in Figure. We have used fourth order forward difference equation with threshold $(Th = 0.3)$ for remove of noises by sampling frequency$f_s = 170Hz$. In Figure 5.6 (c) – (d)it shows the output of the first, 3rd and fourth forward different equation. Figure 5.6(f) shows the filtered ECG signal, where the abrupt baseline shifts removed by proposed algorithm-6. Similarly, proposed algorithm-6 have also applied to eliminate noise, for noise intensity is 0, 0.25, 0.5, and 0.75 and 1 respectively. It is observed that Algorithm-6 does not properly remove the noise with higher noise density. On the other sides the EMG noise and abrupt noise is properly remove by Algorithm with higher noise density. Removal of abrupt shift noise is shown in figure 5.7 at different noise density. Specially the Algorithm-6 is fully support to remove of abrupt noise with higher noise density.

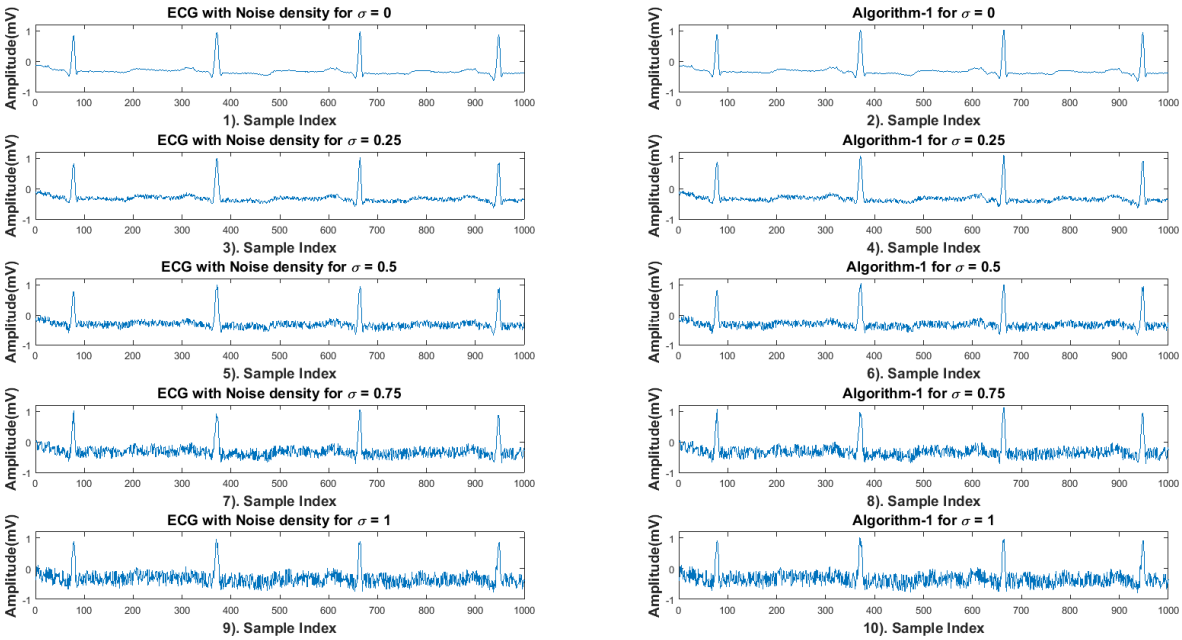

Figure 5.1: The raw ECG signal collected from MIT/BIH Database and its filter ECG signal with different noise density $\sigma = 0, 0.25, 0.5, 0.75, 1$ **for EMG noise by Algorithm-1.**

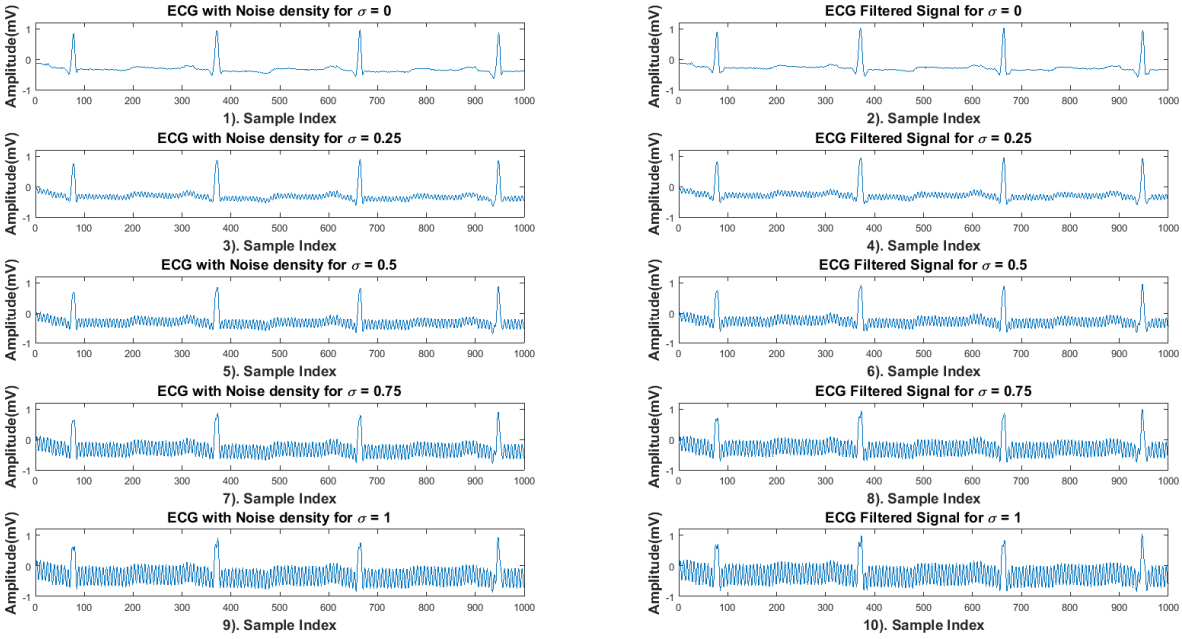

Figure 5.2 : The raw ECG signal collected from MIT/BIH Database and its filter ECG signal with different noise density $\sigma = 0, 0.25, 0.5, 0.75, 1$ **for powerline noise by Algorithm-2.**

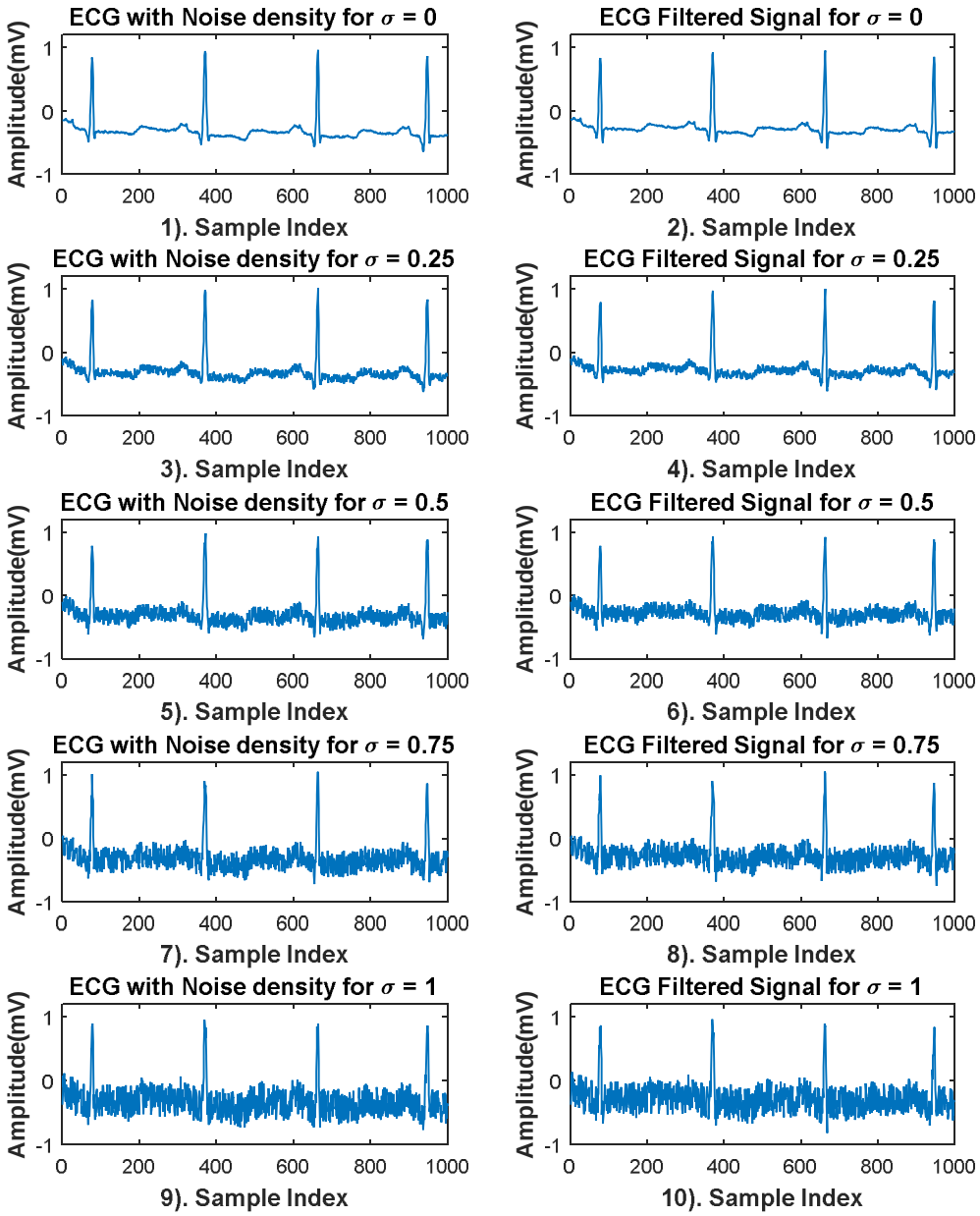

Figure 5.3: The raw ECG signal collected from MIT/BIH Database and its filter ECG signal with different noise density $\sigma = 0, 0.25, 0.5, 0.75, 1$ **for EMG noise by Algorithm-3.**

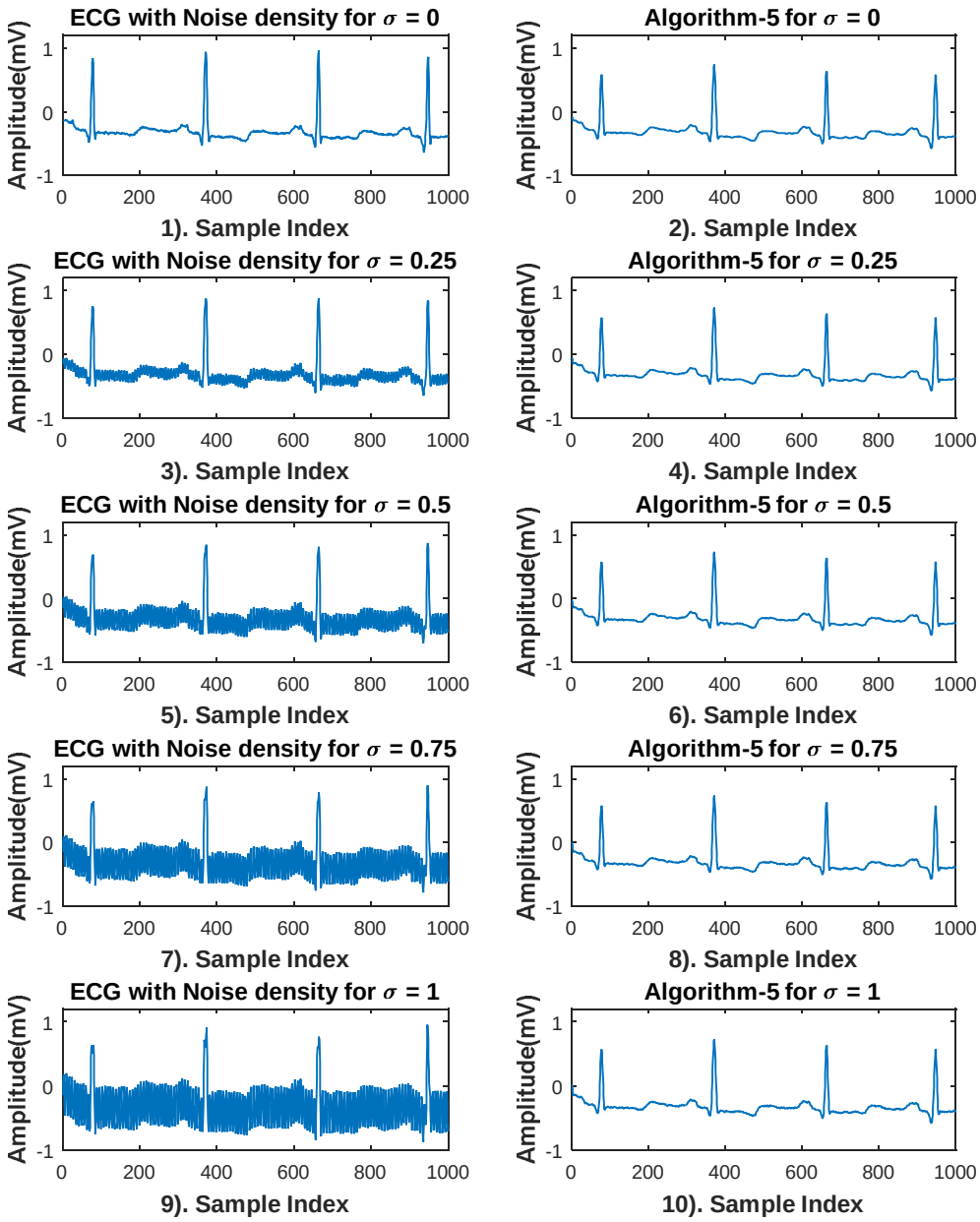

Figure 5.4: The raw ECG signal collected from MIT/BIH Database and its filter ECG signal with different noise density $\sigma = 0, 0.25, 0.5, 0.75, 1$ **for Baseline drift noise by Algorithm-4.**

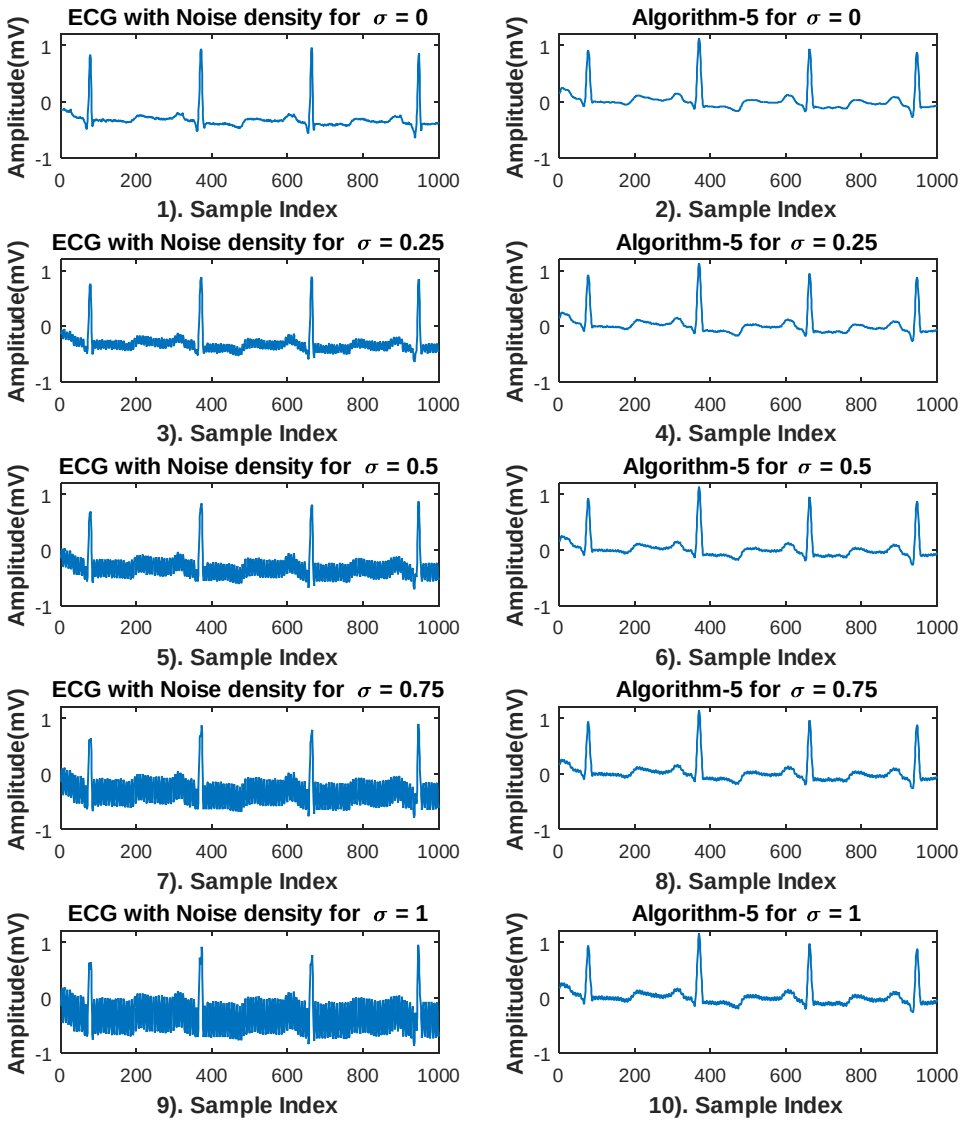

Figure 5.5: The raw ECG signal collected from MIT/BIH Database and its filter ECG signal with different noise density $\sigma = 0, 0.25, 0.5, 0.75, 1$ **for powerline noise by Algorithm-5.**

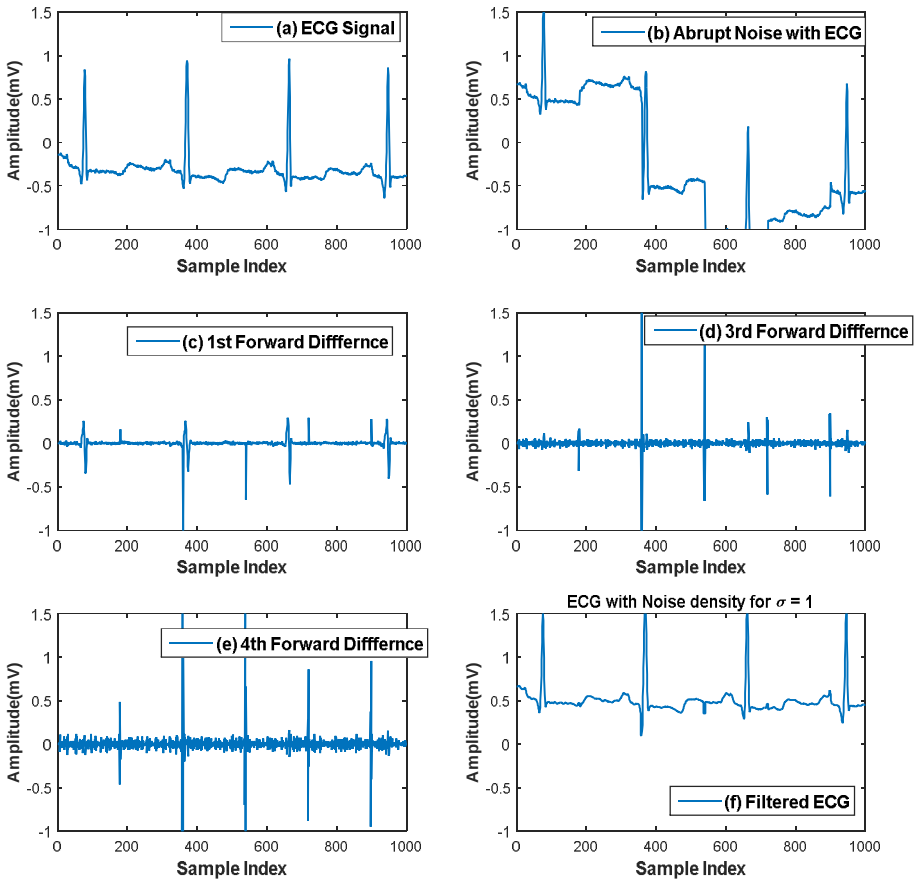

Figure 5.6: Simulation results on abrupt base line shift noise analysis when noise intensity is 100% for **Algorithm-6**.

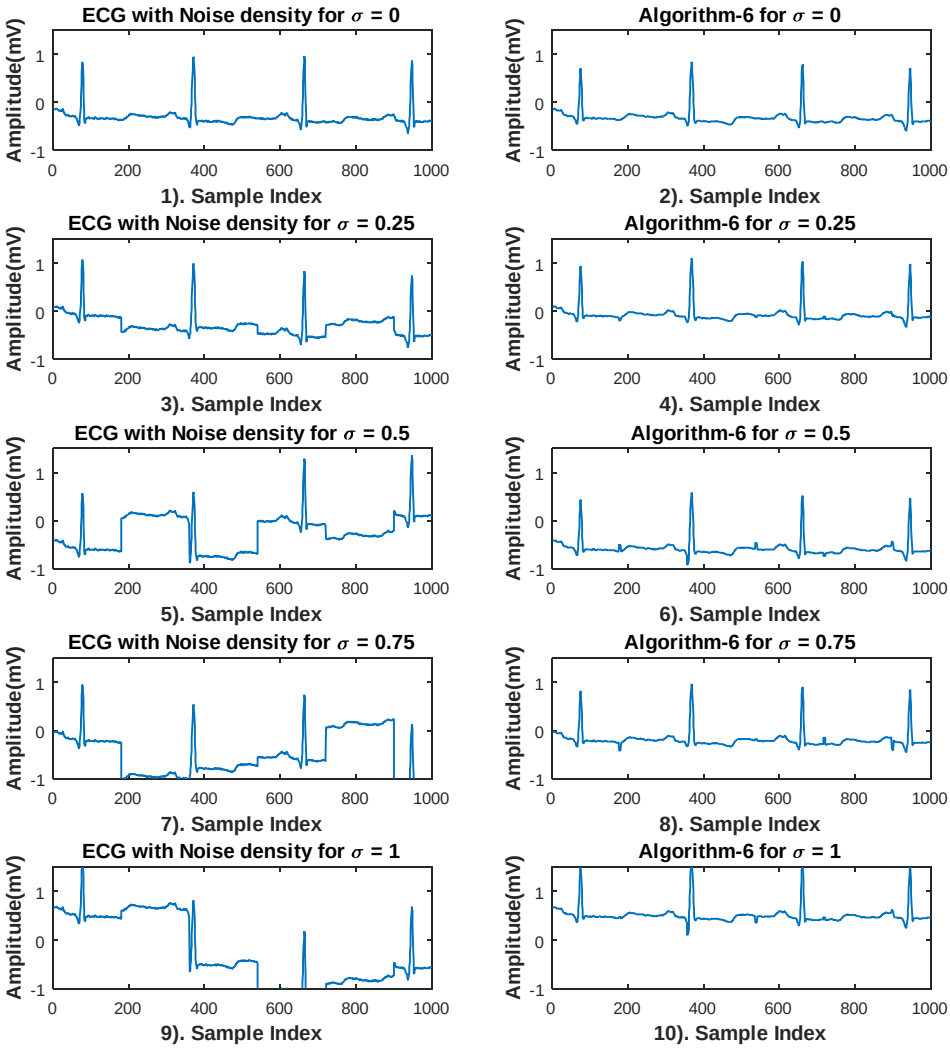

Figure 5.7: The raw ECG signal collected from MIT/BIH Database and its filter ECG signal with different noise density $\sigma = 0, 0.25, 0.5, 0.75, 1$ **for Abrupt noise by Algorithm-6.**

To measure the performance for different noise removal methods, the distortion between original signal and reconstructed signal is measured by mean square error *(*MSE*)*, signal-to-noise ratio (SNR*)* and correlation coefficients values. In this thesis, the performance parameters such as SNR (in dB), MSE, correlation which will prove the robustness of these algorithms are shown in Table I for all proposed algorithms**.** First, we have added the noise into the raw ECG signal at different intensity of noise such as 0, 0.25, 0.5, 0.75, and 1. The proposed Algorithm 4 have acquired highest SNR, lowest MSE and also good correlation coefficients values than Algorithm-1, 2 & 3**.** The Algorithm -1 has achieved 91.737 for SNR, 0.0015162 for MSE and 0.9810 for correlation on an average value in MIT-BIH database as shown in Table 5.1 for power line interference and baseline drift noise. However, in the case of EMG and abrupt noise, the values of SNR, MSE and Correlation value are slightly different than power line interference and baseline drift noise. We have checked that the correlation coefficients value(r), if $r > 0.8$ is generally described as *strong*, whereas $r < 0.5$ is generally described as *weak* in MIT-BIH database. In Table 5.1, Algorithm-1 to 6 shows strong correlation value $(r \approx 1)$ whereas Algorithm-1 shows rang of correlation value $r \approx 0.99$ to $r \approx 0.6$, $r \approx 0.99$ to $r \approx 0.55$ for Algorithm-2, $r \approx 0.99$ to $r \approx 0.56$ for Algorithm-3, $r \approx 0.98$ to $r \approx 0.91$ for Algorithm-4, $r \approx 0.91$ to $r \approx 0.86$ for Algorithm-5 and $r \approx 0.91$ to $r \approx 0.57$ for Algorithm-6 for all noises. Someway the correlation value has decreased depends on the vary of the noise density σ. This result show in visual representation from Figure 5.8-5.13.

Figure 5.8 (a) & (c) shows for SNR value is higher for Algorithm-1 than others Algorithms for powerline noise with $\sigma = 0$. It is gradually decreases with increase of σ, but Algorithm-5 is increased the SNR value after $\sigma = 0.5$ for EMG noise than Algorithm 1,2,3,4, & 6. It also shows the numerical values in Table I. In Figure 5.8 (b), the SNR values of Algorithm-4 show the highest values than other algorithms with the increase of . Figure 5.8 (d), SNR value of Algorithm-1 is higher than others for $\sigma = 0$, but Algorithm-6 show good SNR values than others.

Figure 5.9 (a), (b), (c), & (d) shows for lower MSE value for Algorithm-6 than others Algorithms for with $\sigma = 0$. It is gradually increases with increase of σ, but for abrupt noise, its remain low MSE values. Algorithm-4 & 6 show the lowest MSE value for all noised with different noises. It also shows the numerical values in Table 5.1.

Figure 5.10 (a), (b), & (c) shows for higher correlation coefficient values for Algorithm-4 than others Algorithms for powerline noise, EMG and baseline shift noise with $\sigma =$

$0, 0.25, 0.5, 0.75, 1$. It shows numerically near about 1. Figure 5.9 (d), shows higher correlation coefficient values for Algorithm-6 than others. It also shows the numerical values in Table 5.1.

Figure 5.11 (a) – (f) shows the comparison between SNR and noise density of different noises such as powerline noise, EMG noise, baseline shift noise and abrupt noise for denoising algorithms. The SNR value is increased gradually for Algorithm 1,2,4 &5 of powerline noise and baseline shift noise. Algorithm 3 & 6 has the higher value than other algorithms for EMG noise.

Figure 5.12 (a) – (f) shows the comparison between MSE and noise density of different noises such as powerline noise, EMG noise, baseline shift noise and abrupt noise for denoising algorithms. The MSE value for abrupt noise shows higher value for all noise density (σ) of Algorithm 1 - 5. Whereas Algorithm 6 show lower MSE value than others algorithms.

Figure 5.13 (a) – (f) shows the comparison between MSE and noise density of different noises such as powerline noise, EMG noise, baseline shift noise and abrupt noise for denoising algorithms. The correlation coefficient value for EMG noise shows higher value for all noise density (σ) of Algorithm 1, 3 & 6. Where as Algorithm 2, 4 & 5 show higher correlation coefficient value than others noises.

However, in visual representation, Figures 5.8 – 5.13, the Algorithm 4 and 6 have shown good smoothed ECG signal as compared to Algorithm-1, 2, 3 & 5. In Table 5.1, Algorithm-4 & 6 achieved higher SNR, lower MSE, and good correlation value which is approximately 1 with the vary of noise density. Therefore, the filtered ECG signal and original signal are matched each other. For signal processing application, higher signal-to-noise ratio would be better, that would mean less distortion. So, Algorithm-4 & 6 proved the robustness for de-noised ECG signal than Algorithm-1,2,3 & 5 for four different noises.

Table 5.1: Results of performance parameters for proposed algorithms.

	Methods	**Noises**	**Performance parameters (avg. results of total no. of patients)**	**Percentage of Noise intensity (σ)**				
				0	**0.25**	**0.5**	**0.75**	**1**
Patient Data 100, 105, 107, 108, 109, 111, 112,	Algorithm-1	Power line interference	SNR	60.571	32.784	8.4506	3.7776	2.1292
			MSE	0.000169	0.00424	0.01646	0.03682	0.06532
			Correlation	0.9987	0.9443	0.8225	0.6946	0.5868
		EMG	SNR	60.571	18.344	14.849	8.3965	4.7836
			MSE	0.0001695	0.0019774	0.0073796	0.0165665	0.0290783
			Correlation	0.9987	0.9733	0.9076	0.8230	0.7344
			SNR	60.571	32.784	8.4506	3.7776	2.1292

113, 114, 115, 119, 200, 213		Baseline Drift Noise	MSE	0.000169	0.00424	0.01646	0.03682	0.06532
			Correlation	0.9987	0.9443	0.8225	0.6946	0.5868
		Abrupt Baseline Shift Noise	SNR	60.571	6.3657	1.7134	0.7280	0.3413
			MSE	0.0001	0.0218	0.0811	0.1910	0.4074
			Correlation	0.9987	0.7849	0.5386	0.3704	0.2960
	Algorithm-2	Power line interference	SNR	56.457	21.183	7.3699	3.5317	2.0424
			MSE	0.0024638	0.0065666	0.0188741	0.0393864	0.0681034
			Correlation	0.9924	0.9340	0.8061	0.6753	0.5671
		EMG	SNR	56.457	15.431	4.8328	2.2455	1.2957
			MSE	0.0024638	0.0090143	0.0287825	0.0619461	0.1073518
			Correlation	0.9924	0.9032	0.7336	0.5900	0.4763
		Baseline Drift Noise	SNR	56.457	21.183	7.3699	3.5317	2.0424
			MSE	0.0024638	0.0065666	0.0188741	0.0393864	0.0681034
			Correlation	0.9924	0.9340	0.8061	0.6753	0.5671
		Abrupt Baseline Shift Noise	SNR	56.457	8.2900	2.4606	1.0278	0.5123
			MSE	0.0024638	0.0167793	0.0565299	0.1353372	0.2714708
			Correlation	0.9924	0.8250	0.5954	0.4197	0.3387
	Algorithm-3	Power line interference	SNR	52.975	22.293	8.1414	3.9558	2.3002
			MSE	0.0026257	0.0062396	0.0170855	0.0351633	0.0604732
			Correlation	0.9930	0.9338	0.8045	0.6729	0.5646
		EMG	SNR	52.975	32.730	15.073	7.9476	4.8287
			MSE	0.0026257	0.0042498	0.0092282	0.0175022	0.0288067
			Correlation	0.9930	0.9648	0.8922	0.8023	0.7096
		Baseline Drift Noise	SNR	52.975	22.293	8.1414	3.9558	2.3002
			MSE	0.0026257	0.0062396	0.0170855	0.0351	0.0604732
			Correlation	0.9930	0.9338	0.8045	0.6729	0.5646
		Abrupt Baseline Shift Noise	SNR	52.975104	8.3474503	2.5077935	1.0465039	0.5237861
			MSE	0.0026257	0.0166639	0.0554675	0.1329198	0.2655684
			Correlation	0.9930	0.8091	0.5727	0.3989	0.3223
	Algorithm-4	Power line interference	SNR	91.737	91.644	91.361	90.893	90.244
			MSE	0.0015162	0.0015178	0.0015225	0.0015303	0.0015413
			Correlation	0.9810	0.9809	0.9808	0.9807	0.9804
		EMG Noise	SNR	91.737	79.236	57.918	38.119	27.006
			MSE	0.0015162	0.0017555	0.0024016	0.0036490	0.0051507
			Correlation	0.9810	0.9761	0.9634	0.9396	0.9135
		Baseline Drift Noise	SNR	91.737	91.644	91.361	90.893	90.244
			MSE	0.0015162	0.0015178	0.0015225	0.0015303	0.0015413
			Correlation	0.9810	0.9809	0.9808	0.9807	0.9804
		Abrupt Baseline Shift Noise	SNR	91.737	6.7900	1.9223	0.8112	0.3886
			MSE	0.0015162	0.0204859	0.0723592	0.1714578	0.3578642
			Correlation	0.9810	0.7349	0.4844	0.3225	0.2645
	Algorithm-5	Power line interference	SNR	22.2262	22.2259	22.2250	22.2234	22.2212

			MSE	0.0001134	0.0001134	0.0001135	0.0001136	0.0001138
			Correlation	0.9149	0.9146	0.9134	0.9113	0.9085
		EMG Noise	SNR	22.2262	22.2237	18.2168	16.2016	14.1881
			MSE	0.0001134	0.0001336	0.0114310	0.1157570	0.1170718
			Correlation	0.9149	0.9116	0.9023	0.8839	0.8663
		Baseline Drift Noise	SNR	22.2262	22.2259	22.2250	22.2234	22.221
			MSE	0.0001134	0.0001134	0.0001135	0.0001136	0.0001138
			Correlation	0.9149	0.9146	0.9134	0.9113	0.9085
		Abrupt Baseline Shift Noise	SNR	22.226	10.947	7.5882	5.3408	3.1911
			MSE	0.0001134	0.0146801	0.2364762	0.4080659	0.7278047
			Correlation	0.9149	0.6461	0.4069	0.2636	0.2218
	Algorithm-6	Power line interference	SNR	23.493	18.190	12.389	9.5634	8.2008
			MSE	0.0001403	0.0001431	0.0120310	0.0810310	0.1035000
			Correlation	0.8605	0.8068	0.7893	0.6700	0.5723
		EMG Noise	SNR	22.2262	22.2237	18.2168	16.2016	14.1881
			MSE	0.0001134	0.0001336	0.0114310	0.1157570	0.1170718
			Correlation	0.9149	0.9116	0.9023	0.8839	0.8663
		Baseline Drift Noise	SNR	23.493	18.190	12.389	9.5634	8.2008
			MSE	0.0001403	0.0001431	0.0120310	0.0810310	0.1035000
			Correlation	0.8605	0.8068	0.7893	0.6700	0.5723
		Abrupt Baseline Shift Noise	SNR	23.493	12.764	10.363	9.5443	6.3018
			MSE	0.0001403	0.0001431	0.0011031	0.031031	0.090350
			Correlation	0.8605	0.8162	0.7951	0.7826	0.6970

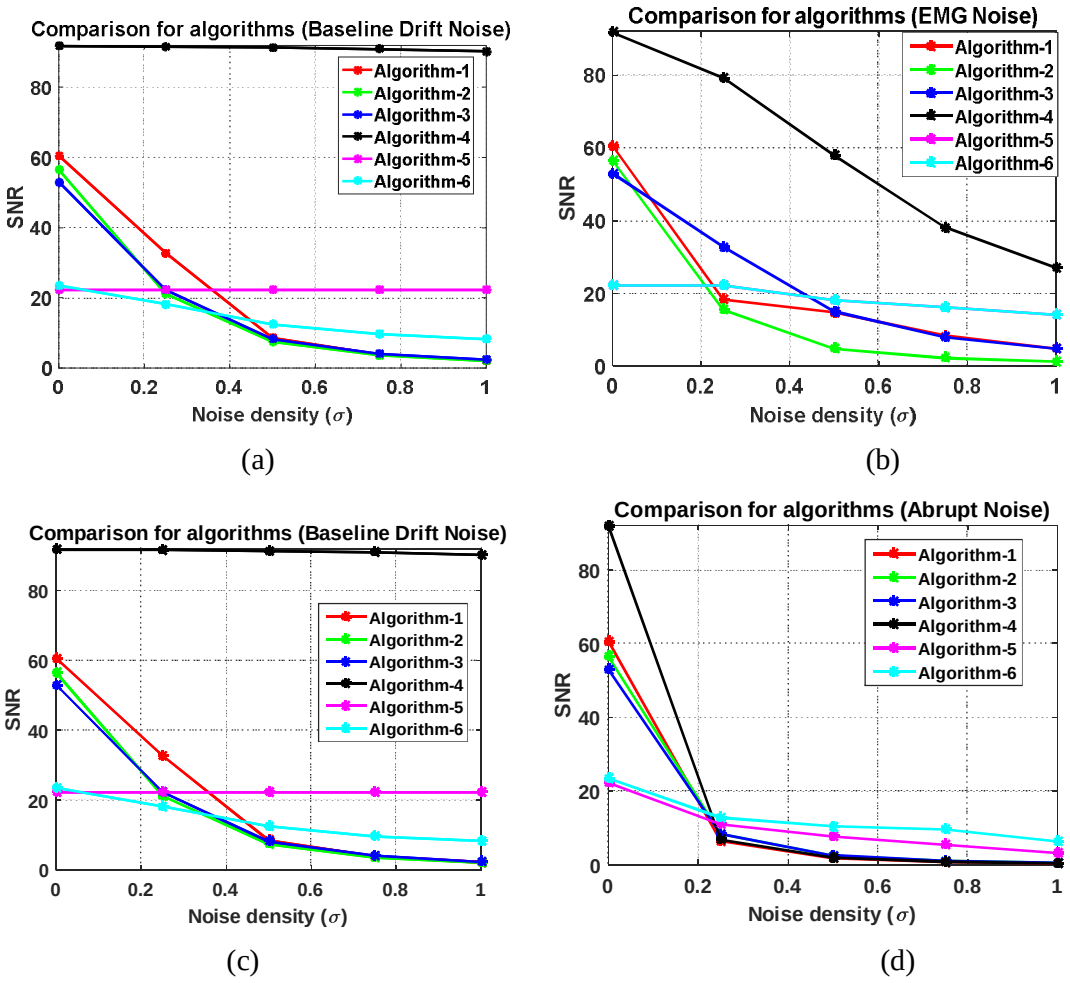

Figure 5.8: Comparison of SNR with noise density for (a) powerline noise (b) EMG noise (c) Baseline Drift noise (d) Abrupt noise of denoising algorithms.

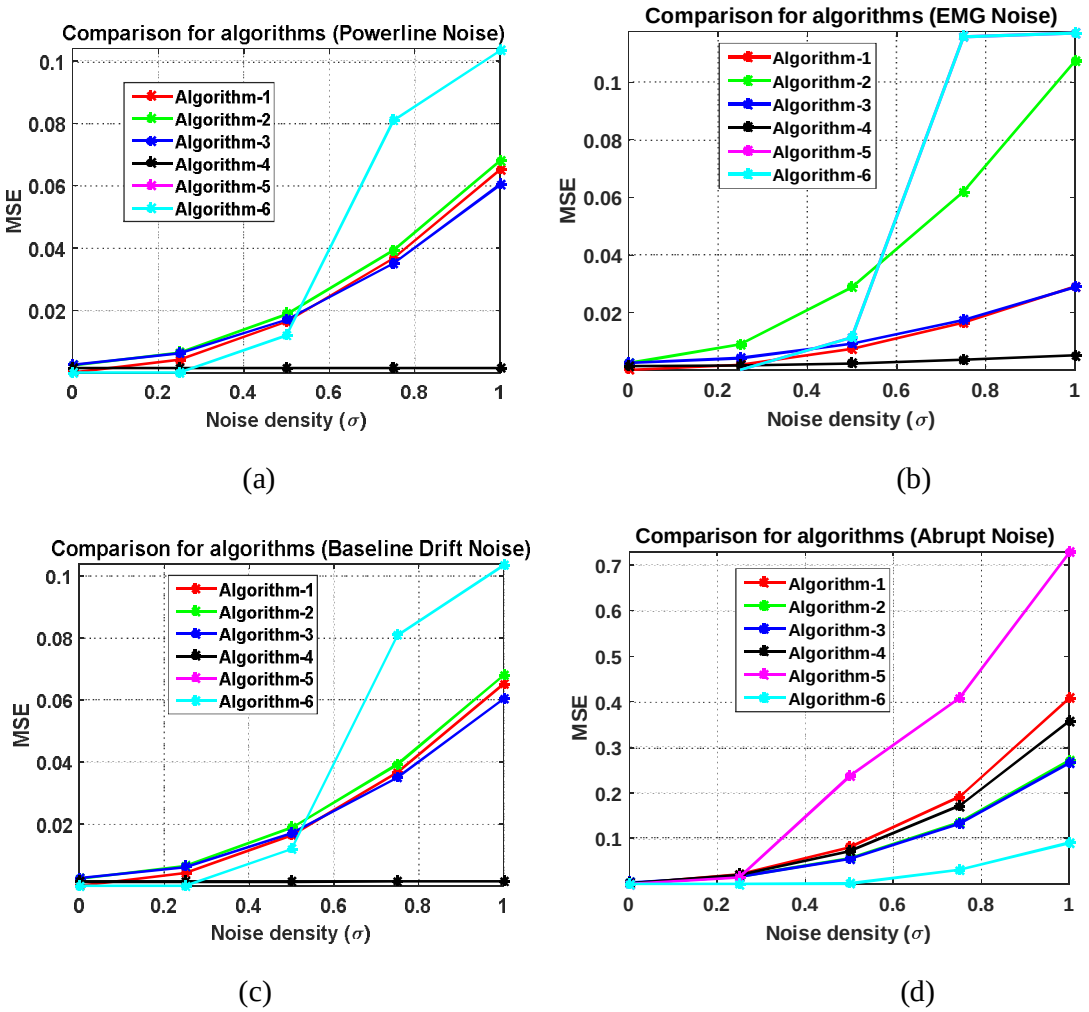

Figure 5.9: Comparison of MSE with noise density for (a) powerline noise (b) EMG noise (c) Baseline Drift noise (d) Abrupt noise of denoising algorithms.

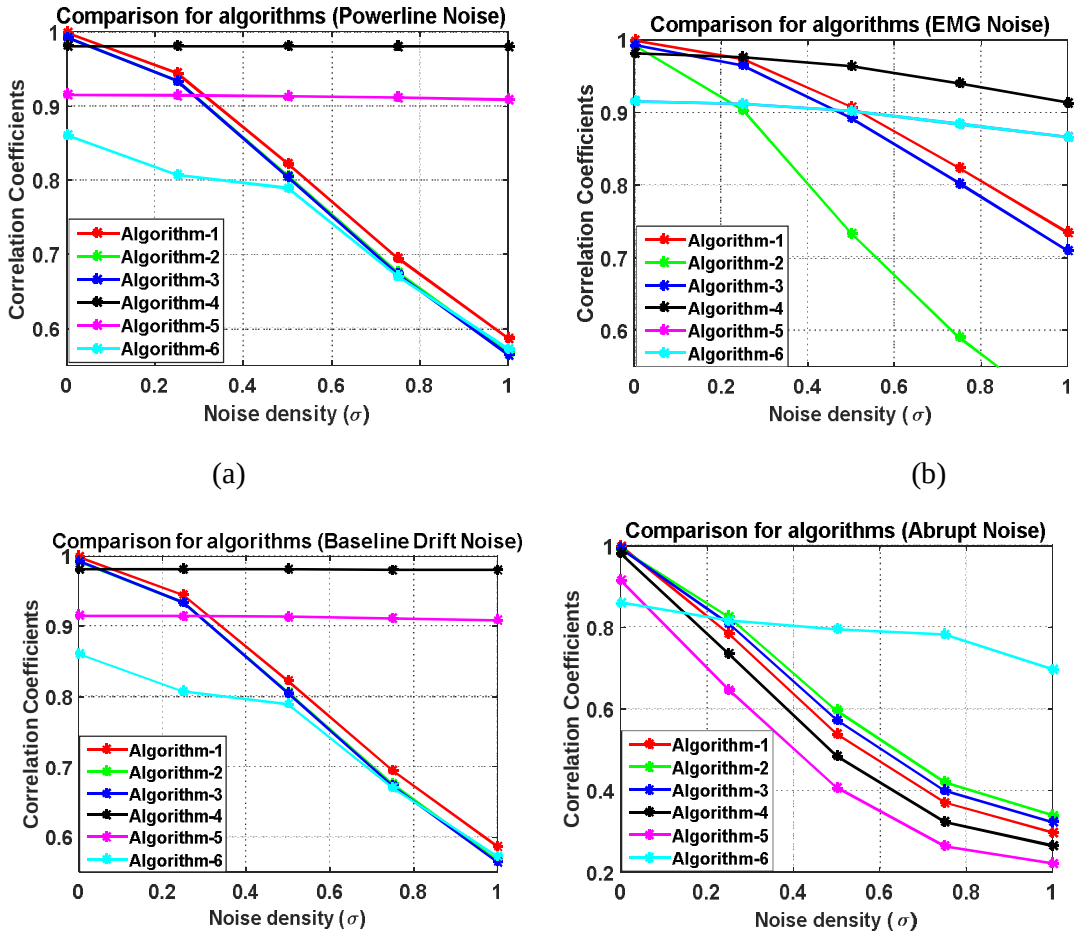

Figure 5.10: Comparison of Correlation coefficient with noise density for (a) powerline noise (b) EMG noise (c) Baseline Drift noise (d) Abrupt noise of denoising algorithms.

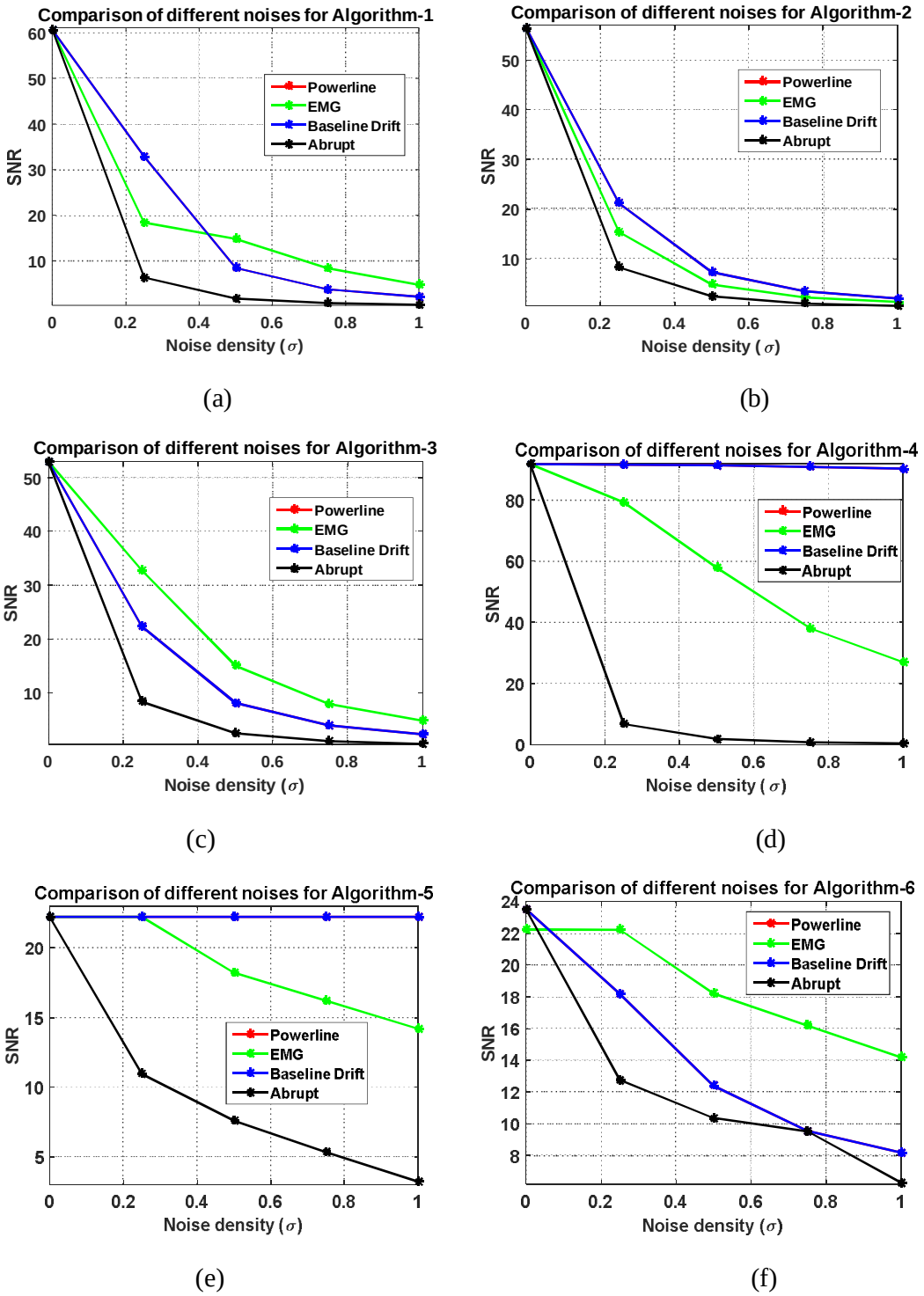

Figure 5.11: Comparison of SNR with noise density for (a) Algorithm-1; (b) Algorithm-2; (c) Algorithm-3; (d) Algorithm-4; (e) Algorithm-5; and (f) Algorithm-6 of different noises.

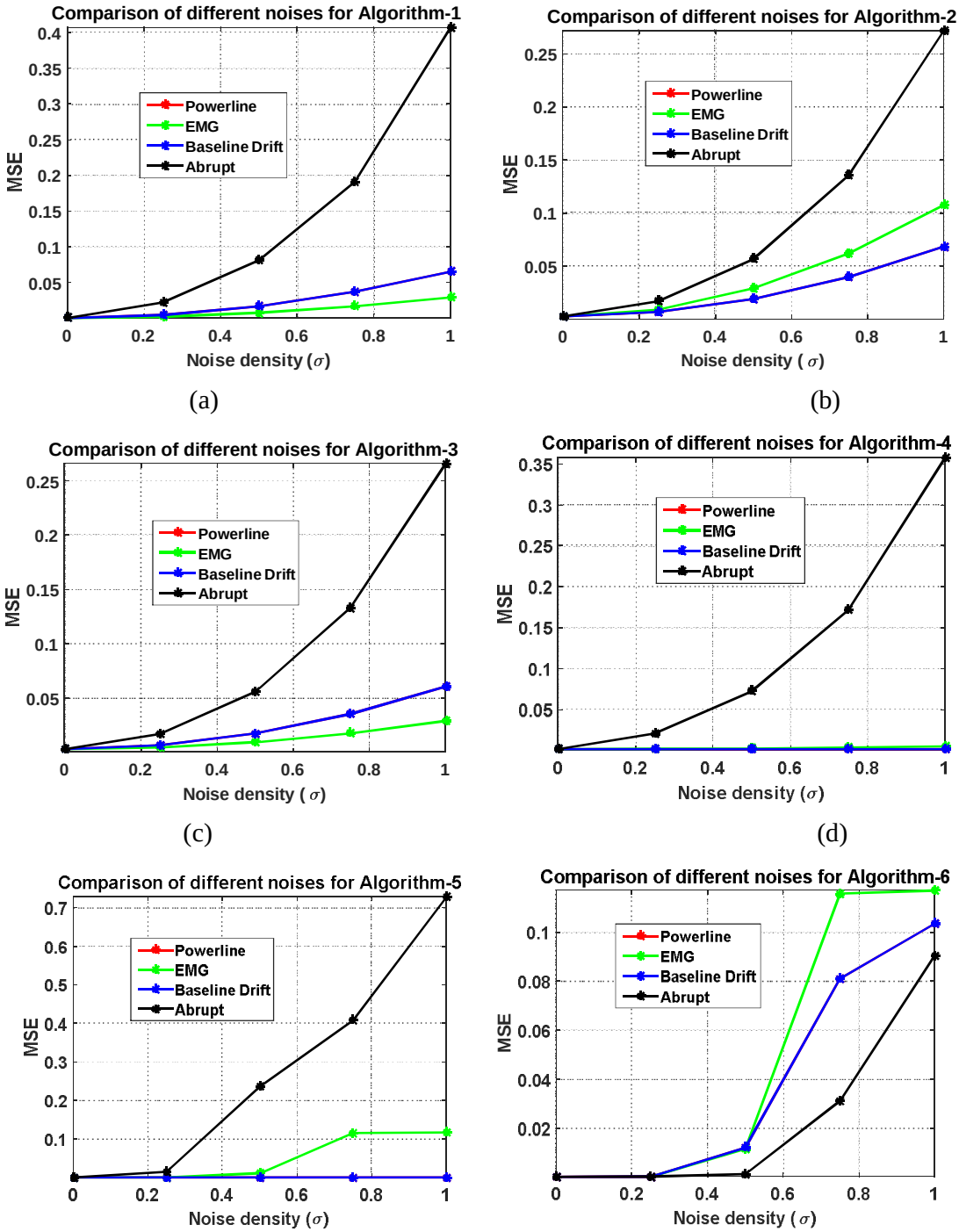

Figure 5.12: Comparison of MSE with noise density for (a) Algorithm-1; (b) Algorithm-2; (c) Algorithm-3; (d) Algorithm-4; (e) Algorithm-5; and (f) Algorithm-6 of different noises.

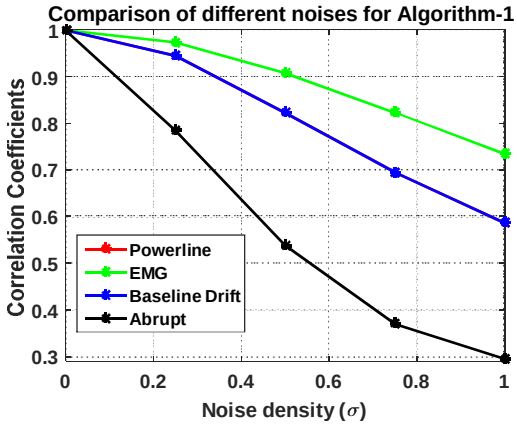

(a)

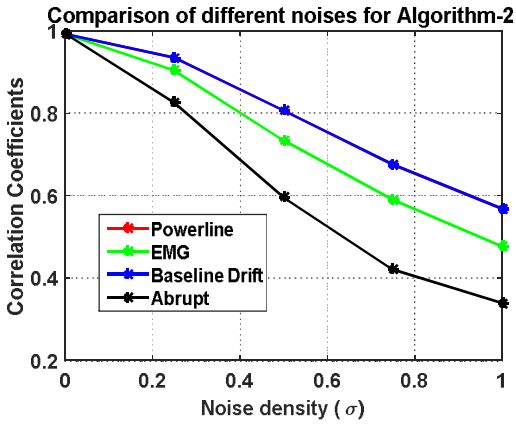

(b)

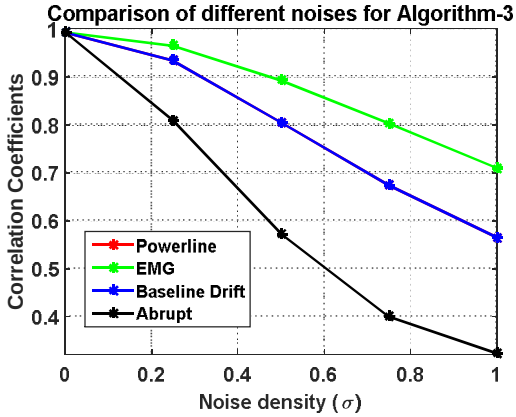

(c)

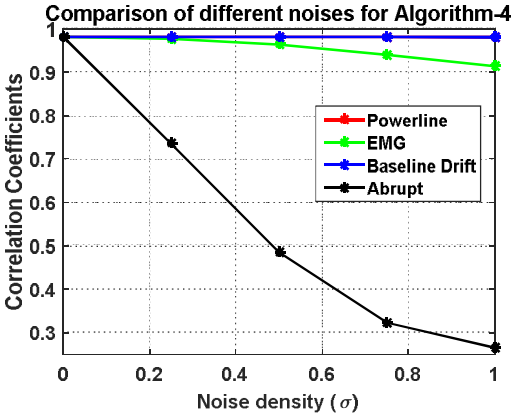

(d)

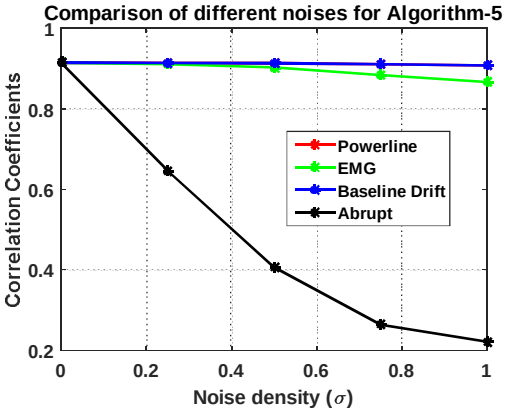

(e)

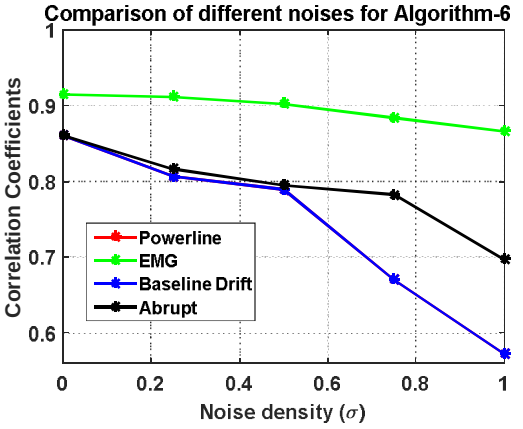

(f)

Figure 5.13: Comparison of correlation coefficient with noise density for (a) Algorithm-1; (b) Algorithm-2; (c) Algorithm-3; (d) Algorithm-4; (e) Algorithm-5; and (f) Algorithm-6 of different noises.

For comparison between the ECG signal and filtered signal by proposed algorithm, we have also considered three processes such autocorrelation, cross-correlation and power spectral density (PSD) for robustness of algorithms. In Figure 5.32-5.35, correlation values for different types of noises of proposed six algorithms have been shown. Figure 5.32 & 5.33, the first subplot indicates that the ECG signal and filtered signal by Algorithm-1, Algorithm-2, Algorithm-3, Algorithm-4, Algorithm-5, and Algorithm-6 with high peaks are good correlated individually by autocorrelation for power line noise with $\sigma = 0$. This shows that the autocorrelation is a periodic function. The second subplot is shown while the high peak shown in filtered signal is present in the ECG signal by cross correlation. This is same as first subplot because autocorrelation and cross-correlation maintain same properties in some cases. Figure 5.33 shows for powerline noise with $\sigma = 0.25$, Figure 5.34 shows for EMG noise with $\sigma = 0.25$ and Figure 5.34 shows for abrupt noise with $\sigma = 0.25$. These shows that if we increase the noise density, the correlation between raw ECG and filter ECG can be fluctuated.

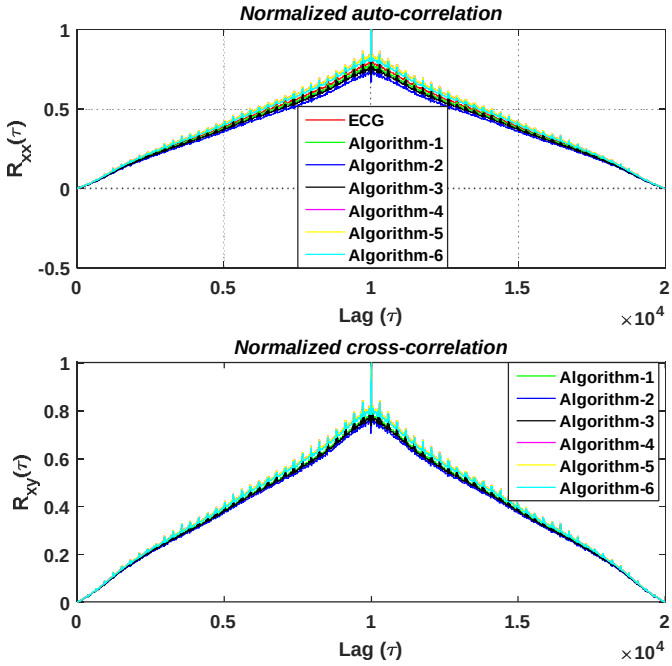

Figure 5.14: Correlation of ECG signal and filtered signal by auto correlation ($R_{xx}(\tau)$) and cross correlation ($R_{xy}(\tau)$) for powerline interference noise with $\sigma = 0$.

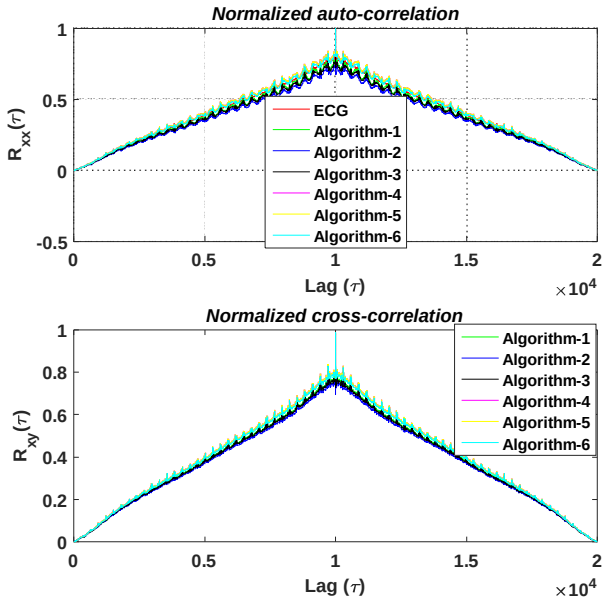

Figure 5.15: Correlation of ECG signal and filtered signal by auto correlation ($R_{xx}(\tau)$) and cross correlation ($R_{xy}(\tau)$) for powerline interference noise with $\sigma = 0.25$.

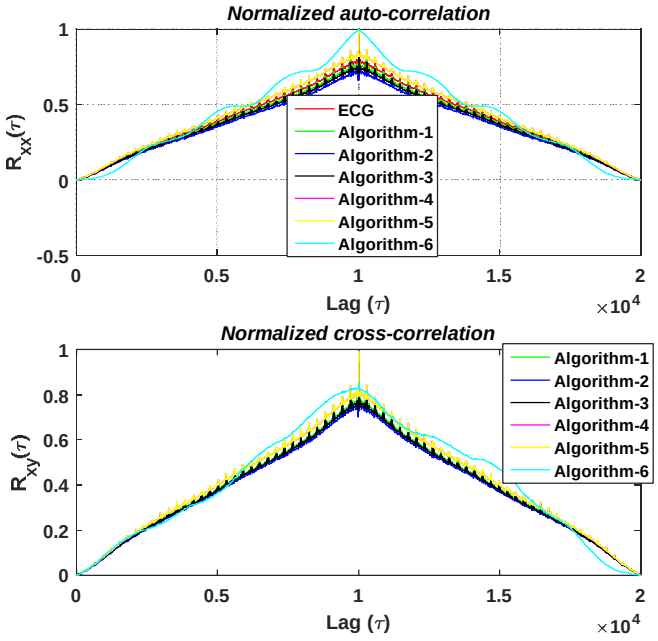

Figure 5.16: Correlation of ECG signal and filtered signal by auto correlation ($R_{xx}(\tau)$) and cross correlation ($R_{xy}(\tau)$) for EMG Noise with $\sigma = 0.25$.

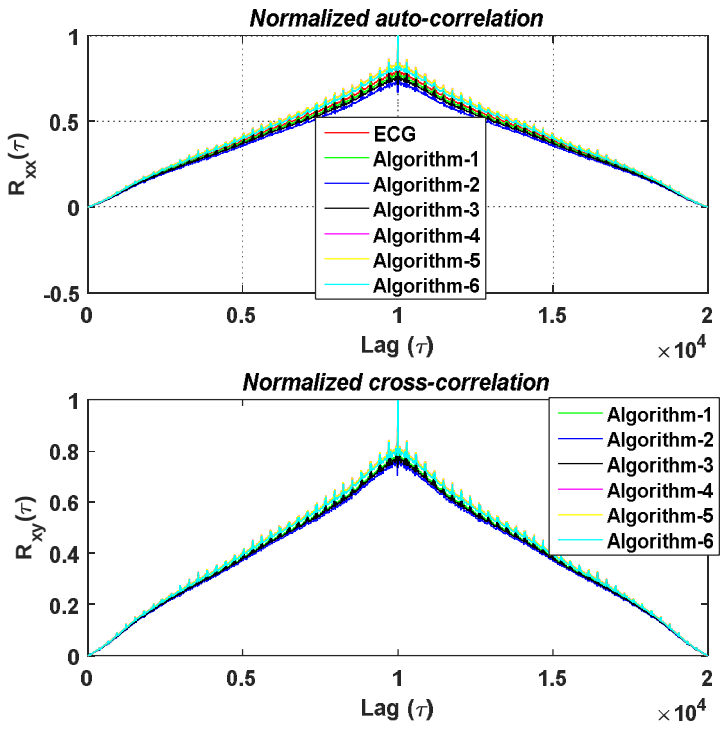

Figure 5.17: Correlation of ECG signal and filtered signal by auto correlation ($R_{xx}(\tau)$) and cross correlation ($R_{xy}(\tau)$) for Abrupt Noise with σ = 0.25.

Power spectral density function (PSD) shows the strength of the variations (energy) as a function of frequency. In other words, it shows at which frequencies variations are strong and at which frequencies variations are weak. The unit of PSD is energy per frequency (width) and can obtain energy within a specific frequency range by integrating PSD within that frequency range. Computation of PSD is done directly by the method called FFT or computing autocorrelation function and then transforming it. To estimate of power spectral density of noisy or filtered signal, we have considered non-parametric methods such as Periodogram, Welch and Lomb-Scargle algorithm **[**24**].** Lomb-Scargle algorithm can compute spectra of nonuniformly sampled signals or signals with missing samples. This algorithm is used to find out nonuniformity of ECG signal of MIT-BIH database.

In Figure 5.18 – 5.23, it can be observed some signals are uniformly collected of ECG signal. Figure 5.18 for Algorithm-1 of EMG noise with different noise density, Figure 5.19 for Algorithm-2 of powerline noise with different noise density, Figure 5.20 for Algorithm-3 of EMG noise with different noise density, Figure 5.21 for Algorithm-4 of baseline drift noise

with different noise density, Figure 5.22 for Algorithm-5 of powerline noise with different noise density, Figure 5.23 for Algorithm-6 of abrupt shift noise with different noise density.

A periodogram calculates the significance of different frequencies in time-series data to identify any intrinsic periodic signals. It shows statistically significant and harmonic is periodic. We have used for test 50 Hz in the noisy signal into ECG signal whereas sampled frequency of each signal 500Hz and then estimate power spectral density by Periodogram, and Welch methods. In Figure 5.18– 5.23 it can be observed that peak of noisy signal is raised because it's added by noise and the larger the amplitude for a given power. The filtered signal by Algorithm- 4 & 6 have smaller amplitude of power than noisy ECG signal and more and more resolution of side lobes of filtered signal than Algorithm 1, 2, 3 & 5. It is clear that the Algorithm 4 & 6 is shown better harmonic frequency than Algorithm 1, 2, 3 & 5.

We also observed the difference between the ECG noisy signal and filtered signal by Spectrogram. The spectrogram shows visual representation of spectrum of frequency in signal as they vary with time. The ECG signal is applied to short time Fourier transform by eight segments with Hamming window of length 512, 256 samples that of each of segment overlaps with 1000Hz sampling frequency. Figure 5.24 for Algorithm-1 of EMG noise with different noise density, Figure 5.25 for Algorithm-2 of powerline noise with different noise density, Figure 5.26 for Algorithm-3 of EMG noise with different noise density, Figure 5.27 for Algorithm-4 of baseline drift noise with different noise density, Figure 5.28 for Algorithm-5 of powerline noise with different noise density, Figure 5.29 for Algorithm-6 of abrupt shift noise with different noise density. Figure 5.24 shows a signal in which the vertical axis is frequency, the horizontal axis is time, and amplitude is shown on a color map. This map shows the amount of energy of ECG signal is displayed as level of yellow color at time and frequency where weak energy appears blue color in the spectrogram. The Algorithm 4 & 6 have shown high amount of energy of ECG signal as yellow and also clearly show blue color which indicates the removal of noise from ECG.

Researchers of biomedical signal processing fields have done some state of the art noise elimination algorithms. We tried to develop some algorithms for research contribution in this field as comparison with some exciting methods as in Table 5.2. The results of this table show that the proposed algorithms have higher results than other reference works. The results show the proposed algorithms have enough robustness in the field of de-noised ECG signal processing applications.

Table 5.2**.** Comparison results of existing methods on ECG dataset**.**

Ref.	**Noises**	**ECG databases(MIT-BIH)**	**Methods**	**SNR**	**PRD (Avg.)**	**MSE (Avg..)**	**Correlation (Avg..)**
[4]	Base line wander	Patient Data 100, 106, 215	LMS NLMS	3.4708 (Avg.) 3.8593 (Avg.)	0.2034 0.2034	0.0653 0.0652	×
	Power line interference,	Patient Data 100, 106, 215	LMS NLMS	7.5909 (Avg.) 7.0324 (Avg.)	6.6319 4.3414	0.0311 0.0310	×
[5]	WGN, Poisson	Patient Data 100	Proposed Algorithm with DWT	×	×	×	×
[6]	Power line interference	Not given patient Data	Band stop filter (3 order FIR filter)	×	×	×	×
	Base line wander		High Pass Filter	×	×	×	×
	Electro myography noise (EMG noise)		Low Pass Filter	×	×	×	×
[7]	Power line interference	Not given patient Data	Linear phase digital filter	×	×	×	×
[8]	Impulsive noise	Not given patient Data.	State Space Recursive Least Square (SSRLS) algorithm	×	×	Below 20dB	×
[9]	Power line	Not given	State Space				

	interference	patient Data.	Recursive Least Square (SSRLS) algorithm				
Proposed Algorithms	Power line interference noise	Patient Data 100, 105, 107, 108, 109, 111, 112, 113, 114, 115, 119, 200, 213	Algorithm-1	60.571	×	0.000169	0.9987
			Algorithm-2	21.183	×	0.0024638	0.9924
			Algorithm-3	52.975	×	0.0026257	0.9930
			Algorithm-4	91.737	×	0.0015162	0.9810
			Algorithm-5	22.2262	×	0.0001134	0.9149
			Algorithm-6	23.493	×	0.0001403	0.8605
	Base line drift noise		Algorithm-1	60.571	×	0.000169	0.9987
			Algorithm-2	21.183	×	0.0024638	0.9924
			Algorithm-3	52.975	×	0.0026257	0.9930
			Algorithm-4	91.737	×	0.0015162	0.9810
			Algorithm-5	22.2262	×	0.0001134	0.9149
			Algorithm-6	23.493	×	0.0001403	0.8605
	EMG noise		Algorithm-1	60.571	×	0.0001695	0.9987
			Algorithm-2	56.457	×	0.0024638	0.9924
			Algorithm-3	52.975	×	0.0026257	0.9930
			Algorithm-4	91.737	×	0.0015162	0.9810
			Algorithm-5	22.2262	×	0.0001134	0.9149
			Algorithm-6	22.2262	×	0.0001134	0.9149

	Abrupt Baseline Shift noise		Algorithm-1	60.571	×	0.0001	0.9987
			Algorithm-2	56.457	×	0.0024638	0.9924
			Algorithm-3	52.975104	×	0.0026257	0.9930
			Algorithm-4	91.737	×	0.0015162	0.9810
			Algorithm-5	22.226	×	0.0001134	0.9149
			Algorithm-6	23.493	×	0.0001403	0.8605

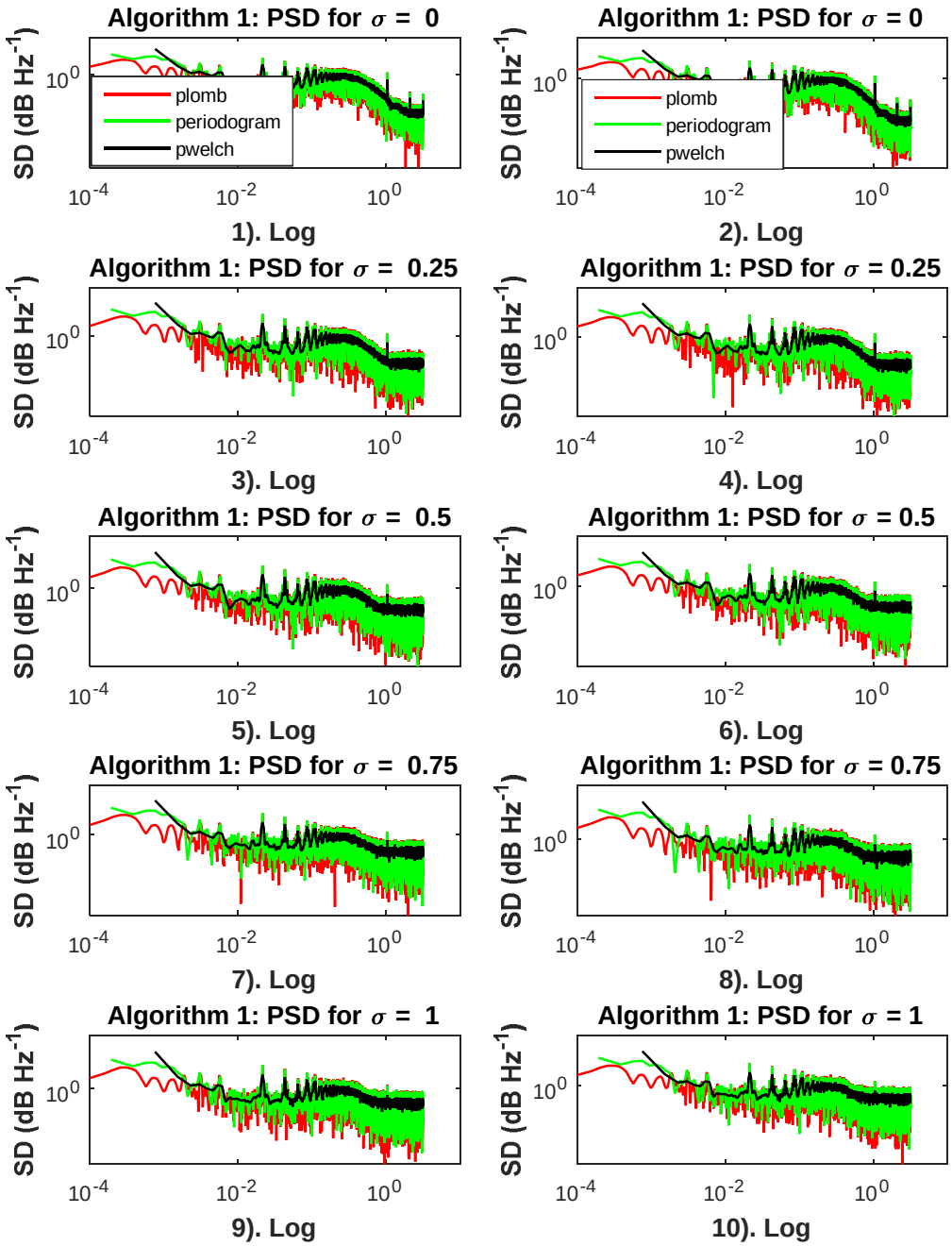

Figure 5.18: Power spectral density of ECG signal and filtered signal by Periodogram, Welch method and Lomb-Scargle algorithm by **Algorithm-1 for EMG noise.**

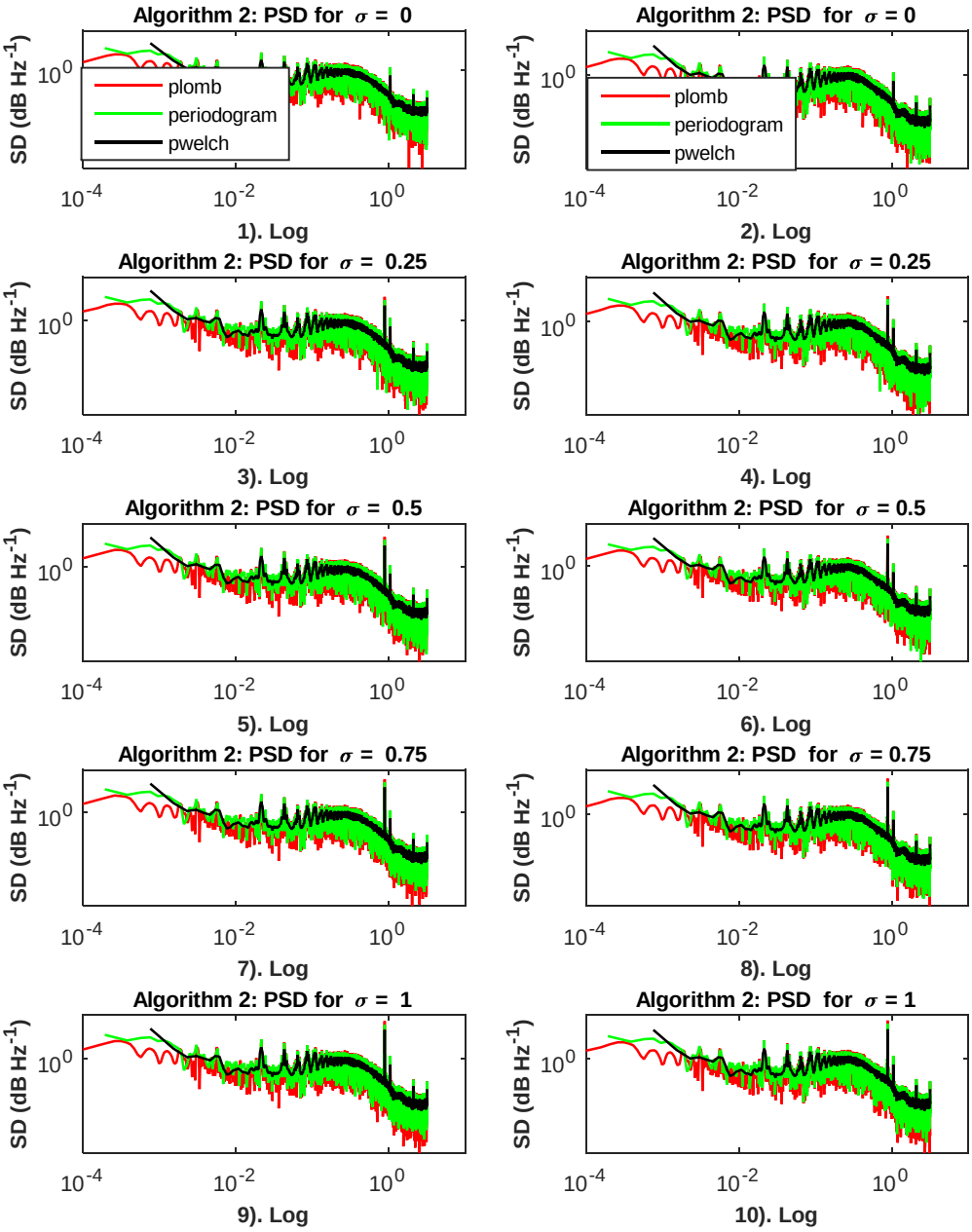

Figure 5.19: Power spectral density of ECG signal and filtered signal by Periodogram, Welch method and Lomb - Scargle algorithm by **Algorithm - 2 for powerline noise.**

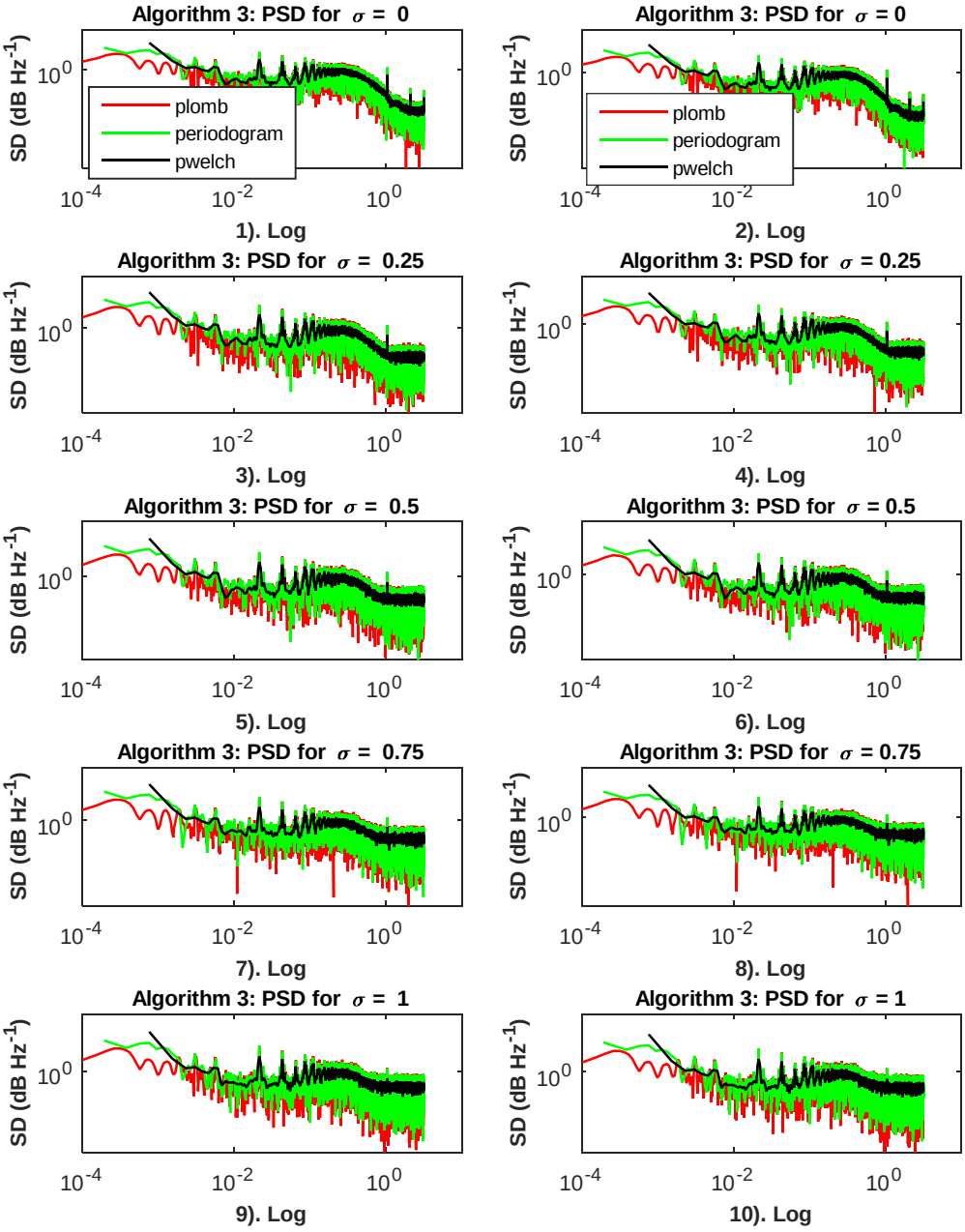

Figure 5.20: Power spectral density of ECG signal and filtered signal by Periodogram, Welch method and Lomb-Scargle algorithm by **Algorithm-3 for EMG noise.**

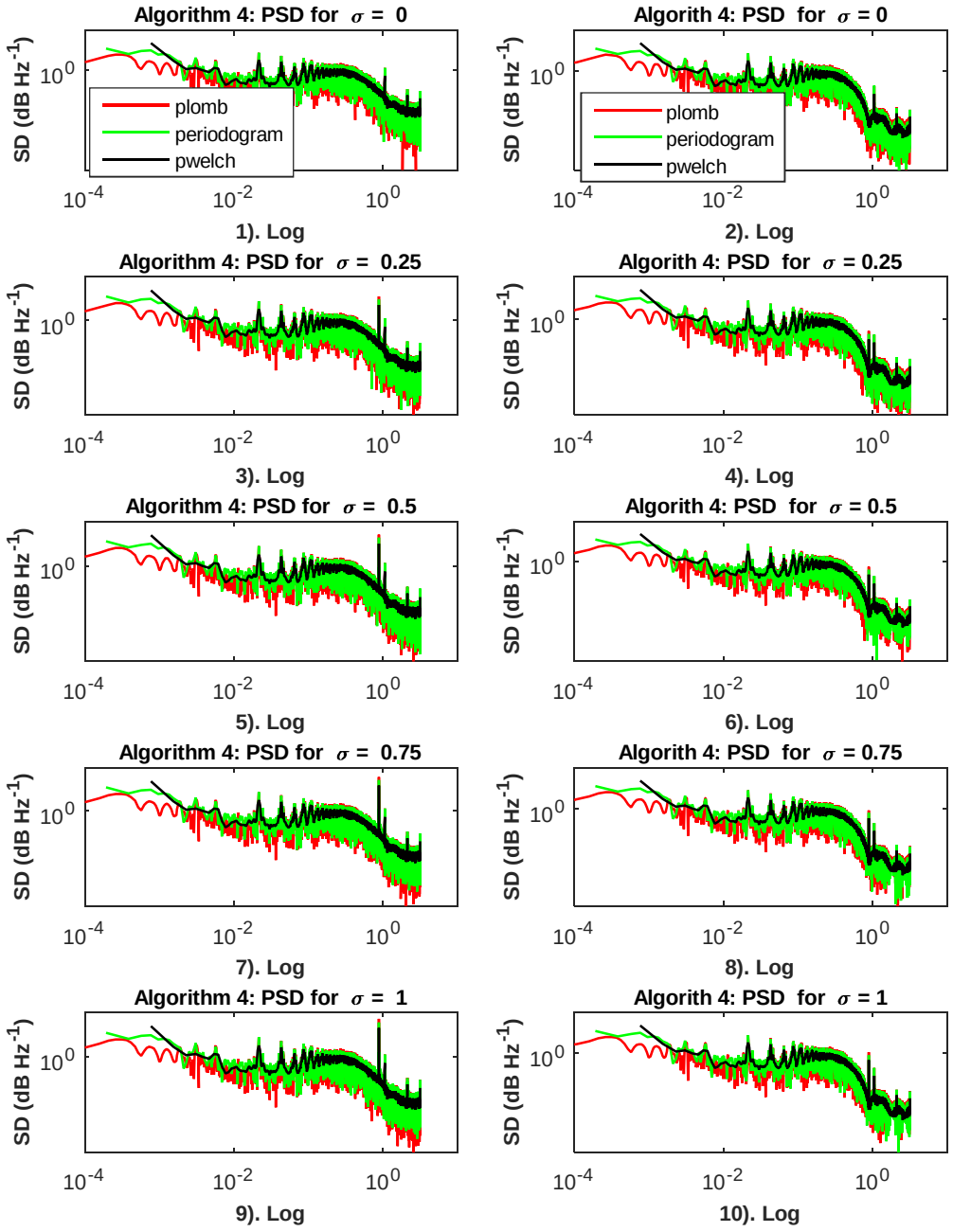

Figure 5.21: Power spectral density of ECG signal and filtered signal by Periodogram, Welch method and Lomb - Scargle algorithm by **Algorithm - 4 for Baseline drift noise.**

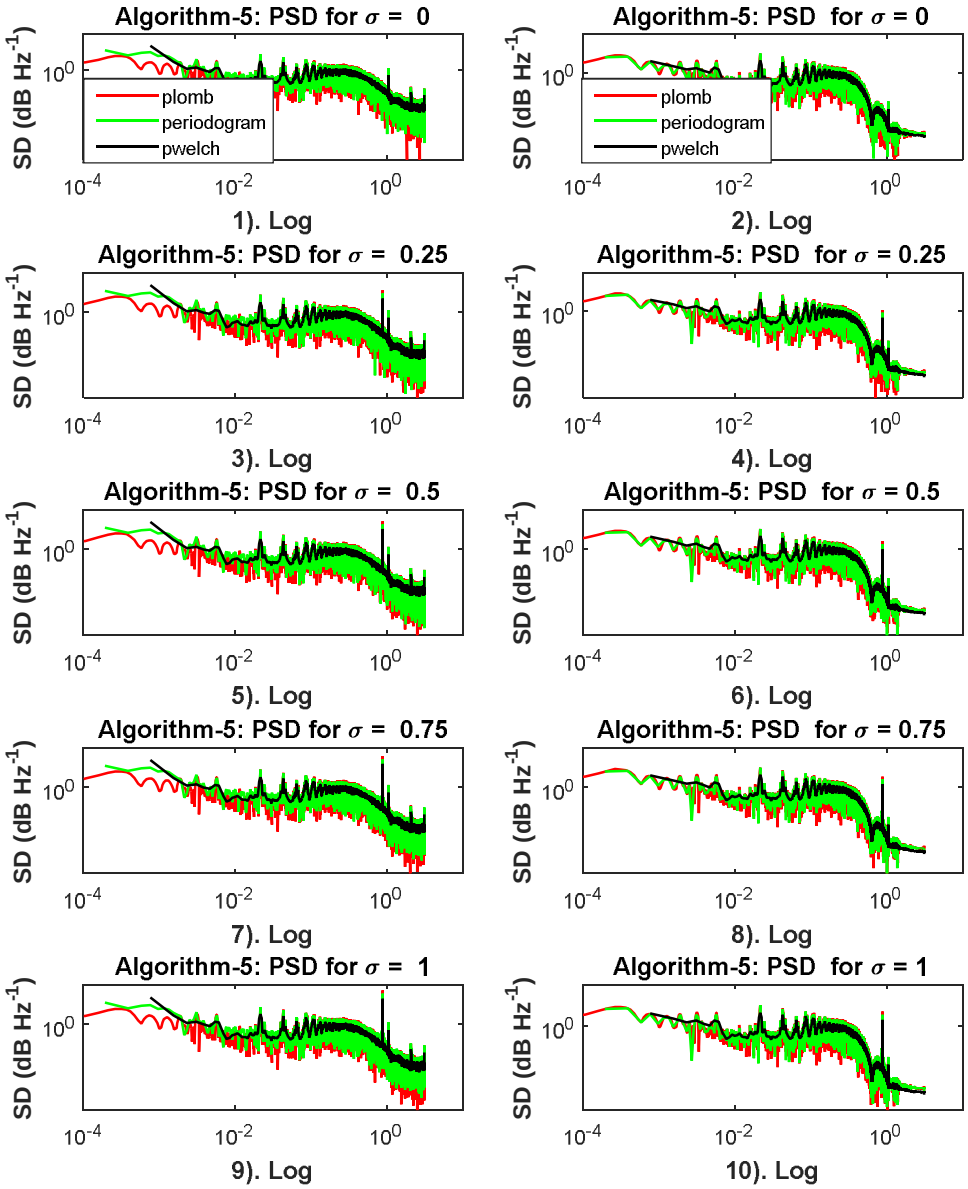

Figure 5.22: Power spectral density of ECG signal and filtered signal by Periodogram, Welch method and Lomb - Scargle algorithm by **Algorithm - 5 for powerline noise.**

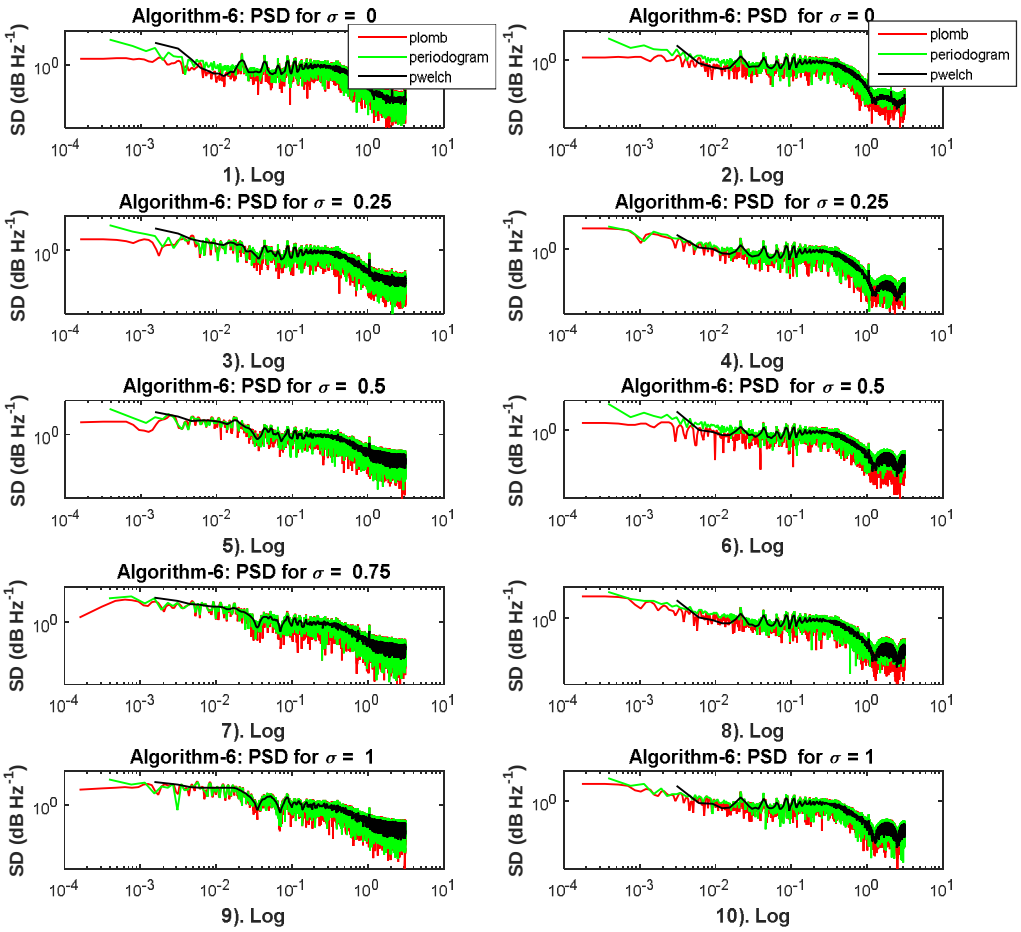

Figure 5.23: Power spectral density of ECG signal and filtered signal by Periodogram, Welch method and Lomb-Scargle algorithm by **Algorithm-6 for Abrupt shift noise.**

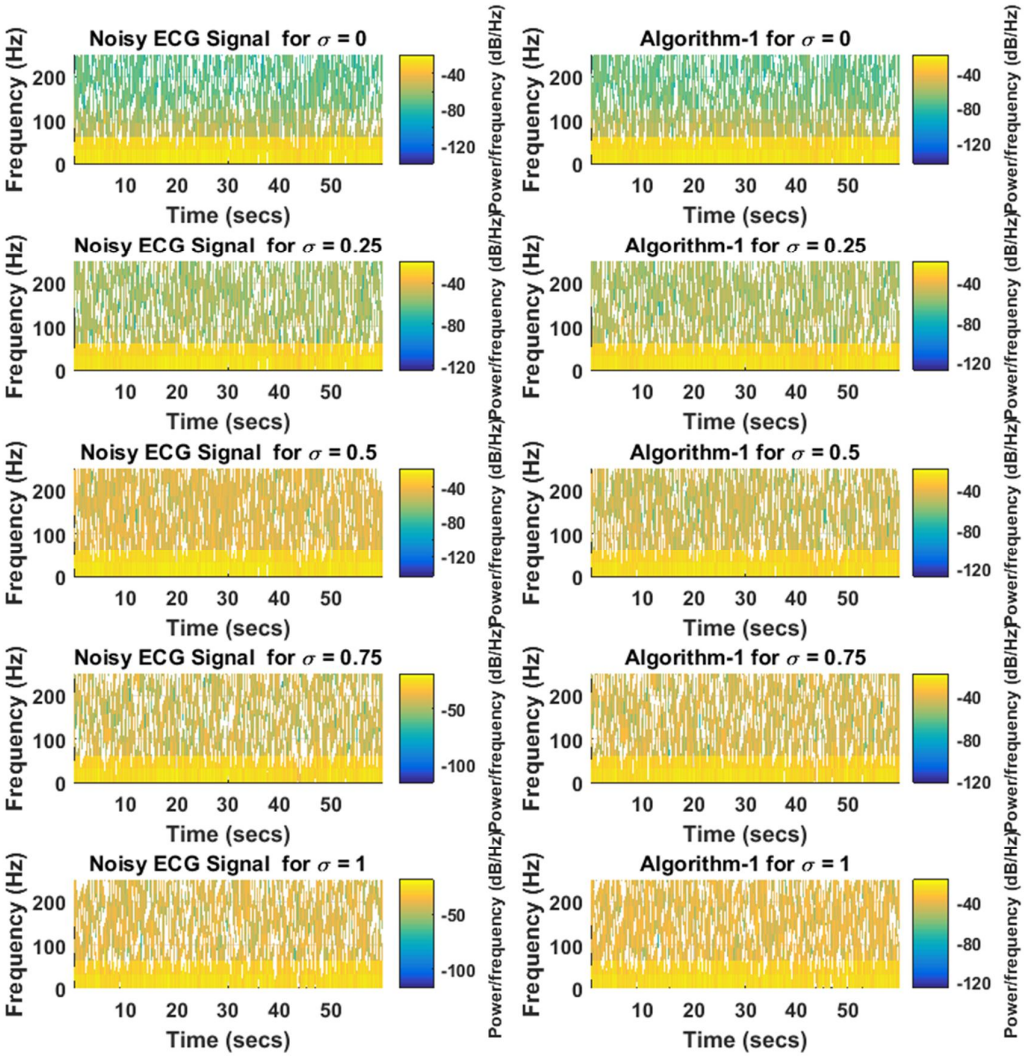

Figure 5.24: Spectrogram of noisy ECG and filtered ECG signal by **Algorithms 1 for EMG noise.**

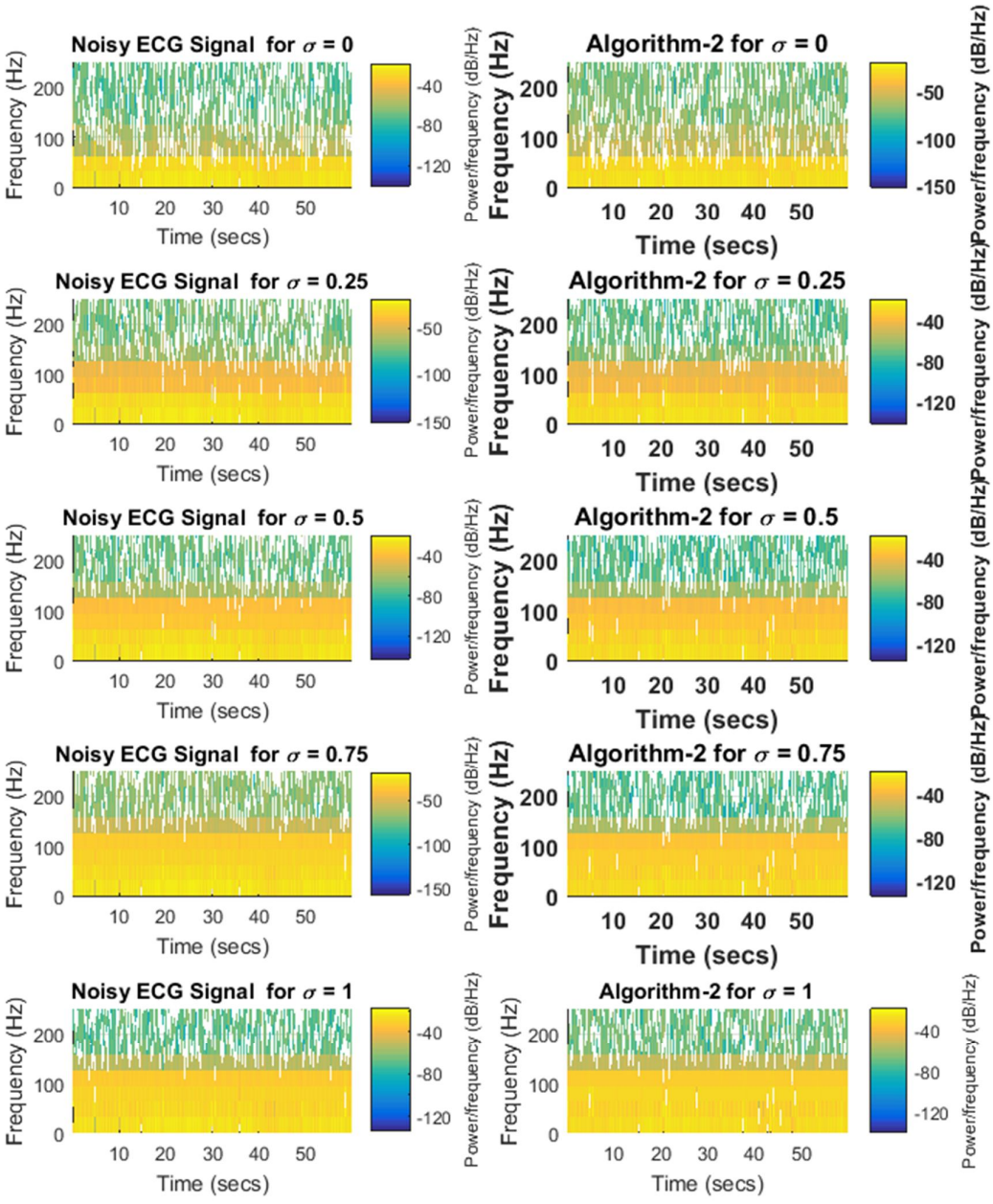

Figure 5.25: Spectrogram of noisy ECG and filtered ECG signal by **Algorithm-2 for powerline noise.**

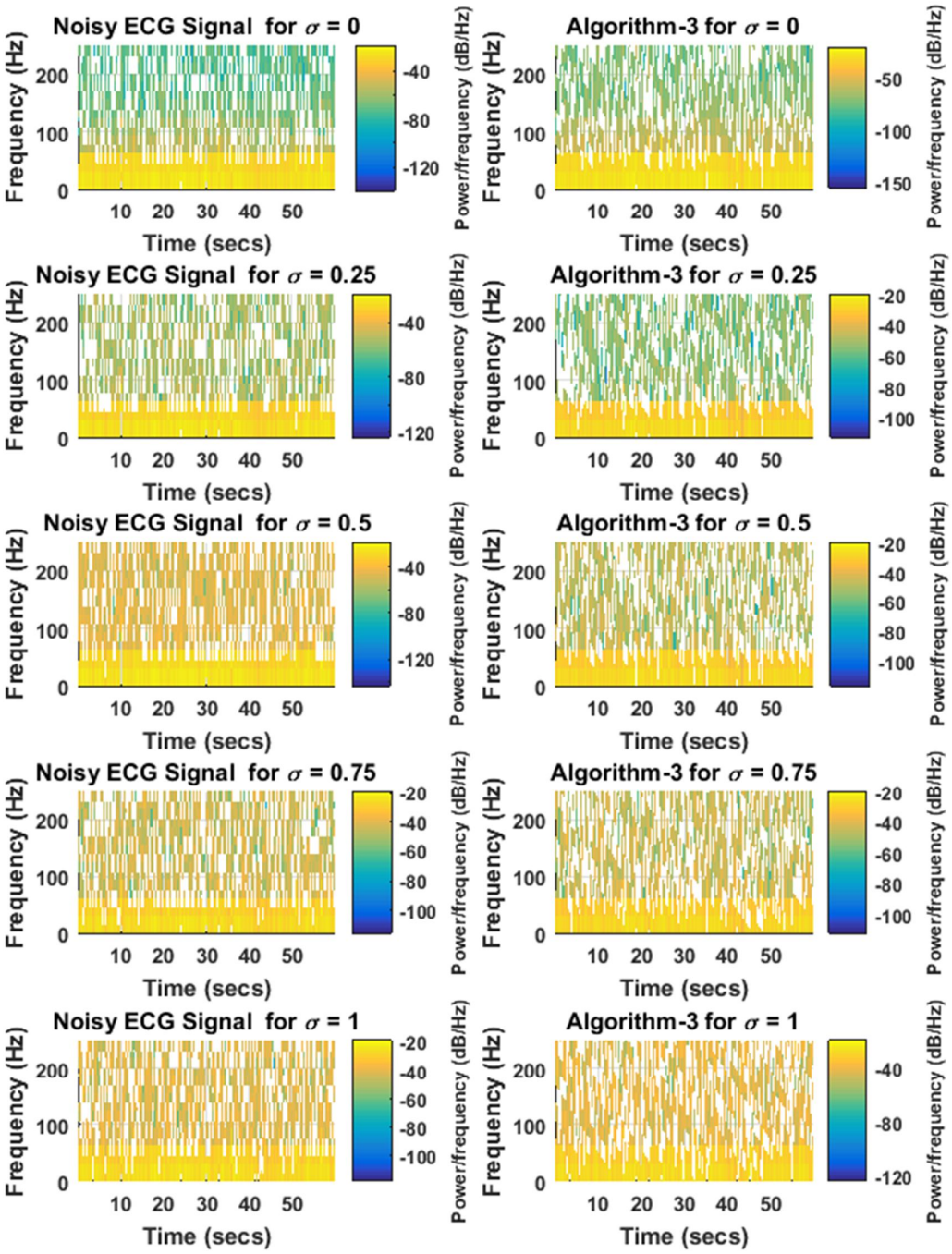

Figure 5.26: Spectrogram of noisy ECG and filtered ECG signal by **Algorithm-3 for EMG noise.**

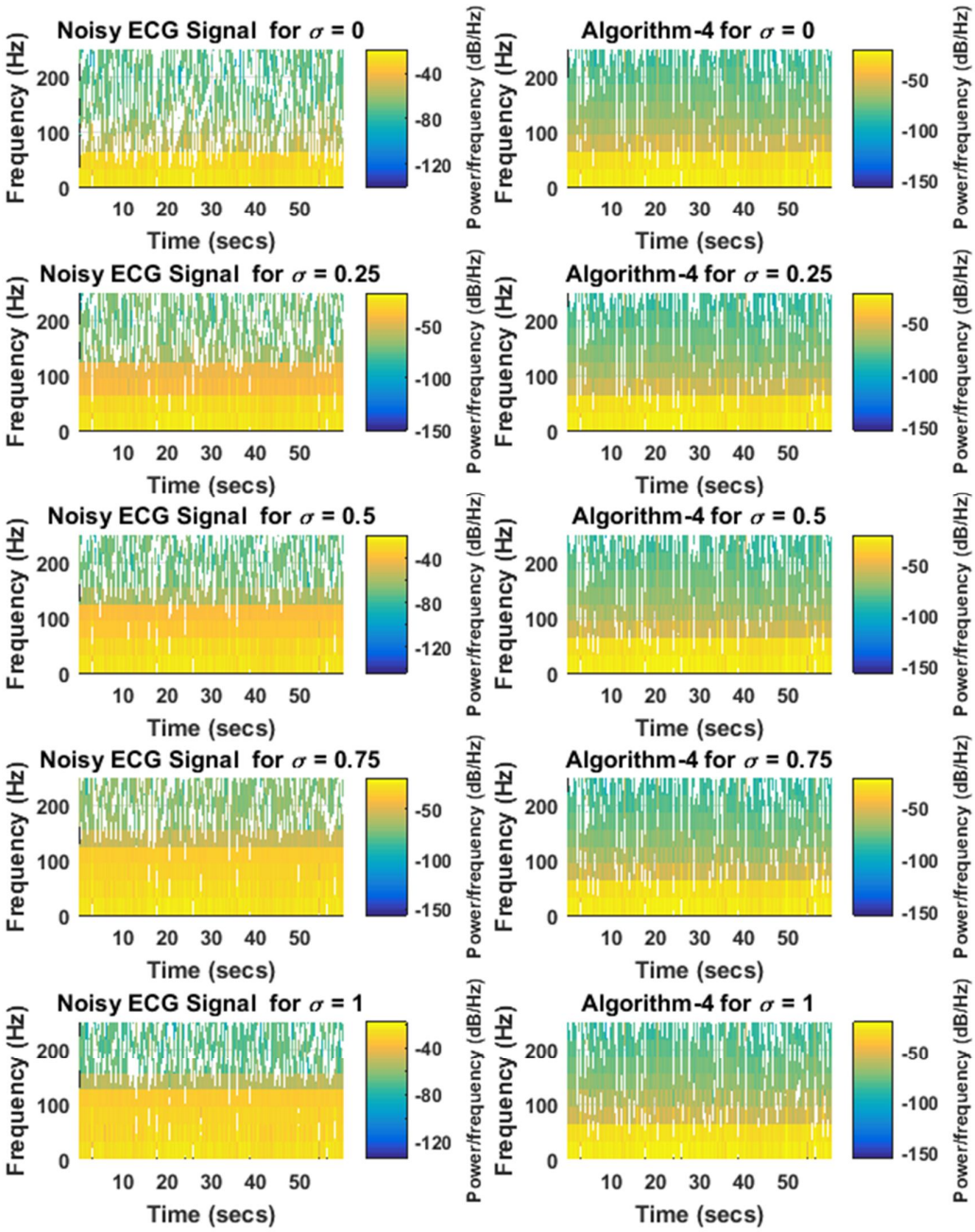

Figure 5.27: Spectrogram of noisy ECG and filtered ECG signal by **Algorithm- 4 for Baseline drift noise.**

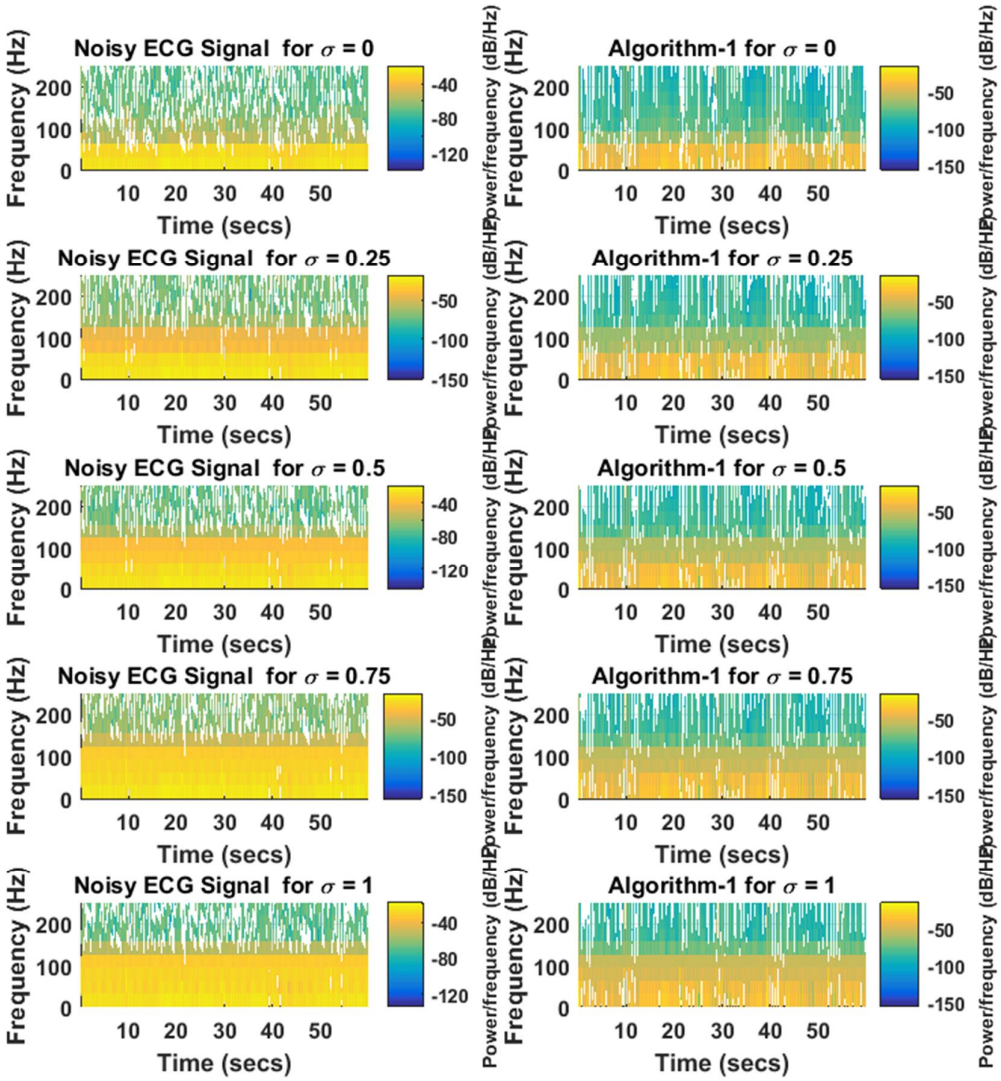

Figure 5.28: Spectrogram of noisy ECG and filtered ECG signal by **Algorithm-5 for Powerline noise.**

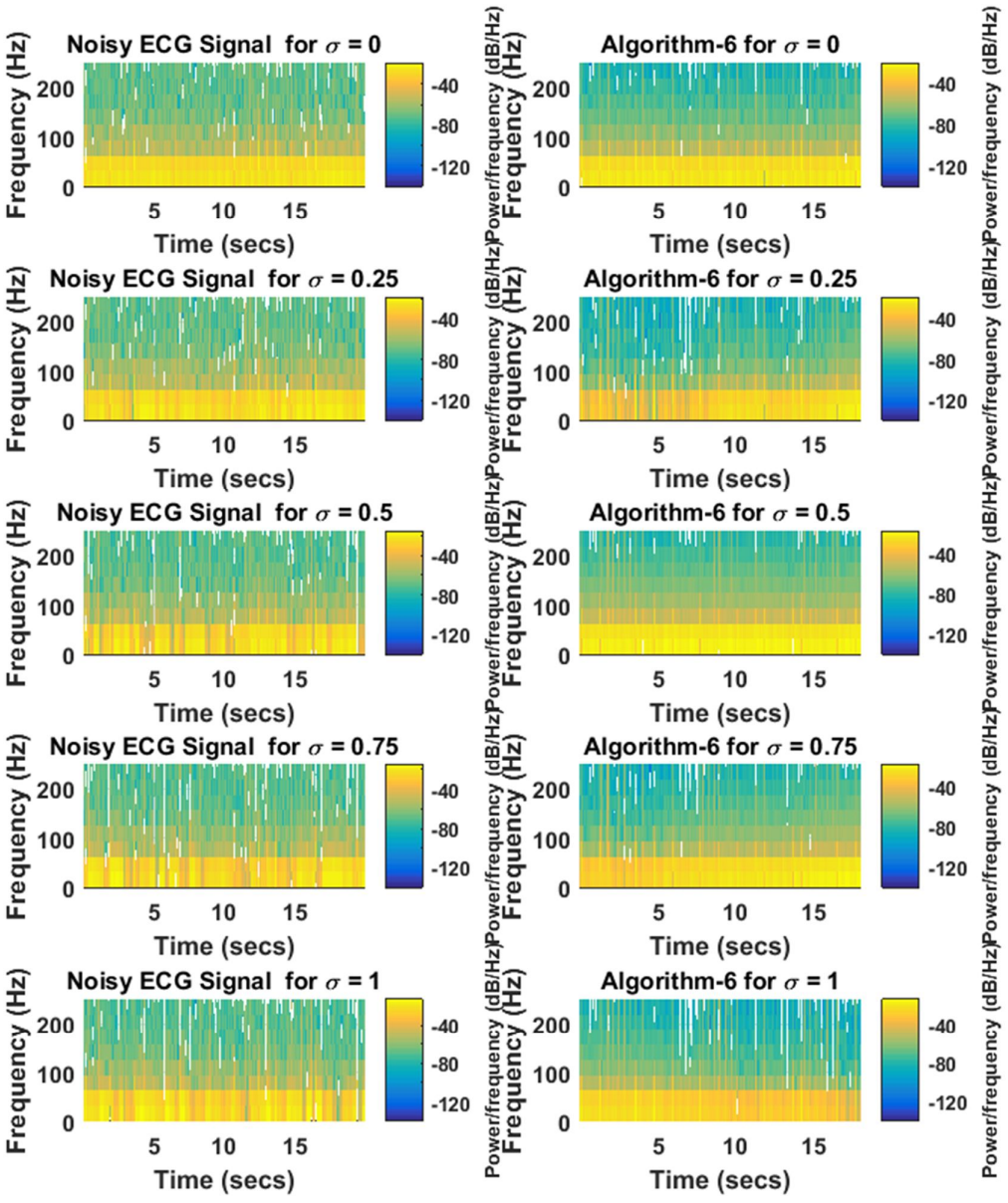

Figure 5.29: Spectrogram of noisy ECG and filtered ECG signal by **Algorithm-6 for Abrupt shift noise.**

5.4 QRS Detection Simulation Results

The performance parameters for detection have used accuracy, sensitivity, specificity, precision [26]. These parameters are defined as follows:

$$\text{Accuracy} = \frac{\text{Total no. of correctly detected sample points}}{\text{Total numbers of sample points}} \times 100$$

$$\text{Sensitivity} = \frac{\text{True Positive}}{\text{True Positive + Fasle Negative}} \times 100$$

$$\text{Specificity} = \frac{\text{True Negative}}{\text{True Negative + Fasle Positive}} \times 100$$

Or

$$\text{Accuracy} = \frac{TP + TN}{TP + FN + TN + FP} \times 100$$

$$\text{Sensitivity} = \frac{TP}{TP + FN} \times 100$$

$$\text{Specificity} = \frac{TN}{TN + FP} \times 100$$

After filtered ECG signal we can detect QRS complex of ECG signal by using Algorithm-4**.** Figure 5**.**31 shows QRS detection for the full sample indexes that was given in MIT-BIH database and Figure 5.30, its small-scale sample indexes**.** The ECG signal obtained after the thresholding is shown 3rd row in Figure 5.30 & 5.31**.** Finally, we have successfully detected the QRS complexes in ECG signal which are shown 4th row in Figure 5.30 & 5**.**31**.** We also present a comparison of results obtained with the algorithms implemented as Table 5.3.

The values presented are the results we got after doing multiple tests with each algorithm, and testing different detection parameters. We can get better results in accuracy, sensitivity, specificity, precision parameters than others with the entire database. For example, in Hamilton & Tompkins or Pan & Tompkins algorithm **[**27, 28**]**, have shown good detection rate but they don't find smaller peak in fixed interval. This algorithm would good sensitivity if local smaller peak would be detected by low interval, however the predictively or precision would be worse. In order to evaluate the performance of proposed algorithm, we calculate several performance criteria, such as, sensitivity, specificity and accuracy. To calculate those factors, at first, we

have to calculate TP, TN, FP and FN. TP beats are those beats which are annotated as 1 or QRS wave both in algorithm and database. TN beats are those beats which are annotated as 0 or lower value of R wave both in algorithm and database. FP beats are those beats which are annotated as 1 or QRS wave algorithm but annotated as 0 or lower value of R wave in database. FN beats are those beats which are annotated as 0 or lower value of R wave in the algorithm but annotated as 1 or QRS wave in the database. The number of TP, TN, FP and FN for each signal is given in Table 5.3.

The proposed detection has acquired the values of detection parameter such as 95.40% accuracy, 99.63% sensitivity, 89.28% specificity, and 98.62% precision. for the patients id 108**.** It proved that our algorithm is simulated properly we can also be observed the results of other patient id in Table 5.4**.**

The comparison of proposed detection method and others state of the art shows in Table 5.5. The referenced methods have considered only single ECG signal. We have given only average value on 4 patient recorded data with three detection parameters such as accuracy, sensitivity and specificity. All the reference authors have worked on only detection parameter of sensitivity.

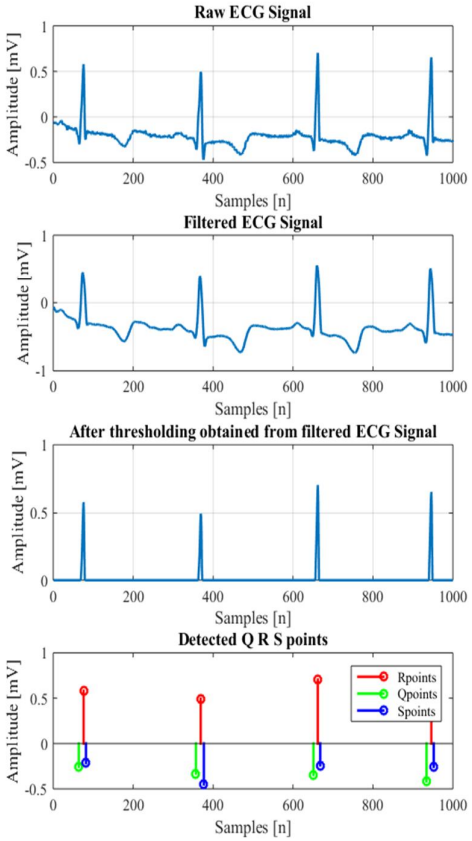

Figure 5.30**:** The detected QRS complexes in ECG signal (small sample indexes[n]).

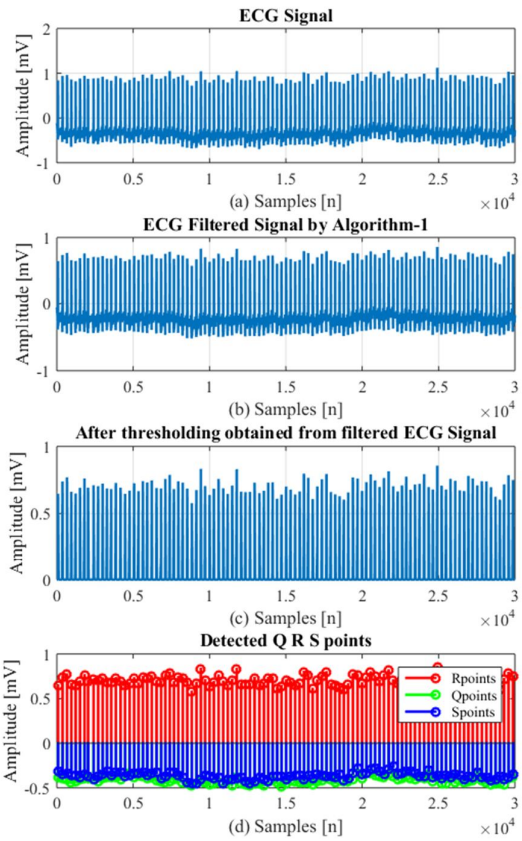

Figure 5.31**:** The detected QRS complexes in ECG signal (Full sample indexes [n]).

Table 5.3: Number of TP, TN, FP and FN for each ECG signal.

Sl. No.	Original ECG Signal (File #)	Total No. of Beats	True Positive TP	True Negative TN	False Positive FP	False Negative FN
1	100	43822	440	39728	3550	104
2	105	40683	811	38288	1439	145
3	107	43827	3444	32830	7398	155
4	108	49309	29004	18035	2165	105

Table 5.4: The calculated value of sensitivity, specificity and accuracy of the tested data.

Sl. No.	Original ECG Signal (File #)	Sensitivity (%)	Specificity (%)	Accuracy (%)
1	100	80.88	91.79	91.66
2	105	84.83	96.37	96.10
3	107	95.69	81.60	82.76
4	108	99.63	89.28	95.40

Table 5.5**:** Comparisons of performance parameters for detection algorithms**.**

Algorithm	**Database**	**Accuracy (%)**	**Sensitivity (%)**	**Specificity (%)**
J. Pan 1985 [11]	MIT-BIH	–	99.30	–
N. Arzeno 2008 [22]	MIT-BIH	–	99.68	–
V. Afonso 1999 [27]	MIT-BIH	–	99.59	–
P. Hamilton 1986 [28]	MIT-BIH	–	99.69	–
J. Martinez 2004 [29]	MIT-BIH, QT, ST-T, CSE	–	99.66	–
C. Li 1995 [30]	MIT-BIH	–	99.80	–
B. Abibullaev 2011 [31]	MIT-BIH	–	97.20	–
Q. Xue 1992 [32]	MIT-BIH	–	99.50	–
D. Coast 1990 [33]	AHA	–	97.25	–
R. Poli 1995 [34]	MIT-BIH	–	99.60	–
A. Martinez 2010 [35]	MIT-BIH, QT, ST-T,TWA	–	99.81	–
Proposed	MIT-BIH	91.48 (on average from Table IV)	90.27(on average from Table IV)	89.76(on average from Table IV)

5.5 Summary

Many researchers have done some state of the art noise removal algorithms. We did some research contribution in this field as comparison in our proposed noise removed algorithms as in Table 5.2 and QRS detection algorithm. in Table 5.5. This table shows that the proposed algorithms are the highest results than other reference works. The results are shown in average of SNR, PRD, MSE, correlation coefficients values because each signal of MIT-BIH database is simulated and figure out in average of all signals for comparisons.

Chapter 6

Conclusion and Future Work

6.1 Conclusion

We have successfully filtered ECG signal and also detected the QRS complex in ECG signal. The results show higher signal-to-noise ratio, good PRD, low MSE and also positive correlation values which represent strong correlation between ECG signal and filtered signal. The simulation results have shown that proposed denoising algorithms are better for diagnostics purposes of ECG and proposed QRS detection algorithms are more efficient for detection of heart diseases. The proposed detection achieved higher accuracy, sensitivity, specificity and precision value than other conventional methods. The heart beat rate will be measured accurately and 100% accuracy from the detected QRS complexes by proposed detection algorithm and also specified the heart diseases based on database.

6.2 Future work

In this thesis work a noble approach is to remove the power line interference, EMG interference, base line drift, abrupt shift in base line from ECG signal. The future work is to remove composite noises which is most accurately replicates an actual ECG signal by incorporating all four aforementioned types of noises into one. In this case, the maximum noise level was constructed by reducing the maximum noise levels for each of the previous described noise types to 50% of maximum and then summing them.

References

[1] F. Strasser, M. Muma and A. M. Zoubir, "Motion Artifact Removal in ECG Signals using Multi-Resolution Thresholding," *20th European signal processing conference (EUSIPCO2011)*, Bucharest, Romania, August 27-31, 2012.

[2] E. Ifeachor. and B.W. Jervis, "Digital Signal Processing: A Practical Approach," 2nd Edition, *Publisher: Pearson Education India*, 2002,

[3] http://www.nhs.uk/Conditions/electrocardiogram/Pages/Introduction.aspx

[4] U. Biswas, A. Das, S. Debnath and I. Oishee, "ECG signal denoising by using least-mean-square and normalized-least-mean-square algorithm based adaptive filter," *International Conference on Informatics, Electronics & Vision (ICIEV)*, 2014.

[5] S. M. R. Islam, X. Huang, and D. Sharma, "Wavelet Based Denoising Algorithm of the ECG Signal Corrupted by WGN and Poisson Noise," in *2012 International Symposium on Communications and Information Technologies (ISCIT)*, pp. 165–168, 2012.

[6] A. D. Jeyarani, T. J. Singh, "Analysis of noise reduction techniques on QRS ECG waveform - by applying different filters," *Recent Advances in Space Technology Services and Climate Change (RSTSCC)*, pp. 149 – 152, Nov. 2010.

[7] Y. Lian and P. C. Ho, "ECG noise reduction using multiplier-free FIR digital filters," *7th International Conference on Signal Processing*, 2004. Proceedings. ICSP '04, vol. 3, pp. 2198-2201, 2004.

[8] A. Mirza, S. M. Kabir, S. Ayub, S. A. Sheikh, "Impulsive Noise Cancellation of ECG signal based on SSRLS," Proceedings *of the 2015 International Conference on Soft Computing and Software Engineering (SCSE'15)*, vol. 62, pp. 196-202, 2015.

[9] M. Butt, N. Razzaq, I. Sadiq, M. Salman and T. Zaidi, "Power Line Interference removal from ECG signal using SSRLS algorithm," *2013 IEEE 9th International Colloquium on Signal Processing and its Applications (CSPA)*, , Kuala Lumpur, pp. 95-98, 2013.

[10] M. Elgendi, M. Jonkman, F. D. Boer," Improved QRS Detection Algorithm using Dynamic Thresholds," International *Journal of Hybrid Information Technology*, vol. 2, no. 1, pp. 65-80, January, 2009.

[11] J. Pan and W. J. Tompkins, "A real-time QRS detection algorithm," IEEE *Transactions on Biomedical Engineering*, vol. BME-32, No. 3, pp. 230-236, March, 1985.

[12] R. G. Lee, I. Chou, C. C. Lai, M. H. Liu, M. J. Chiu, "A Novel QRS Detection Algorithm Applied to The Analysis for Heart Rate Variability of Patients with Sleep Apnea," *Biomedical Engineering applications*, Basis & Communications, vol. 17, no. 5, pp. 44-48, October 2005.

[13] Q. Xue, Y. H. Hu, and W. J. Tompkins, "Neural-network-based adaptive matched filtering for QRS detection," *IEEE Transaction Biomedical Engineering*, vol. 39, no. 4, pp. 317–329, April 1992.

[14] V.S. Chouhan and S.S. Mehta, "Detection of QRS complexes in 12-lead ECG using adaptive quantized threshold," *International Journal of Computer Science and Network Security,* vol. 8, no.1, pp. 155-163, 2008.

[15] http://www.heart.org/HEARTORG/Conditions/HeartAttack/Symptoms

[16] K. P, Gettes LS, J. J.Bailey,R. Childers,B. J. Deal, E. W.Hancock, G.V.Herpen, J. A.Kors, P. Macfarlane, D. M.Mirvis, O. Pahlm, P. Rautaharju, G. S.Wagner, M. Josephson, J. W. Mason , P. Okin, B. Surawicz, and H. Wellens," Recommendations for the standardization and interpretation of the electrocardiogram: part I," *International Society for Computerized Electrocardiology*, Circulation 2007 Mar 13; 115(10) pp. 1306-24.

[17] Jhon G. Webster, "*Medical instrumentation application and design*," 3rd edition, *Publisher: John Wiley & Sons.Inc,* Chapter-6, pp. 248.

[18] J. D. L. Carlo, "Surface Electromyography: Detection and Recording," *DelSys Incorporated*, pp. 2-6, 2002.

[19] G. M. Friesen, T. C. Jannett, M. A. Jadallah, S. L. Yates, S. R. Quint, and H. T. Nagle, "A Comparison of the Noise Sensitivity of Nine QRS Detection Algorithms," *IEEE Transactions on Biomedical Engineering*, Vol 37, No. 1, pp. 85 -98, 1990.

[20] P. Ciarlini, P. Barone, "A recursive algorithm to compute the baseline drift in recorded biological signals," *Comput. Biomed. Res.* 21, pp. 221–226, 1988.

[21] C.R. Meyer, H.N. Keiser, "Electrocardiogram baseline noise estimation and removal using cubic splines and state space computation techniques," *Comput. Biomed. Res.* 10 pp. 459–470, 1977.

[22] N. Arzeno, Z. D. Deng, and C. S. Poon, "Analysis of first-derivative based QRS detection algorithms," *IEEE Transactions on Biomedical Engineering*, vol. 55, no. 2, pp. 478-484, 2008.

[23] R. Barraco, D. Persano Adorno, M. Brai, "ECG signal analysis using wavelet transform," Theory *Biosci*. 130: 155-163, 2011.

[24] Monson H. Hayes “Statistical Digital Signal Processing and Modeling,” *John Wiley & Sons, Inc*. ISBN: 978-0-471-59431-4.

[25] MIT-BIH Arrhythmia Database: www.physionet.org.

[26] H. U. Amin, A. S. Malik, R. F. Ahmad, N. Badruddin, N. Kamel, M. Hussain, W. T. Chooi “Feature extraction and classification for EEG signals using wavelet transform and machine learning techniques,” *Australasian Physical & Engineering Sciences in Medicine*, vol 38, issue 1, pp. 139-149, March 2015.

[27] V. Afonso, W. J. Tompkins, T. Nguyen, and S. Luo, “ECG beat detection using filter banks,” *IEEE Transactions on Biomedical Engineering*, vol. 46, no. 2, pp. 192-202, 1999.

[28] P. S. Hamilton and W. J. Tompkins, “Quantitative investigation of QRS detection rules using the MIT/BIH arrhythmia database,” *IEEE Transactions on Biomedical Engineering*, vol. BME-33, no. 12, pp.1157-1165, 1986.

[29] J. Martinez, R. Almeida, S. Olmos, A. Rocha, and P. Laguna, “A wavelet based ECG delineator: evaluation on standard databases,” *IEEE Transactions on Biomedical Engineering*, vol. 51, no. 4, pp. 570-581, 2004.

[30] C. Li, C. Zheng, and C. Tai, “Detection of ECG characteristic points using wavelet transforms,” *IEEE Transactions on Biomedical Engineering*, vol. 42, no. 1, pp. 21-28, 1995.

[31] B. Abibullaev and H. Seo, “A new QRS detection method using wavelets and artificial neural networks,” *Journal of Medical Systems*, vol. 35, no. 4, pp. 683-691, 2011.

[32] Q. Xue, Y. Hu, and W. J. Tompkins, “Neural-network-based adaptive matched filtering for QRS detection,” *IEEE Transactions on Biomedical Engineering*, vol. 39, no. 4, pp. 317-329, 1992.

[33] D. Coast, R. Stern, G. Cano, and S. Briller, “An approach to cardiac arrhythmia analysis using hidden Markov models,” *IEEE Transactions on Biomedical Engineering*, vol. 37, no. 9, pp. 826-836, 1990.

[34] R. Poli, S. Cagnoni, and G. Valli, “Genetic design of optimum linear and nonlinear QRS detectors,” *IEEE Transactions on Biomedical Engineering*, vol. 42, no. 11, pp. 1137-1141, 1995.

[35] A. Martinez, R. Alcaraz, and J. J. Rieta, “Application of the phasor transform for automatic delineation of single-lead ECG fiducial points," *Physiological Measurement*, vol. 31, no. 11, pp. 1467-1485, 2010.

List of Publications

Journal Paper

[1] **Jannatul Robaiat Mou**, Sheikh Md. Rabiul Islam , Xu Huang and Keng Liang Ou, "Noise Removal and QRS Detection of ECG Signal," *Journal of Biomedical Engineering and Medical Imaging*, Volume 3, No 4, pp. 1-17, August (2016).

IEEE Conference Paper

[1] **Jannatul Robaiat Mou**, Sheikh Md. Rabiul Islam, Xu Huang, Keng Liang Ou, "A New Approach of Noise Elimination Methodology of ECG Signal," *International Conference on Electrical, Computer and Communication Engineering (ECCE)*, pp. 921-927, February 16-18, 2017, Cox's Bazar, Bangladesh.

[2] Sudip Deb, Sheikh Md. Rabiul Islam, **Jannatul Robaiat Mou**, Md. Tariqul Islam, "Design and Implementation of Low Cost ECG Monitoring System for the Patient using Smart Device," *International Conference on Electrical, Computer and Communication Engineering (ECCE)*, pp. 774-778, February 16-18, 2017, Cox's Bazar, Bangladesh.